DEPARTMENT OF THE AIR FORCE

AIR UNIVERSITY

AIR FORCE INSTITUTE OF TECHNOLOGY

Wright-Patterson Air Force Base, Ohio

SECURITY CLASSIFICATION OF THIS PAGE

REPORT DOCUMENTATION PAGE

Form Approved
OMB No 0704-0188

1a REPORT SECURITY CLASSIFICATION UNCLASSIFIED	1b RESTRICTIVE MARKINGS
2a SECURITY CLASSIFICATION AUTHORITY	3 DISTRIBUTION/AVAILABILITY OF REPORT Approved for public release;
2b DECLASSIFICATION/DOWNGRADING SCHEDULE	distribution unlimited
4 PERFORMING ORGANIZATION REPORT NUMBER(S) Air Force Institute of Technology (AU) Wright-Patterson AFB Ohio 45433-6583	5 MONITORING ORGANIZATION REPORT NUMBER(S)
6a NAME OF PERFORMING ORGANIZATION / 6b OFFICE SYMBOL (If applicable)	7a NAME OF MONITORING ORGANIZATION
6c ADDRESS (City, State, and ZIP Code)	7b ADDRESS (City, State, and ZIP Code)
8a NAME OF FUNDING/SPONSORING ORGANIZATION / 8b OFFICE SYMBOL (If applicable)	9 PROCUREMENT INSTRUMENT IDENTIFICATION NUMBER
8c ADDRESS (City, State, and ZIP Code)	10 SOURCE OF FUNDING NUMBERS PROGRAM ELEMENT NO / PROJECT NO / TASK NO / WORK UNIT ACCESSION NO

11. TITLE (Include Security Classification)

Compression Testing of Carbon Fibers (Unclassified)

12. PERSONAL AUTHOR(S)

Thomas A. Downe, Captain, U.S. Air Force

13a. TYPE OF REPORT	13b. TIME COVERED	14. DATE OF REPORT (Year, Month, Day)	15. PAGE COUNT
MS Thesis	FROM _____ TO _____	1989 November	167

16. SUPPLEMENTARY NOTATION

17. COSATI CODES			18. SUBJECT TERMS (Continue on reverse if necessary and identify by block number)
FIELD	GROUP	SUB-GROUP	
11	04		Compression, Carbon Fibers
11	02	01	

19. ABSTRACT (Continue on reverse if necessary and identify by block number)

Title: Compression Testing of Carbon Fibers

Thesis Advisors: Lt. Col. Thomas Schuppe, Department of Operational Sciences
Dr. A. M. Palazotto, Department of Aeronautics

Abstract on back.

20 DISTRIBUTION/AVAILABILITY OF ABSTRACT	21 ABSTRACT SECURITY CLASSIFICATION
☒ UNCLASSIFIED/UNLIMITED ☐ SAME AS RPT ☐ DTIC USERS	Unclassified

22a NAME OF RESPONSIBLE INDIVIDUAL	22b TELEPHONE (Include Area Code)	22c OFFICE SYMBOL
A. M. Palazotto, PhD.	513-255-2998	AFIT/ENY

DD Form 1473, JUN 86 Previous editions are obsolete SECURITY CLASSIFICATION OF THIS PAGE

AFIT/GSO/ENS/89D-4

COMPRESSION TESTING OF CARBON FIBERS

THESIS

Thomas A. Doyne
Captain, USAF

AFIT/GSO/ENS/89D-4

Approved for public release; distribution unlimited

AFIT/GSO/ENS/89D-4

COMPRESSION TESTING OF CARBON FIBERS

THESIS

Presented to the Faculty of the School of Engineering

of the Air Force Institute of Technology

Air University

In Partial Fullfillment of the

Requirements for the Degree of

Master of Science in Space Operations

Thomas A. Doyne

Captain, USAF

December 1989

Acknowledgements

I would like to express my sincere gratitude to my thesis advisors, Lieutenant Colonel Thomas Schuppe and Professor A. M. Palazotto and, my thesis reader Major Dave Robinson for their expert advice, guidance and genuine concern throughout the course of this work. Also, the support given by the WRDC Materials Laboratory is deeply appreciated. A special thanks to Dr. Charles Lee and Dr. Chyi-Shan Wang of the University of Dayton Research Institute, UDRI, who introduced and guided me through the fascinating world of experimental research.

I would also like to thank Kenneth Lindsey, of UDRI, whose extensive knowledge of the micro-tensile testing machine made this study possible. Sincere thanks is also given to Bill Click for allowing me to use the facilities of the Mechanical Characterization Laboratory and to all those who helped and befriended me.

I would like to thank my beautiful wife who survived eighteen months of separation in Colorado Springs while I worked to complete my studies in Dayton OH. Finally, I would like to thank my parents for their love and support over the past year and a half.

Table of Contents

List of Figures

List of Tables

ABSTRACT

Understanding the compressive properties of composites is key to the development of new high performance composites required for the next generation of aerospace structures. One important aspect of composite compressive properties is the fiber compressive properties. A method has been developed for testing composite fibers in direct compression by using the Tecam Micro Tensile Testing Machine (MTM-8). The MTM-8 had been used successfully to measure the compressive properties of polymer fibers. This study demonstrated the MTM-8's ability to compression test carbon fibers that required gage lengths on the order of .1 mm to prevent Euler buckling. The data was then compared to the properties determined by other test methods such as: the elastica loop, the bending beam, recoil, and composite specimen tests.

The compressive strengths and the stress strain curves for T300, a PAN fiber, P100 and P55, both pitch fibers. The strength of the T300 fiber could not be determined because the glue holding the ends of the fiber failed before the fiber did. This method did determine the strength of the P100 and P55 fibers. The apparent (measured) compressive and tensile modulus were found to be the same for all three fibers. The apparent moduli varied with gage length for all three fibers in the same manner as the polymer fibers of the previous study. The [illegible] data

variability reduced the confidence of the actual moduli values determined from the machine compliance curves. The fiber strengths determined with the MTM-8 can be related to the strengths predicted by the rule of mixtures for composites almost one-to-one with least squares analysis.

COMPRESSION TESTING OF CARBON FIBERS

I. INTRODUCTION

Background

In materials engineering, composites are a class of materials made by embedding fibers of one type of material within another material, called the matrix. In general, composite materials possess high strength for their weight, and as a result, composites have been the subject of intensive research in aerospace engineering. The best examples of the use of composites in space are the payload bay doors of the Space Shuttle (17:736). Major new space programs, such as the Space Station, also require lightweight materials with high strength and stiffness. Therefore, composite materials are logical candidates for use in the Space Station. Research is being conducted to improve the performance of composites so that they may be used in such applications (20).

The properties of a composite material are related to the properties of both the fiber and the matrix. This relationship is approximated by the rule of mixtures, which shows that the fiber's properties are the dominant factor in

determining the composite's properties. Fibers with high moduli of elasticity (high stiffness) have been embedded in matrix materials, such as epoxy, to create new, higher performance composites. An interesting finding of high-performance composite research was the fact that the compressive strength does not necessarily increase with increase in the fiber's stiffness. This phenomenon increased the interest in understanding the compressive strength of composites, as well as their constituent fiber and matrix materials. Previously, information about fiber compressive strength was calculated from the rule of mixtures and was therefore based on the compressive strength of the composite, and not on any testing of the fiber (20).

The disparity between the compressive strengths of many high-performance composites has resulted in a multifaceted research effort to understand and improve the compressive properties of such composite materials. One facet of the research is concerned with the development of new fibers. Another facet is concerned with gathering information on existing fibers to better understand the correlation between the fiber's properties and the ultimate properties of composites fabricated with that type of fiber (20).

The development of new fibers is an active area of research. Currently, test specimens are used to determine the tensile and compressive strengths and the modulus of elasticity of composites that use the new fibers (20). However, new fibers are initially made in such small quantities that test specimens of composite materials cannot be fabricated. A test method which can characterize a fiber's compressive properties and then relate those properties to the composite's properties is highly desired, because of the savings in time and expense of composite test specimen fabrication. Such a method of assessing a new fiber's potential in a composite would speed the development of new composites.

Compression Test Methods

Because the fiber's compressive strength is of particular interest, several methods have been used to study this property. These methods are as follows: 1) the bending beam test; 2) elastica loop test; 3) recoil test and; 4) fiber embedded in resin test (12:5). Each of these tests will be discussed in greater detail in Chapter 2. However, the use of these tests leads to a scatter of compressive strength data for a given type of fiber, and thus results do not always correlate well with the strengths

calculated from the rule of mixtures of composites (20). A more direct test method would be of great value to researchers.

The Tecam Micro-Tensile Testing Machine, the MTM-8, originally designed to test small diameter specimens in tension, has been modified for direct compression testing of composite fibers. The MTM-8 will be described further in Chapter 3 and in Appendix A. The MTM-8 has been used to determine the compressive strengths of several different polymeric fibers (8). These polymeric fibers have a diameter of approximately 10 - 15 micrometers. In this study, the MTM-8 will be used to test carbon fibers which have diameters of 5 - 10 micrometers.

Problem Statement

The purpose of this study is to determine the compressive strengths of different carbon fibers with the MTM-8 and then correlate the results to the compressive strength of the fibers, as calculated using the rule of mixtures with data from composite specimens. The correlation of the MTM-8 compressive data will be compared to the correlations of the other compressive test methods' data to determine which test method achieves the best correlation to the rule of mixtures. In the process of this

study, several sub-objectives will be met, which are as follows:

1. The compressive properties of carbon fibers will be found using the MTM-8

2. The procedures for utilizing the MTM-8 will be further refined during the data collection.

Two common types of carbon fibers will be examined in this study, polyacrylonitrile (PAN) fibers and pitch-based fibers. Chapter 2 provides a detailed description of these fibers.

II. BACKGROUND

Overview

A review of the basic concepts of materials engineering is beneficial because of the nature of this type of research. This chapter will review - 1) the rule of mixtures for composite materials; 2) carbon fibers; 3) compression failure modes and; 4) compression test methods.

Rule of Mixtures for Composite Materials

The rule of mixtures is an empirical equation that relates the stiffness of a composite, as measured by Young's modulus, to the moduli of its fiber and matrix. For uniaxial composites, the rule is expressed as follows:

$$E_1 = E_f v_f + E_m v_m \qquad (1)$$

where E_1 is the apparent Young's modulus of the composite in the fiber direction, E_f and E_m are the moduli for the fiber and matrix respectively and, v_f and v_m are the volume fractions of the fiber and matrix in the composite (10:91).

The key assumptions of this macromechanical approach to characterizing a composite material's properties are:

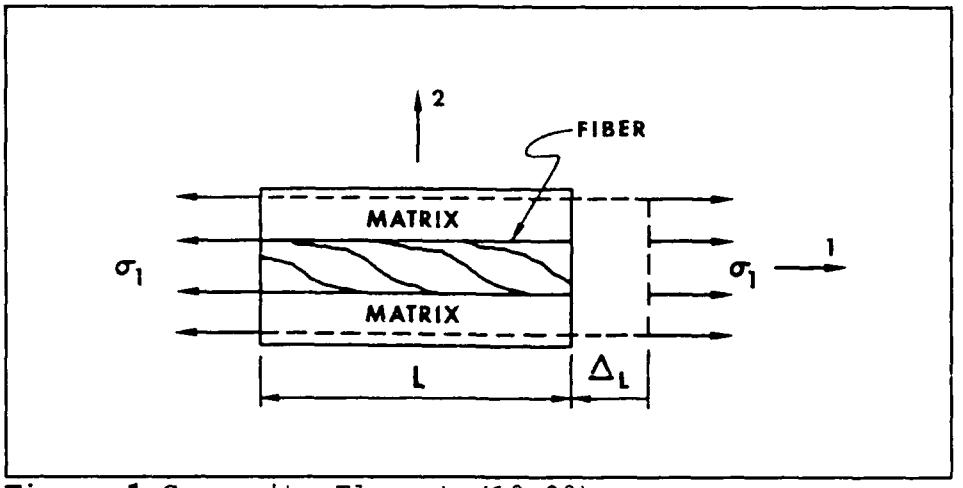

Figure 1 Composite Element (10:90)

1. the composite contains only unidirectional fibers

2. the strains in the fiber direction are the same for both the fiber and matrix

3. The constituent materials behave elastically (10:90).

Equation 1 can be used to calculate a value for the compressive strength of a fiber, provided that the moduli of the composite and matrix are known. For many matrix materials, $E_m << E_f$ (13:111), or V_m may be assumed equal to 0 (16), therefore, equation 1 can be reduced to:

$$E_c = E_f V_f \qquad (2)$$

Equation 2 can be modified by replacing the modulus terms with their Hooke's Law equivalents as follows:

$$\frac{\sigma_c}{\varepsilon} = \frac{\sigma_f V_f}{\varepsilon} \qquad (3)$$

where σ_c and σ_f are the strengths of the composite and fiber respectively. Simplifying equation 3 and solving for the strength of the fiber (13:112), one obtains:

$$\sigma_f = \frac{\sigma_c}{V_f} \tag{4}$$

Equation 4 is the most common method of determining a fiber's compressive strength because compression testing of composite specimens is much easier than compression testing of small diameter fibers. However, a large quantity of fiber is required to fabricate the composite specimens, and such a quantity of fiber is not normally available for new experimental fibers. Existing commercially produced fibers have been and are being compression tested in order to find a correlation between the actual fiber strength and the fiber strength predicted by the rule of mixtures from composite test data. If this correlation is found, the potential of new fibers for use in a composite can be evaluated using only a small number of fibers.

Carbon Fibers

Carbon fibers have been used extensively in modern composites because of their high stiffness and high

tensile strength. Carbon fibers are a class of fibers that are 80 - 90 wt. % (percent by weight) carbon, with diameters ranging between 5 - 15 micrometers (17:205).

Carbon fibers are manufactured from various precursors (starting materials). The most common precursors are rayon, polyacrylonitrile (PAN), and pitch (17:197). Carbon fibers based on rayon were first developed by Thomas Edison for use in his incandescent lamps. However, by 1909, tungsten filaments replaced carbon fibers and interest in carbon fibers waned until the 1950's. Research was then focused on the use of carbon fibers for use in rockets and missiles. The first use of polyacrylonitrile (PAN) was reported by Tsunoda in 1960. Research on the use of pitch as a precursor for carbon fibers began in the mid-1960's (17:197-199). Since this thesis is focusing on the compressive strengths of PAN and pitch based fibers, these fibers will be explained in detail.

PAN fibers. Polyacrylonitrile is a long linear molecule consisting of a hydrocarbon backbone with nitrile (carbon-nitrogen) groups attached along its length.

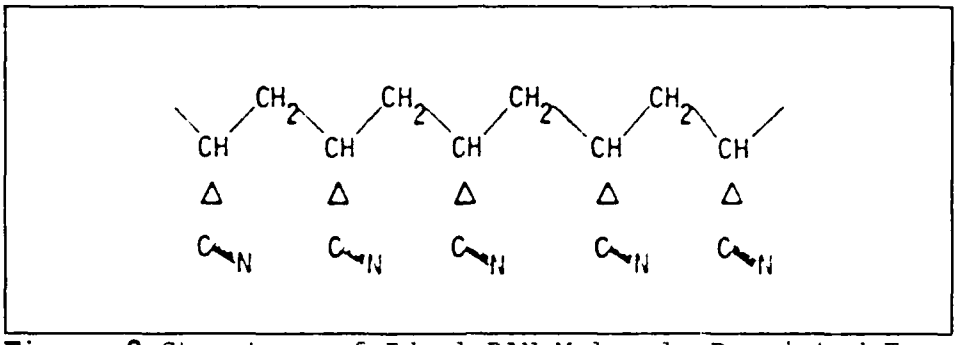

Figure 2 Structure of Ideal PAN Molecule Reprinted From (17:200)

The PAN fiber manufacturing process consists of the following steps:

1. Spinning and stretching the precursor
2. Stabilization at 220 degrees C under tension
3. Carbonization at ~ 1500 degrees C in an inert atmosphere (17:200).

The spinning and stretching of the PAN precursor form the fiber and align the molecules parallel to the fiber axis, which improves the fiber mechanical properties. Stabilization of the fibers continues the alignment of the molecules and prevents any relaxation (loss of molecular alignment) during the carbonization step. Carbonization is simply the heat treatment of the stabilized fiber to remove the majority of the noncarbon elements. Approximately 55 - 60 wt. % (percent by weight) is lost during this step. The resulting fiber is 80 - 95 wt. % carbon, with a highly aligned molecular

structure. When the carbonization is continued until the fiber is +99% carbon, the fiber is classified as a graphite fiber (17:200-207).

Pitch-based fibers. Pitch is a very common precursor for carbon fibers. Pitch is a mixture of by-products of petroleum refining and is considered to be a waste product since it is difficult to refine into petroleum products. As a result, pitch is a plentiful and inexpensive source of carbon for fiber manufacture (17:214).

The most popular method of manufacturing pitch fibers is the mesophase pitch process. The steps to this process are as follows:

1. Heat to 400-500° C to transform the pitch into the mesophase (a liquid crystalline) state
2. Spin the mesophase into filaments
3. Thermoset and carbonize the fibers (17:214).

This process is analogous to PAN fiber fabrication. The spinning transforms the pitch into fibers and aligns the molecules along the fiber axis. Thermosetting prevents relaxation during the carbonization. Carbonization removes the noncarbon elements, leaving a fiber 80 - 95%

carbon by weight. The resulting pitch fibers are considered high-performance fibers because they can have a modulus as high as 128 Msi (880 GPa) and a compressive strength as high as 320 ksi (2205 MPa) (17:217). The cross section texture of pitch fibers will vary depending on the spinning process. Some fibers exhibit a radial texture while others exhibit onion skin or random textures.

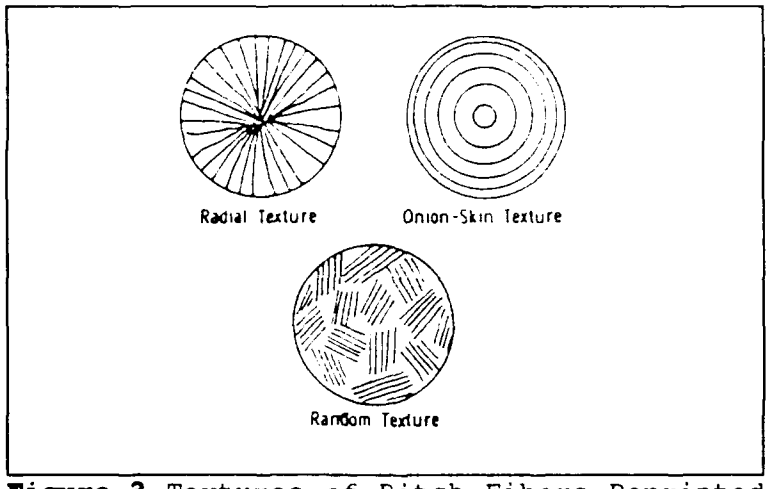

Figure 3 Textures of Pitch Fibers Reprinted From (17:217)

Fiber Compressive Behavior

Composite fibers will behave in a variety of ways when subjected to compressive loads. Three modes of behavior are of interest in this research: kinkband formation, buckling, and material failu

Kinkband formation. Kinkband formation in a composite fiber is a microbuckling mode of fracture. One proposed mechanism for kinkband formation is buckling along planes of easy shear slip, as depicted in Figure 4. From their study of the compressive failure of

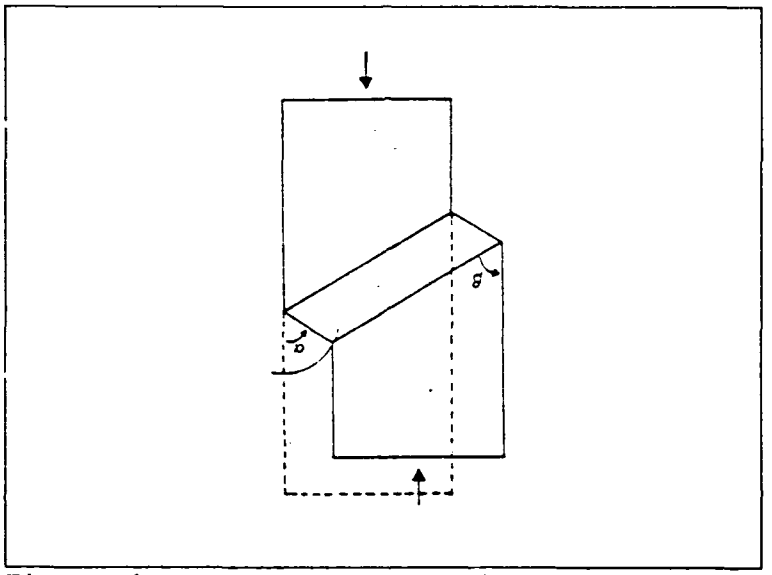

Figure 4 Ideal Kinkband Reprinted From (6:37)

single carbon fibers, Hawthorne and Teghtsoonian (9) showed that kinkband formation was based on the anisotropic nature of the fibers. As the molecular orientation of the fiber increased, the fiber's anisotropy increased, which changed the fracture mode to microbuckling (kinkband formation) (9). Test such as the elastica loop, bending beam, and fiber embedded in resin

tests have been used to examine the nature of kinkband formation in various types of fibers (9, 7, 6, 11).

Buckling. Buckling is simply a very large deformation resulting from a very small increase of compressive load (4:1). The stress that causes buckling can be very different than the compressive

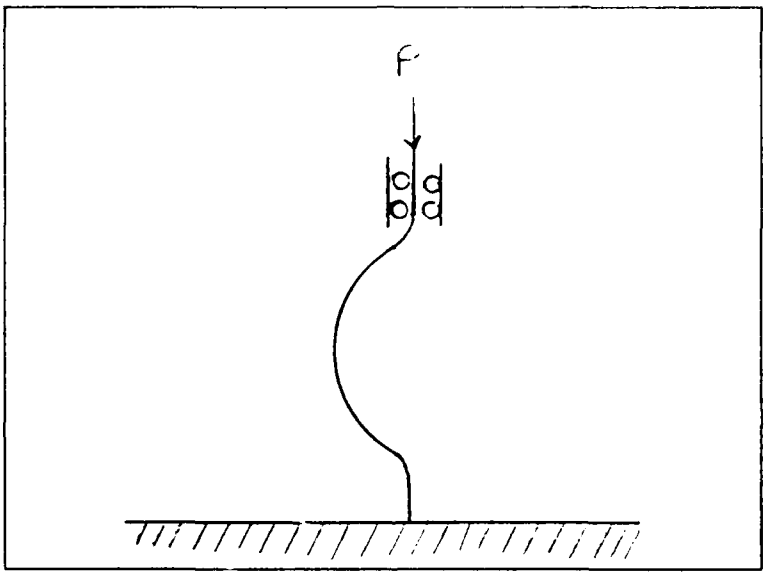

Figure 5 Euler Buckling of a Simply Clamped, Linear Elastic Prismatic Column

stress that causes material fracture. As a result, buckling is to be avoided. By assuming the fibers to be simply clamped, linear elastic prismatic columns, the following Euler buckling equation can be used to estimate the load at which the fibers will buckle instead of break for a given fiber length:

$$P_{cr} = \frac{4\pi^2 EI}{L^2} \quad (5)$$

where

P_{cr} = critical load
E = tensile modulus
I = area moment of inertia for a linear material
L = gage length of the fiber (4:22)

Euler buckling occurs when the potential energy of the fiber increases to the bifurcation point. The bifurcation point is the point where two different energy states are equally likely to exist in the fiber, thereby causing instability in the fiber (8:7).

Material failure. Material failure is simply loading the fiber in compression until the point of fracture, without buckling occurring. This point determines the compressive strength of the fiber.

Compression Test Methods

Carbon fibers formed from PAN and pitch precursors have been widely used for composite materials. While carbon fiber composites have excellent tensile strength, in general, these composites tend to be weaker in compression. In an effort to better understand composite compressive strength, fiber compressive properties are being examined. Several different methods have been

developed for testing composite fibers. These methods are as follows: 1) elastica loop test; 2) bending test; 3) recoil test; 4) fiber embedded in resin and; 5) direct compression test.

Elastica loop test. The elastica loop test was used by Allen (1) during his research on the properties of polymer fibers. The test loads the fiber as shown in Figure 6.

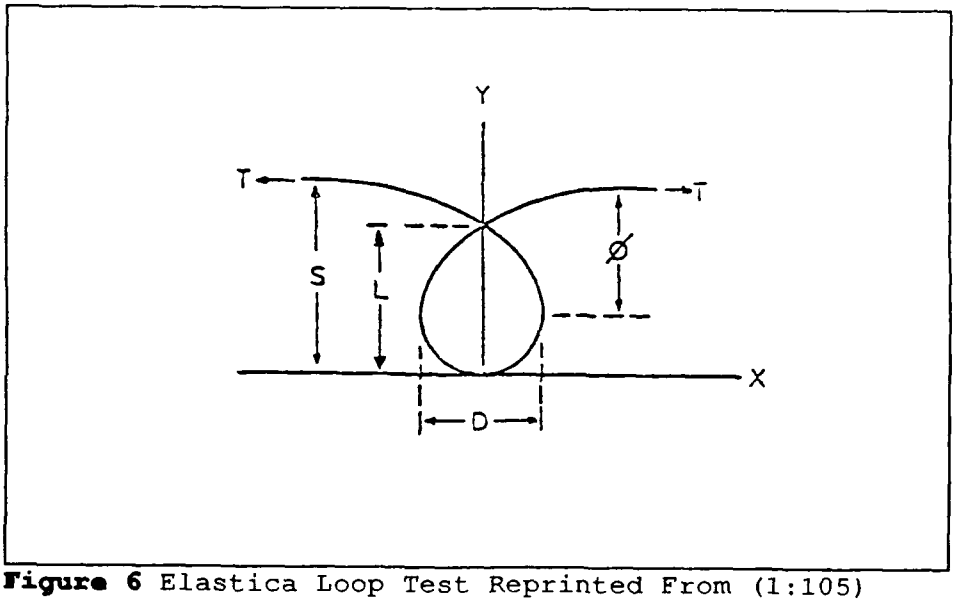

Figure 6 Elastica Loop Test Reprinted From (1:105)

The stress analysis is based on equating the elastic strain energy in an element of the looped fiber with the work done in creating the looped fiber. The stress field on the concave side of the fiber is compressive (1:117). Since the fiber is loaded simultaneously in compression

and tension, the true axial compressive strength is difficult to determine.

Bending beam test. The bending beam test is so named because the fiber is mounted to a beam which is then loaded as shown in Figure 7. The fiber is glued to a beam that is deflected upward by a roller forced inward toward the clamped end of the beam. Assuming a perfect bond between the fiber and the beam, the strain at a given point should be the same for both the fiber and the beam. The strain is then calculated for a given point on the beam and equated to the fiber at that point. The compressive strength is then calculated from Hooke's law:

$$\sigma_c = E_t \varepsilon_c \qquad (6)$$

which assumes that the tensile and compressive modulus are the same and that fiber behavior is linear up to the point of failure. The latter assumption is most likely untrue and will result in overestimating the compressive strength (8:3).

Recoil test. The recoil test method forces linear stress-strain behavior by dynamically loading the fiber. A single fiber is loaded in tension and then cut at its midpoint. Each half of the cut fiber recoils back toward

the clamps, thereby inducing a compressive stress wave.

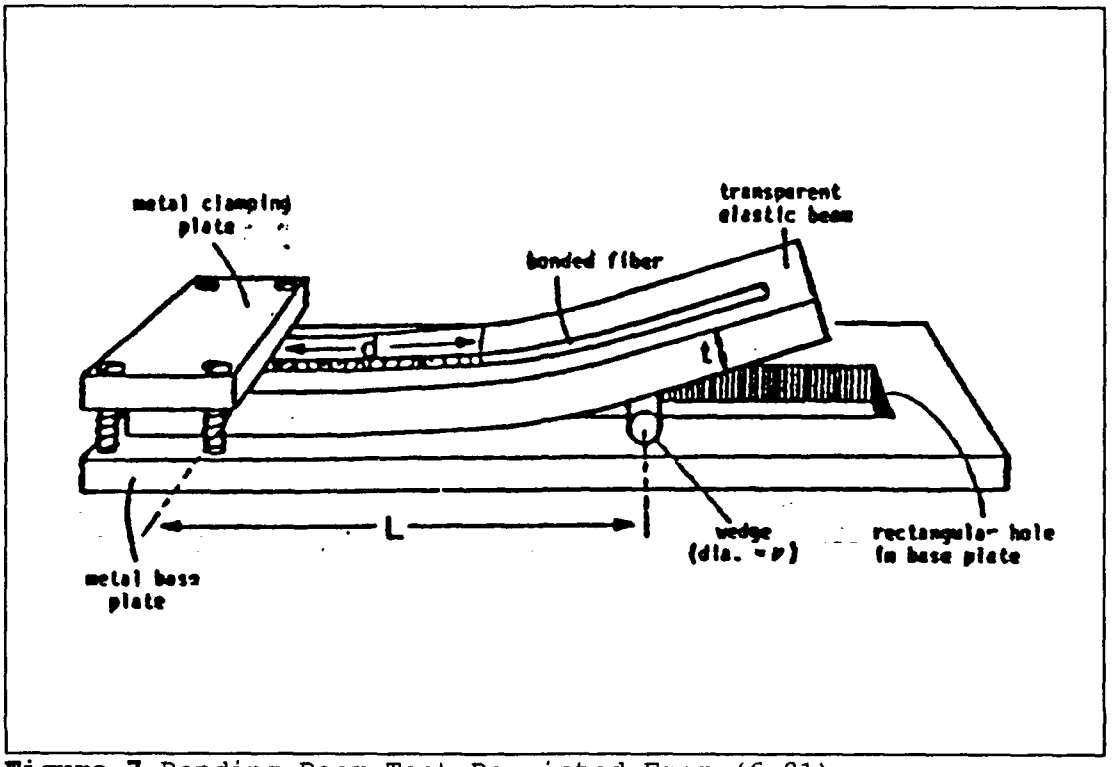

Figure 7 Bending Beam Test Reprinted From (6:81)

The kinetic energy of the fiber is transformed into strain energy and the compressive strength can be derived. This test assumes the fiber recoils directly back along the axis of the fiber and does not account for any lateral motion. In addition, this method is unable to determine the compressive modulus (20).

Fiber embedded in resin test. In this test, a single fiber or fiber bundle is embedded in a resin test sample. The sample is then subjected to a compressive

load and the fiber is examined. Dobbs et al. subjected unidirectional Kevlar fiber composite specimens to compressive loads and extracted the fibers in order to compare them to the fibers tested with the elastica loop method and the bending beam method (Dobbs:963). Keller embedded a bundle of polymer fibers in a clear matrix material and examined the compressed fiber using x-ray diffraction (11). Both of these studies examined kinkband formation.

Direct compression test. Polymer fibers were tested in direct compression using a modified Tecam MTM-8 Micro-Tensile testing machine (8). This work validated the procedures for using the MTM-8 to compression test polymer fibers. The machine compliance (error) was determined, as well as the moduli of elasticity and compressive strengths of different polymer fibers. Great care must be used when mounting the fiber into the MTM-8 in order to prevent any off-axis loading due to mis-alignment. The MTM-8 can apply compressive loads on a fiber and will be used in this study of the compressive characteristics of carbon fibers.

End effects. The stress distribution across the cross-section of a fiber is affected by the method of mounting in the testing machine. End effects cause a three dimensional stress field in the fiber that may cause the fiber to fail before its maximum compressive strength is reached. One method of estimating the fiber gage length required to avoid end effects is with the following equation:

$$\frac{L_f}{d} = \frac{E_t^{.5}}{G^{.5}} \qquad (7)$$

where

L_f = fiber gage length
d = fiber diameter
E_t = fiber tensile modulus
G = fiber shear modulus (8:8)

While this relation was developed with a polymer fiber, this equation should provide an estimate of the minimum gage length needed to avoid edge effects.

Summary

This chapter has provided a review of the materials engineering concepts pertinent to this study. The rule of mixtures for composites, carbon fibers, compression failure modes and the different compression test methods must be understood in order for the results of this study

to be understood. The next chapter presents the experimental methodology developed with these concepts.

III. Methodology

Introduction

Several different types of carbon fibers were tested with the MTM-8 in order to determine their compressive strengths. In addition to compressing the fibers, the MTM-8 measured the resulting deformations so that a stress-strain curve could be constructed. Three commonly used carbon fibers were tested, T300 fiber (a PAN fiber), P55 and P100 fibers (two pitch-based fibers). These fibers were obtained from Union Carbide Corporation. This chapter will discuss 1) fiber gage lengths, 2) test equipment, 3) test procedures and, 4) data analysis. Appendix A presents a detailed description of the MTM-8 and the procedures for its use. Appendix B lists the equipment used in this study, including the computers and the software.

Fiber Gage Length

Fiber gage length is determined by Euler Buckling and end effects criteria. Euler Buckling determines the upper bound of the gage length and end effects determine the lower bound of the gage length. The Euler buckling equation, equation (6) discussed in Chapter 2, and equation (5), also discussed in Chapter 2, were used to calculate the bounds for the gage

lengths. The table below lists the range of gage lengths for the fibers. The gage lengths are converted to metric units because the MTM-8 is calibrated for metric units. The upper bounds were calculated using the predicted compressive strengths of the fibers from the rule of mixtures for composites.

Table I Range of Gage Lengths for the Carbon Fibers

Fiber Type	Compressive Strength (ksi)	Tensile Modulus (Msi)	Shear Modulus (Msi)	Upper Bound (mm)	Lower Bound (mm)
T300	417	34	3.2	.07	.016
P100	70	100	*	.59	*
P55	123	55	*	.33	*

*Shear Modulus unavailable for the calculation

Test Equipment

The MTM-8 is an optical-mechanical device that can load a fiber in either tension or compression and measure the resulting displacement. Since the MTM-8 is mechanical, the usual sources of error associated with electronic equipment are not present. A detailed description of the MTM-8 and its operation is provided in Appendix A.

Fibers are placed in either tension or compression with the MTM-8 (see Figure 8) through a series of micrometers, torsion arms and levers. Rotating the load

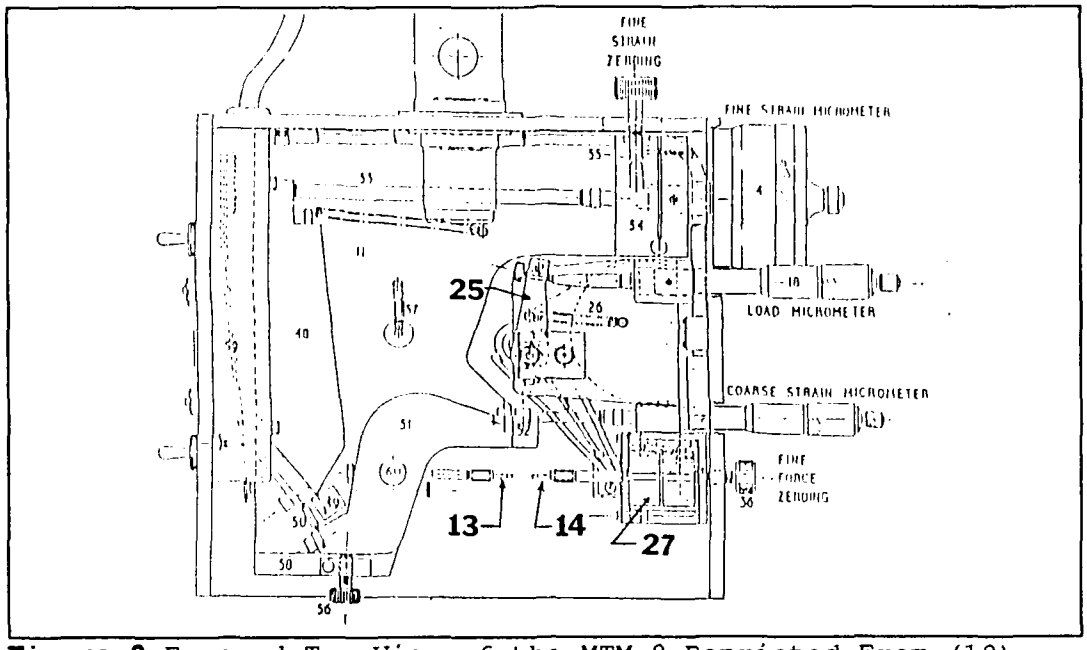

Figure 8 Exposed Top View of the MTM-8 Reprinted From (19)

micrometer, 18, loads the fiber by applying a moment to the torque arms, 26, through the lever, 25, which causes the left anvil, 13, to move towards or away from the right anvil, 14. The resulting deformation of the mounted fiber causes a mirror, 27, to move. When reviewed through the telescope, the mirror movement causes an image formed from the mirrors to split. The greater the deformation, the greater the image is split. (see Figure 9) . Re-aligning the images with the fine strain micrometer, 14, measures the displacement to hundreds of Angstroms. The load and displacement measurements can then be used to plot a stress-strain curve for the tested fiber.

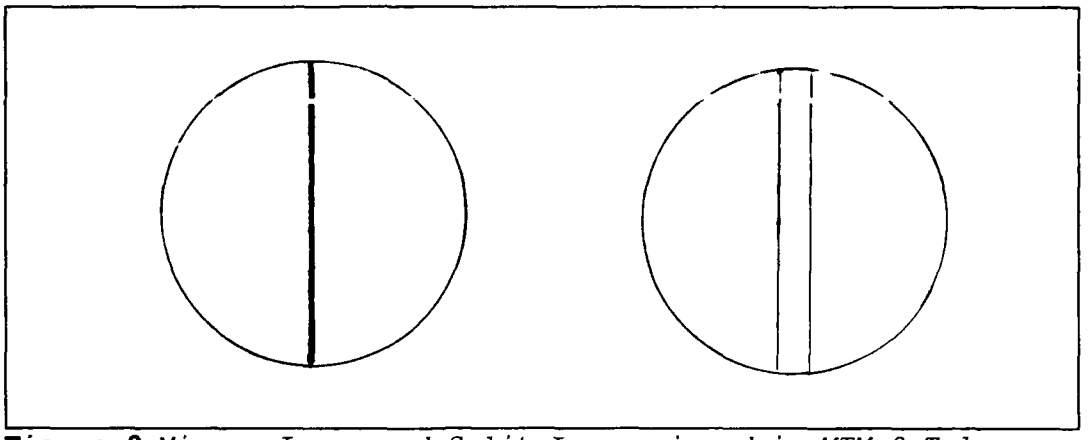

Figure 9 Mirror Image and Split Image viewed in MTM-8 Telescope

Test Procedures

Fibers were mounted in the MTM-8 by gluing the ends of the fibers to the anvils with 1,5 diphenylcarbazide, a thermoplastic glue. This glue was used because it could be melted and then quickly solidify at room temperature without affecting its material properties. The fiber was first glued to the right anvil and then to the left anvil.

Fiber alignment during the mounting process is of paramount importance to ensure pure axial loading of the fiber. Lateral alignment of the fiber was checked with the travelling microscope. The vertical alignment was checked with the focus of the traveling microscope. A fiber in focus is in the focal plane and, therefore, is vertically aligned. If the fiber was mis-aligned, then the glue on either anvil was melted and the left anvil, which has three dimensional adjustment capabilities, was adjusted. Once the

fiber was aligned, then the zero load point was set on the load micrometer. Next, the glue on the left anvil was remelted and the anvil was moved in towards the right anvil to set the desired gage length. Finally, the glue on each anvil was melted and re-hardened in order to minimize or eliminate any residual stresses that might be in the fiber embedded in the glue. Mounting and aligning the fibers was a painstaking process due to the frailty of the fibers. The entire testing process for one fiber would require up to 60 minutes. As experience was gained in the procedure the required time for the process was reduced to an average of 40 minutes.

Since the precision of the MTM-8 is assumed to be constant, the load increments were set at equal intervals to obtain good results for the resulting stress-strain curve (18:152). The load was incremented by 0.05 on the scale of the load micrometer, which equated to a load of 0.42 g. This load increment gave a noticeable image split and an average of 10 data points for the stress-strain curves.

Approximately 30 of each type of fiber were tested to failure so that the central limit theorem (CLT) could be invoked. The CLT states that if the sample size is large enough, then the sample mean is approximately normally

distributed (14:6). A detailed discussion of statistical analysis is provided in Appendix C.

The moduli determined from the stress-strain curves are not equal to the true fiber moduli because of the MTM-8's machine compliance (displacement). The relationship of the apparent modulus to the actual modulus is derived from Hooke's law and is expressed:

$$\frac{1}{E_a} = \frac{1}{E_c} + \frac{L_m}{\sigma_f} \cdot \frac{1}{L_f} \qquad (8)$$

where

E_a = apparent fiber modulus
E_c = corrected fiber modulus
L_f = fiber gage length
L_m = machine compliance
σ_f = fiber stress (8:22)

This relationship has been shown to hold for polymeric fibers tested in either tension or compression (8). The gage lengths for each set of fibers were varied between 0.27 and 0.11 mm in order to verify the applicability of equation 8 holds.

Data Analysis

The data of interest in this study is the failure compressive strength of the tested fibers and the compressive modulus of the fibers. As previously stated,

a minimum of 30 fibers were tested so that the CLT could be used in the statistical analysis of the fiber data. The following are the steps which were used to analyze the collected data:

1. A check to ascertain if the data can be considered to be a sample from a normally distributed population. The statistical analysis techniques used in this study assume the data is normally distributed.

2. An examination of the data for any bias such as researcher experience with the test equipment.

3. If the data can be assumed to be normally distributed, then the mean observed strength is the maximum likelihood estimator of the fiber compressive strength (5:231). The basic statistics of the data were calculated with the software package STATISTIX (15).

4. A calculation, using STATISTIX, of the unweighted least squares regression for $1/E_a = 1/L_f$ and the associated Fitness test and R^2 values. The F-test and R^2 values indicate how well the regression fits the observed data.

5. A plot of the fitted regression values verses the residual values to determine data variability and

nonlinearity if indicated by step 4 Fitness test results and R^2 values.

6. A recalculation of the least squares regression with transformed data or a weighting variable as indicated by step 5.

Chapter 4 presents the results of this statistical procedure. Appendix C presents a detailed summary of the theory underlying this analysis and presents all the steps used in the data analysis for all three fiber types.

IV. RESULTS AND DISCUSSION

Introduction

Three carbon fibers were tested in direct compression with the TECAM MTM-8. The T-300 fiber is a PAN carbon fiber with an average diameter of about 5 micrometers. The P55 and P100 fibers are pitch-based carbon fibers with average diameters of approximately 10 micrometers. The MTM-8 was used to plot a stress strain curve and to find the ultimate axial compressive strength of each fiber. An in-depth discussion of the statistical analysis is presented in Appendix C. Stress-strain curves for all the fibers tested and used in the analysis are presented in Appendices D, E and F.

T300 Fiber

The T300 fiber was the first fiber to be tested because its Euler Buckling gage length was the smallest of the three fibers. If the MTM-8 could successfully test this fiber, then it should be able to test the other fiber types with little difficulty.

Figure 10 Photograph of a T300 Fiber Buckling

A T300 fiber with a 0.6 mm gage length was compressed in the MTM-8, in order to test the assumption of Euler Buckling with clamped end conditions. The fiber buckled in the classic Euler buckling manner for clamped end conditions, as can be seen in Figure 10.

The maximum gage length predicted for the T300 fiber from the Euler buckling equation is 0.07 mm. The initial attempts at mounting fibers at this small gage length failed because the glue kept bridging the 0.07 mm gap. Fibers were then tested at a longer gage length, 0.11 mm, to further check the assumption of Euler buckling.

In all, 34 T300 fibers were tested to their breaking point. With the first 16 fibers, the mounting glue prematurely fractured thereby increasing the gage length of the fiber and allowing the fiber to fail at a much lower stress. Table II shows the results of these tests. A two tailed t-test was performed to verify if the mean strength of these tests, 103 ksi, was statistically different than the 173.33 ksi predicted by the Euler buckling equation. The test did confirm that the two strengths were statistically different.

Table II Statistics of Tests Using the Old Glue

DESCRIPTIVE STATISTICS (ksi)

VARIABLE	MEAN	S.D.	N	MEDIAN	MINIMUM	MAXIMUM
OLD GLUE	103.0	43.5	16	91.75	59.56	214.3

Several modifications in the experiment were implemented to investigate this mode of glue failure. The first modification was testing other types of fibers to check if this glue failure was specific to the T300 fiber. The second modification was to replace the year-old glue with new glue ordered from the manufacturer.

The next modification was the plotting of stress-strain curves to see if the curves were linear and that the MTM-8 was performing properly. In addition, the modulus could be found and the modulus-gage length relationship, verified for the polymer fibers, could be checked (8).

Four PBT as-spun fibers and four P100 fibers were tested in the MTM-8. Both diameters of the fiber types, approximately 20 micrometers and approximately 10 micrometers respectively, were significantly thicker than the T300 fiber diameter. No glue damage was observed before or after fiber failure for any of these fibers, therefore the glue failure appears to be associated with only the T300 fiber tested at higher compressive strengths.

Next, new 1,5 diphenylcarbazide glue replaced the year-old 1,5 diphenylcarbazide glue that had been previously used. A two sample t-test was (see Table III) used to compare the mean compressive strength of the 16 fibers mounted with the old glue to the mean strength of the 10 fibers mounted with the new glue. Both sets of fibers had a gage length of 0.11 mm. STATISTIX automatically performs the test twice - first, assuming

Table III Two Sample T-Test For Old Glue Use vs. New Glue Use

TWO SAMPLE T TESTS FOR OLD GLUE VS NEW GLUE

VARIABLE	MEAN STRENGTH	SAMPLE SIZE	S.D.	S.E.
OLD	103.0 ksi	16	43.50	10.87
NEW	178.4 ksi	10	30.32	9.589

	T	DF	P
EQUAL VARIANCES	-4.79	24	0.0001
UNEQUAL VARIANCES	-5.20	23.6	0.0000

	F	NUM DF	DEN DF	P
TESTS FOR EQUALITY OF VARIANCES	2.06	15	9	0.1379

CASES INCLUDED 26

the two samples have equal variances and then assuming they have unequal variances. A test for equality of variance is also performed so the appropriate test results can be used. The test (see Table III) indicates that the means are from two different populations with equal variances and therefore, the old glue data can be omitted from any further statistical analysis. The tests with the new glue resulted in a higher mean failure strength (see Table IV for the basic statistics) that was much closer to the predicted strength Euler buckling

stress.. The mean strength of 178.4 ksi differed from the predicted buckling stres of 173.3 ksi by only 2.9%.

Table IV T300 Compressive Strength (ksi) Results

DESCRIPTIVE STATISTICS (ksi)

VARIABLE	MEAN	S.D.	N	MEDIAN	MINIMUM	MAXIMUM
NEW	178.4	30.3	10	179.8	137.8	240.4

A two tailed t-test was performed, and the test indicated that the observed strength and the predicted strengths can be considered equal. This result is another confirmation of the assumption of clamped end conditions.

The stress-strain curves (see Figures 11 and 12) for both the old glue and the new glue were linear, indicating that the MTM-8 was operating properly and that the fibers were behaving elastically prior to the point of buckling.

In one instance of testing a fiber with the new glue, the glue failed and the fiber buckled but did not break. The compressive loading was then reduced and the fiber was then placed under a tensile load until failure

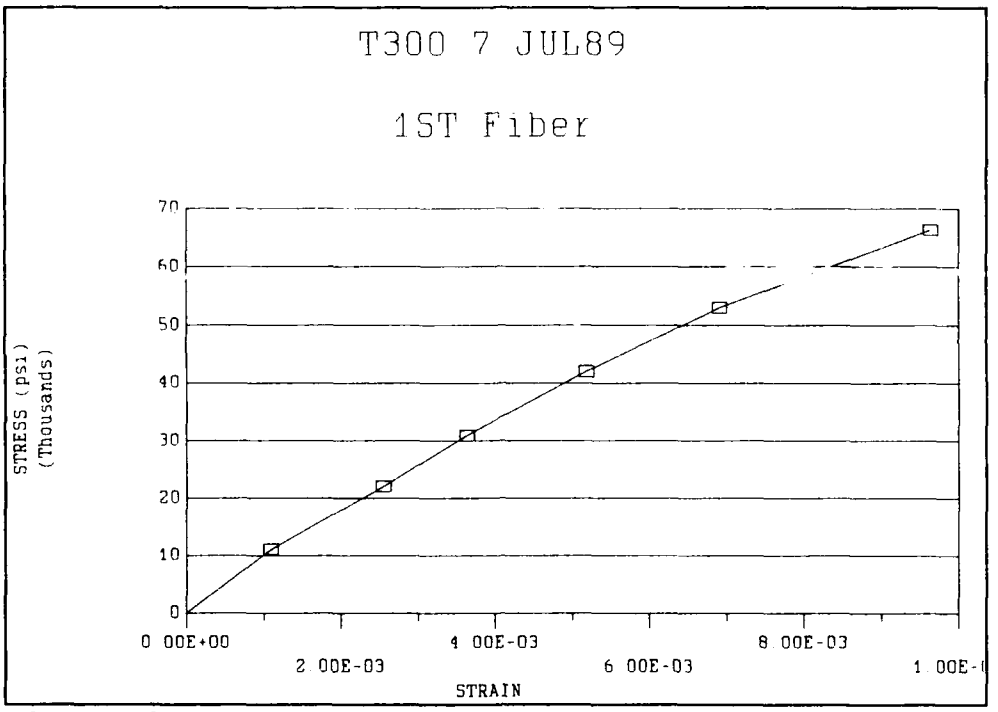

Figure 11 Compressive Stress-Strain Curve for T300 Fiber Mounted With the Old Glue

(see Figure 13). This stress strain curve graphically illustrates the fiber buckling with the change in slope of the curve between the last two points on the compressive loading portion. The graph also shows that the measured compressive modulus and the measured tensile modulus are the same. A paired t-test performed with data from additional fibers, also tested tension to compression, showed that the tensile and compressive moduli are the same. Finally, a least-squares regression

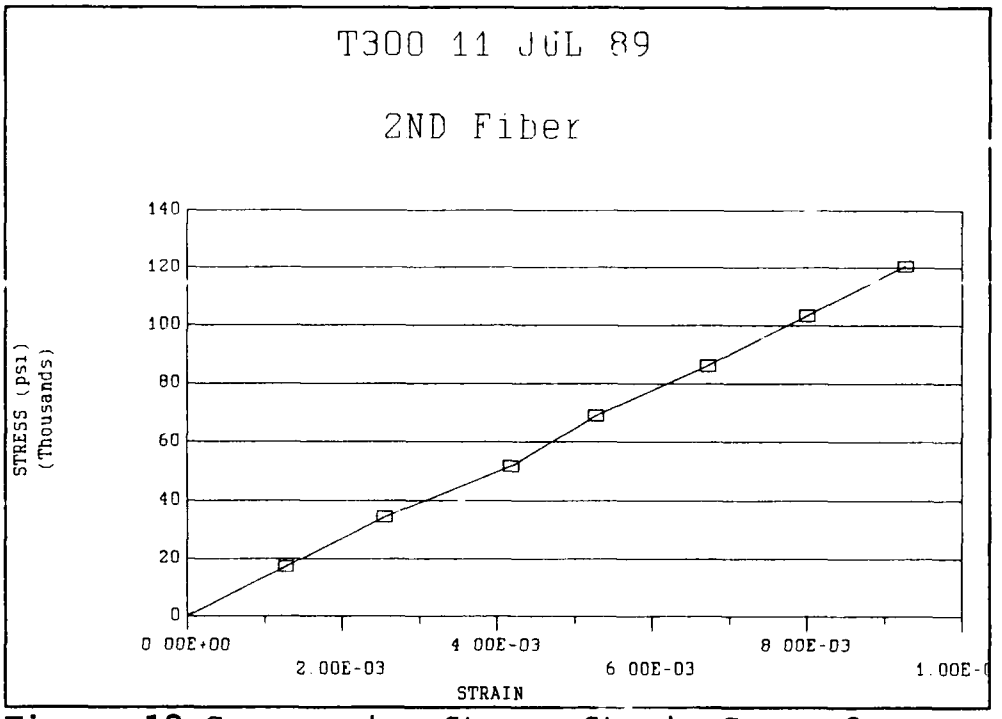

Figure 12 Compressive Stress-Strain Curve for T300 Fiber Mounted With the New Glue

analysis was performed on all the fibers mounted with the new glue to check if the inverse of the measured modulus/inverse gage length relationship found during the polymer fiber testing still held true for the T300 fiber. Since a least-squares regression assumes the data being analyzed is from a normally distributed population, STATISIX was used to calculate a Wilk-Shapiro number for the modulus data, which is a measure of the normality of a given set of data. The number calculated (.9398) strongly indicates that the modulus data is normally

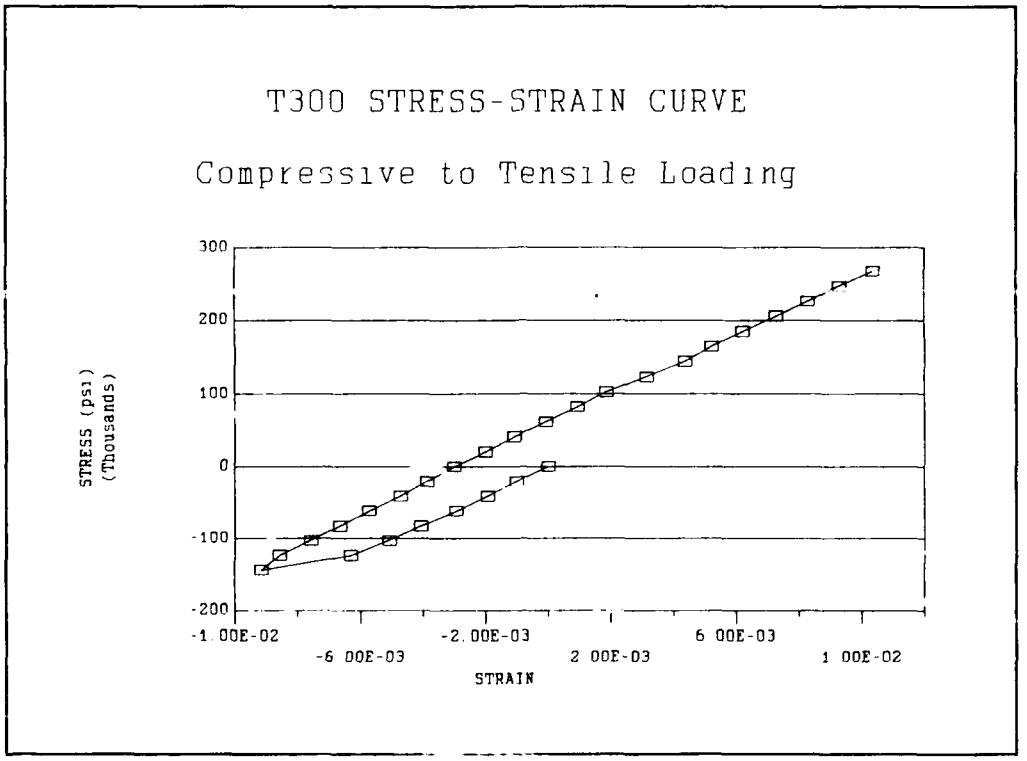

Figure 13 A T300 Fiber Loaded In Compression and then Tension

distributed thereby satisfying the normality assumption required for a least squares analysis. The results of the weighted least squared analysis are listed in Table V.

The regression results show a definite relationship between the inverse of the apparent modulus and the inverse of the gage length. However, the regression also shows that the intercept should be zero because of the large amount of variation in the apparent modulus for the 0.11 mm gage length. The small R^2 value indicates that

Table V Weighted Least Squares Analysis For T300 Data

WEIGHTED LEAST SQUARES LINEAR REGRESSION OF $1/E_a$

WEIGHTING VARIABLE: L_f^2

PREDICTOR VARIABLES	COEFFICIENT	STD ERROR	STUDENT'S T	PVALUE
CONSTANT	8.6038E-03	3.1671E-02	0.27	0.7894
$1/L_f$	6.2625E-03	3.7854E-03	1.65	0.1175

CASES INCLUDED	18		
DEGREES OF FREEDOM	16		
OVERALL F	2.737	P VALUE	0.1175

ADJUSTED R SQUARED	0.0927
R SQUARED	0.1461
RESID. MEAN SQUARE	2.736E-06

the regression does not account for much of the variation in the data. Figure 14 shows the amount of variation in the observed data as well as the fitted regression line. The probable causes for this variation include:

1) Machine error
2) Weak glue-fiber bonding
3) Weak glue-anvil bonding
4) Gage length measurement errors

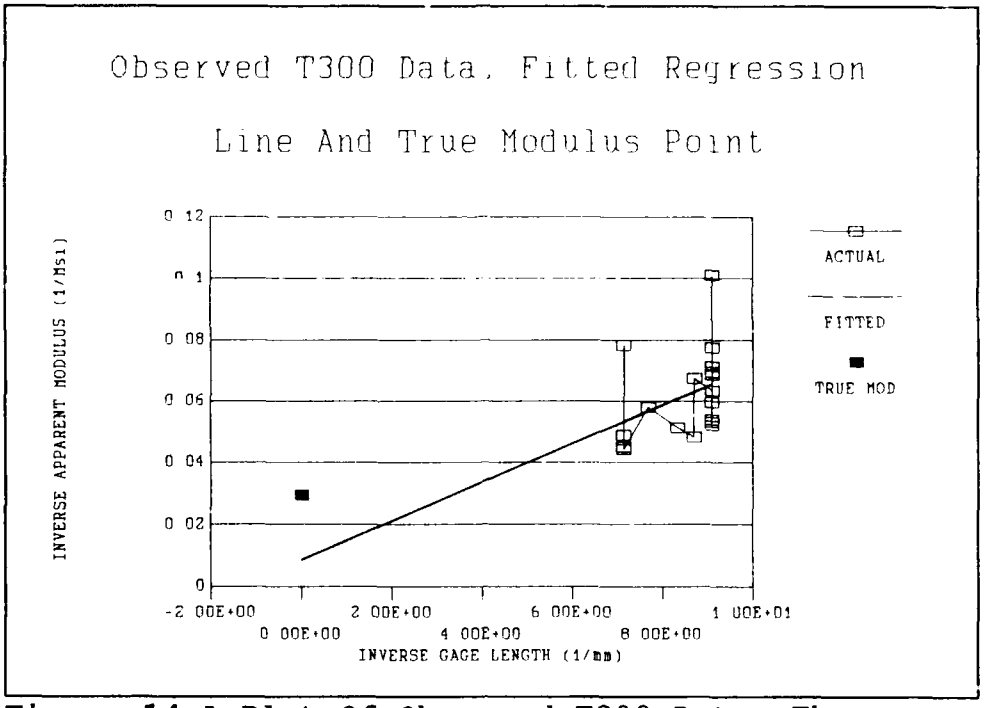

Figure 14 A Plot Of Observed T300 Data, The Fitted Regression Line and The True Modulus Point

After gaining several months experience mounting fibers, five T300 fibers were successfully mounted at a gage length of .065 mm for testing in the MTM-8. Table VI lists the results of the testing. The fibers failed at an average of 200 ksi which is far below the 400 ksi predicted by the rule of mixtures from composite data. Glue damage was observed in every case after the fiber failure. The glue could not hold the fibers and prevent the fibers from buckling. Figure 15 is a stress-strain

Table VI Results of Tests on T300 With .065 mm Gage Length

DESCRIPTIVE STATISTICS (ksi)

VARIABLE	MEAN	S.D.	N	MEDIAN	MINIMUM	MAXIMUM
Strength	200.1	27.84	5	206.0	161.9	235.4

curve of one of the fibers. The curve changes slope at a load of approximately 200 ksi indicating that excessive deformation occurred before the fiber failure.

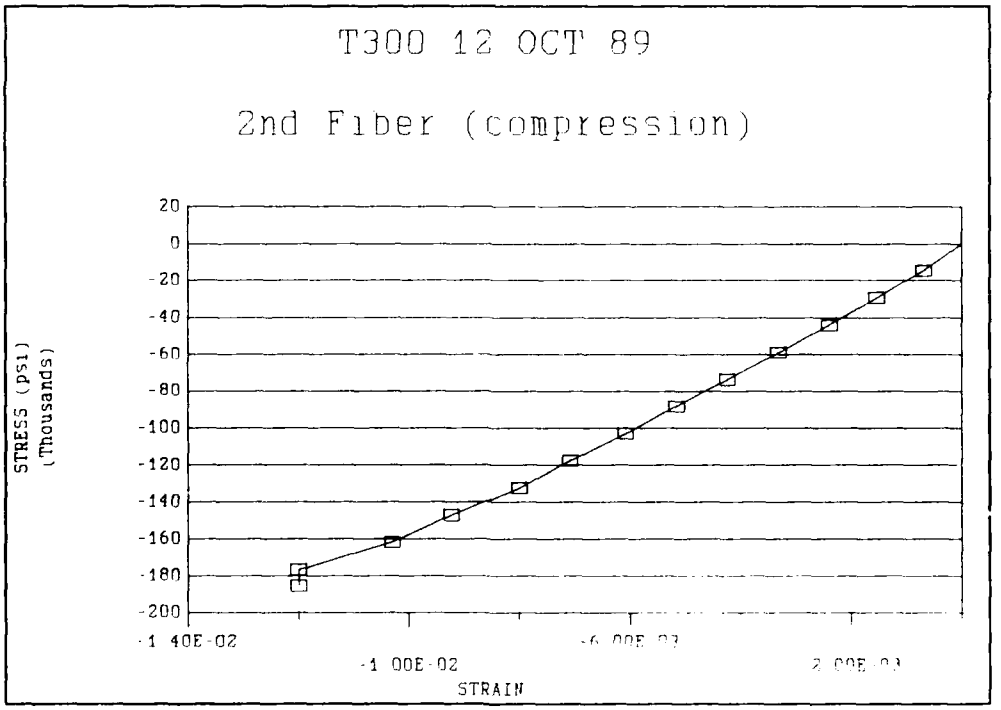

Figure 15 Stress-Strain Curve For T300 Fiber Showing Glue Failure

P100 Fiber

A total of 35 P100 fibers were tested in the MTM-8. No glue damage was observed before or after any fiber failure. The data from the first 13 fibers were not used because of a bias caused by researcher experience with mounting the fiber. The strength of the fibers showed an upward trend when plotted in order of testing. Appendix C contains the details of the statistics. As a result, the data from these first fibers was not used in the subsequent analysis.

Table VII shows the results of the fiber testing. The

Table VII Results of P100 Testing

DESCRIPTIVE STATISTICS (ksi)

VARIABLE	MEAN	S.D.	N	MEDIAN	MINIMUM	MAXIMUM
Strength	115.9	31.7	22	111.9	55.93	185.0

average strength of 115.9 ksi which is much higher than the 70 ksi predicted from the rule of mixtures. A two

tailed t-test indicated that the observed strength and the predicted strength can be considered as unequal.

Figure 16 is an example of a typical stress-strain curve for the P100 data. The curve is linear, indicating

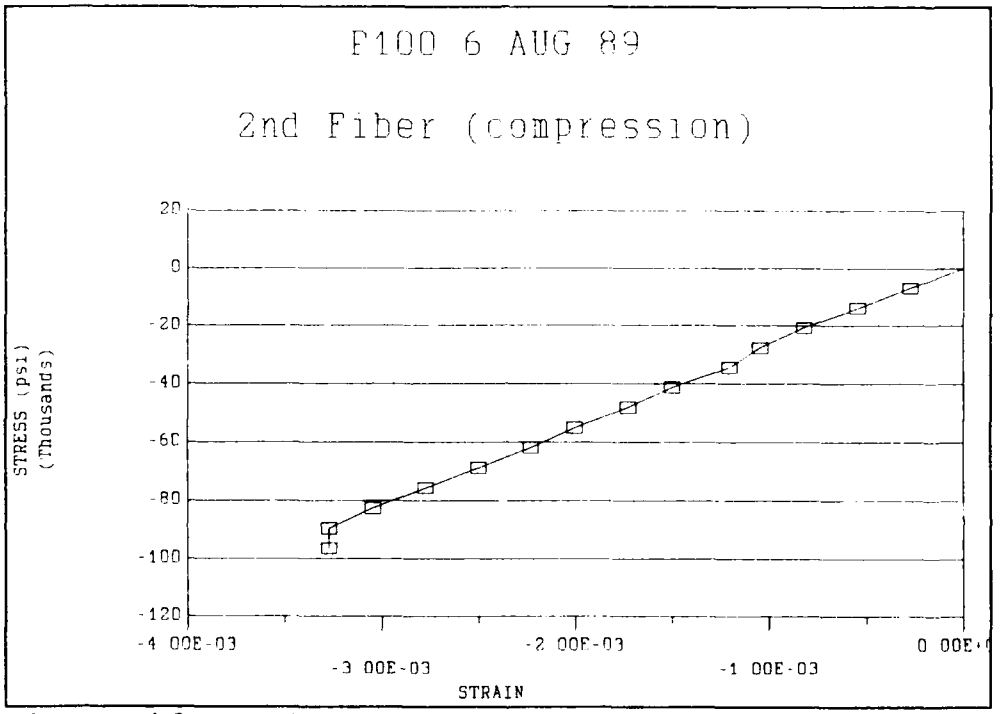

Figure 16 A P100 Stress-Strain Curve

that the fiber behaved elastically until failure. Figure 17 shows a stress-strain curve for a fiber loaded from tension into compression. A paired t-test indicates the apparent compressive and tensile moduli are the same, as is predicted by continuum mechanics.

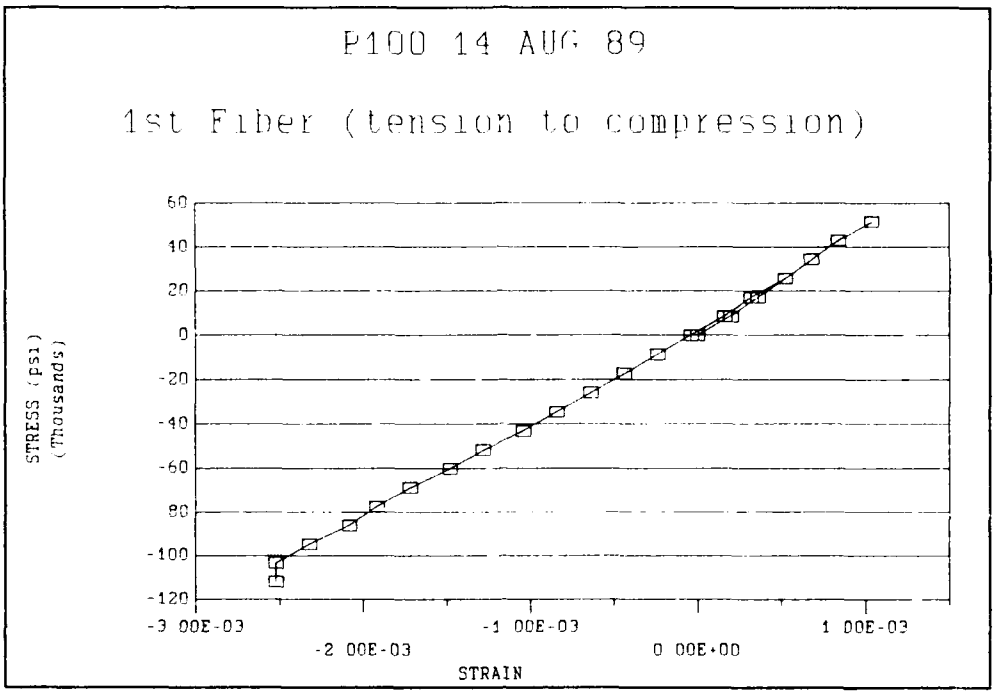

Figure 17 A Stress-Strain Curve of a P100 Fiber Loaded Tension to Compression

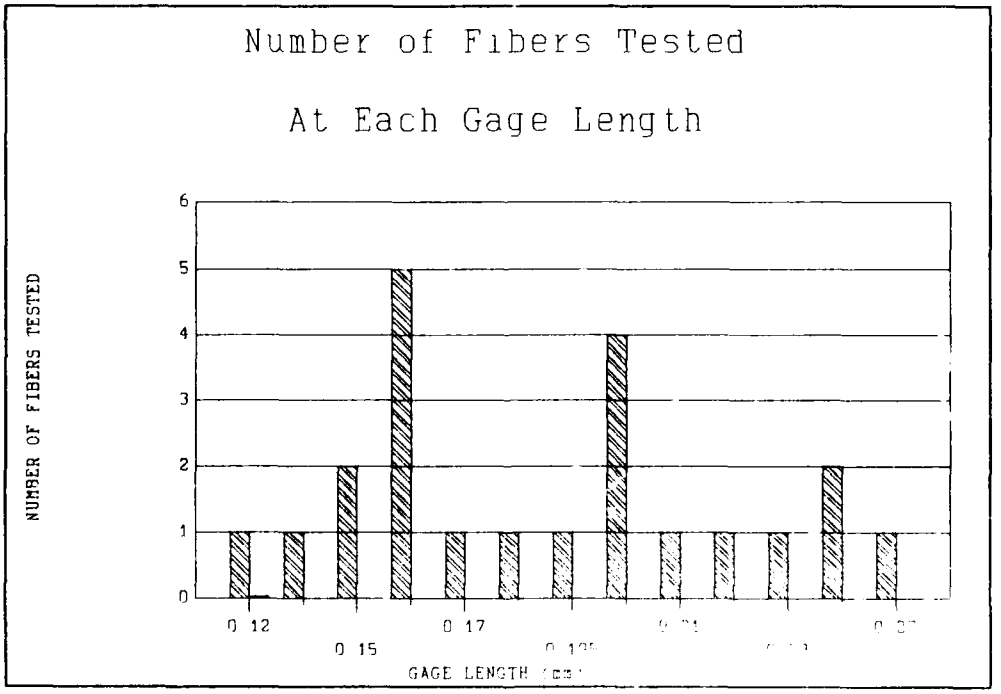

Figure 18 A Plot of The Number of Fibers Tested At Different Gage Lengths

The maximum gage length predicted for the P100 fiber by the Euler buckling criteria is 0.59 mm. The gage lengths of the P100 fibers were systematically varied between 0.11 mm and 0.27 mm to facilitate the calculation of a least squares analysis relating the inverse of the apparent modulus to the inverse of the gage length.

Table VIII shows the results of the weighted least squares regression analysis. The results show that this

Table VIII The Results of the Weighted Least Squares Regression of the P100 Data

WEIGHTED LEAST SQUARES LINEAR REGRESSION OF $1/E$ TO $1/L_f$

WEIGHTING VARIABLE: L_f^2

PREDICTOR VARIABLES	COEFFICIENT	STD ERROR	STUDENT'S T	P
CONSTANT	1.5794E-02	7.7448E-03	2.04	.0549
$1/L_f$	3.5060E-03	1.4891E-03	2.35	.0289

CASES INCLUDED	22		
DEGREES OF FREEDOM	20		
OVERALL F	5.543	P VALUE	0.0289
ADJUSTED R SQUARED	0.1779		
R SQUARED	0.2170		
RESID. MEAN SQUARE	1.942E-06		

relationship holds for the P100 fiber. However, the small R^2 value indicates that the model does not account

for the large amount of variation in the observed data. The intercept point equates to 63 Msi which is much smaller than the actual modulus of 100 Msi. This difference is due to the large variation in the observed data (see Figure 19), which caused the intercept point to deviate from the expected value. The plot of the actual data and the regression function clearly illustrates the large amount of variation in the observed data. The

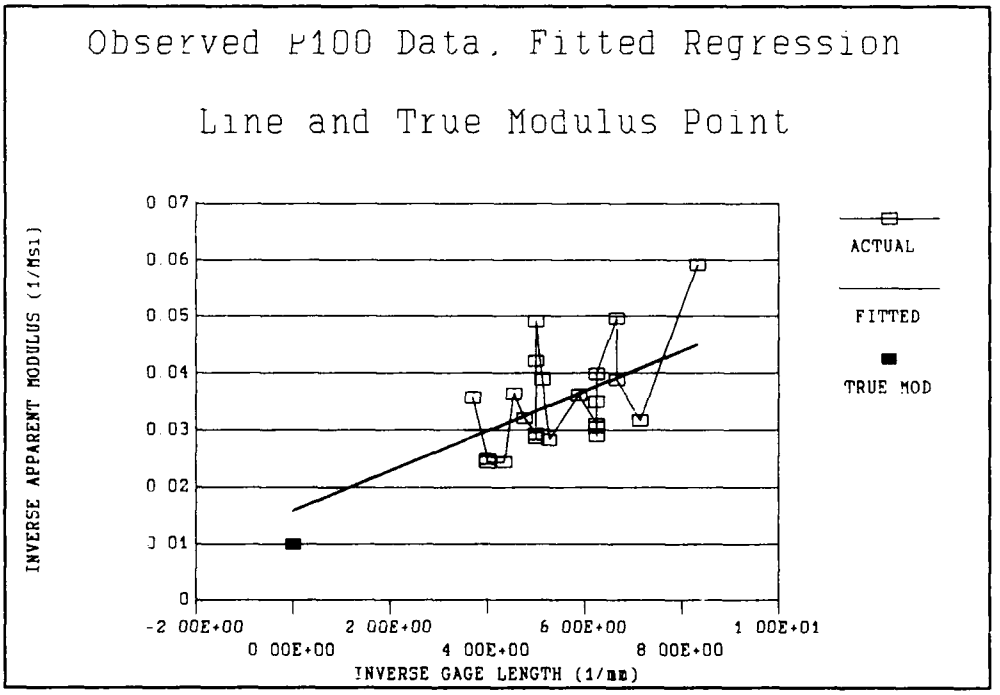

Figure 19 A Plot of The Obeserved Data, The Regression Line And The True Modulus Point

probable causes for this variation are the same as those listed for the T300 fiber:

1) Machine error
2) Weak glue-fiber bonding
3) Weak glue-anvil bonding
4) Gage length measurement errors

The variation shown in Figure 19 appears to decrease as the gage length increases. This decrease could be attributed to the fact that the percentage of strain error decreases (for a given amount of gage length measurement error) as the gage length increases.

P55 Fiber

A total of 30 P55 fibers were tested in the MTM-8. All the data collected was usable due to the fact that no bias was detected in the data.

Table IX shows the basic results of this testing. The average observed strength is 112.3 ksi which is lower than the 123 ksi predicted from the rule of mixtures. While the difference between the strengths is only 8.9%, a two tailed t-test indicates that this difference is statistically significant and therefore the strengths cannot be considered equal. This test assumes the variation associated with the 123 ksi is zero, which is

not true. However, this t-test was used in place of the two sample t-test because the information required for the two sample t-test was unavailable.

Table IX The Results of The P55 Testing

DESCRIPTIVE STATISTICS (ksi)

VARIABLE	MEAN	S.D.	N	MEDIAN	MINIMUM	MAXIMUM
Strength	112.3	15.44	30	112.7	82.70	141.0

The stress-strain curves for the P55 fibers are linear, indicating that the fibers behaved elastically up to the point of failure. Figure 20 is a typical stress-strain curve for the P55 fibers. Fibers were also tested in both tension and compression to check if the apparent tensile and compressive moduli are the same. Figure 21 shows that the tensile and compressive moduli are the same.

The maximum gage length predicted by the Euler buckling criteria is 0.33 mm. The gage lengths of the fibers were varied between 0.11 mm and 0.25 mm (refer to Figure 22) to facilitate a weighted least squares

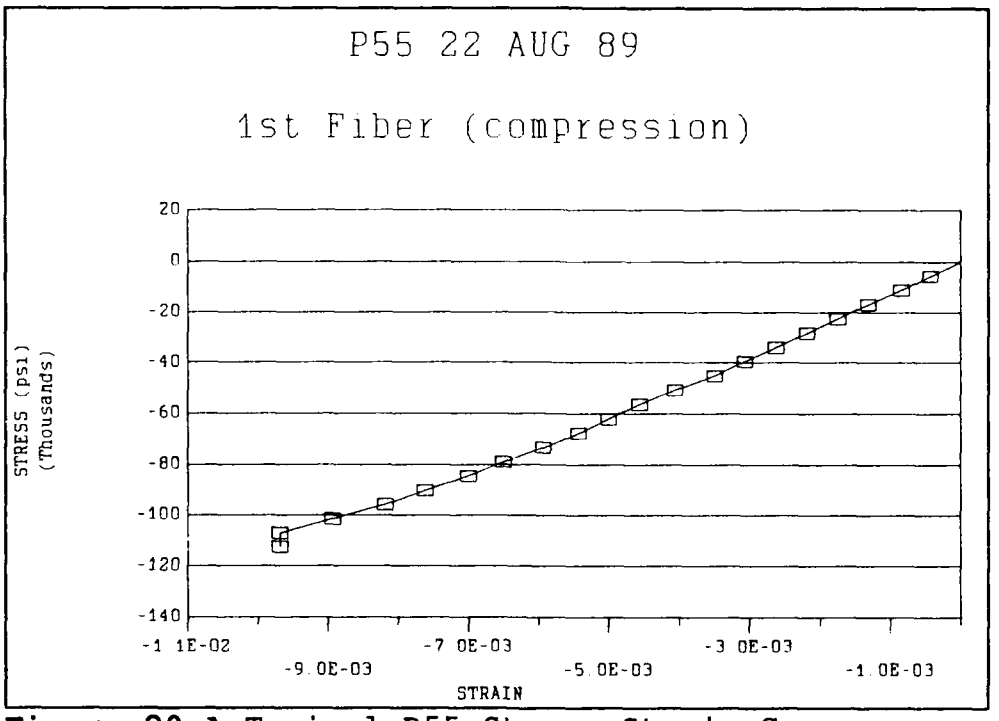

Figure 20 A Typical P55 Stress-Strain Curve

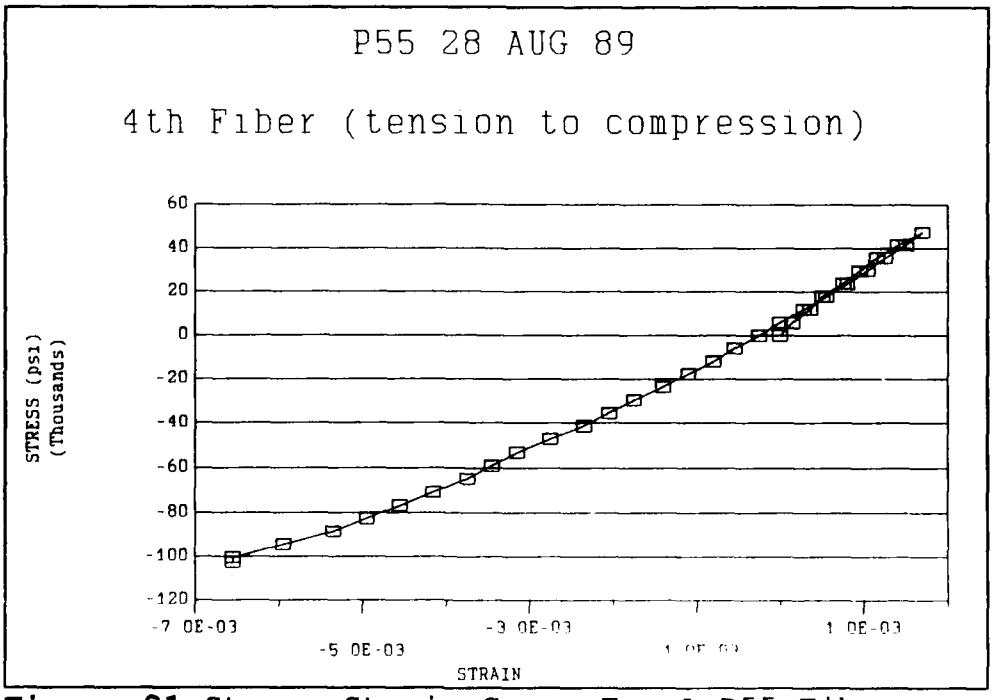

Figure 21 Stress-Strain Curve For A P55 Fiber Loaded In Tension And Compression

analysis of the inverse modulus - inverse gage length. The regression was performed to check if Equation 8

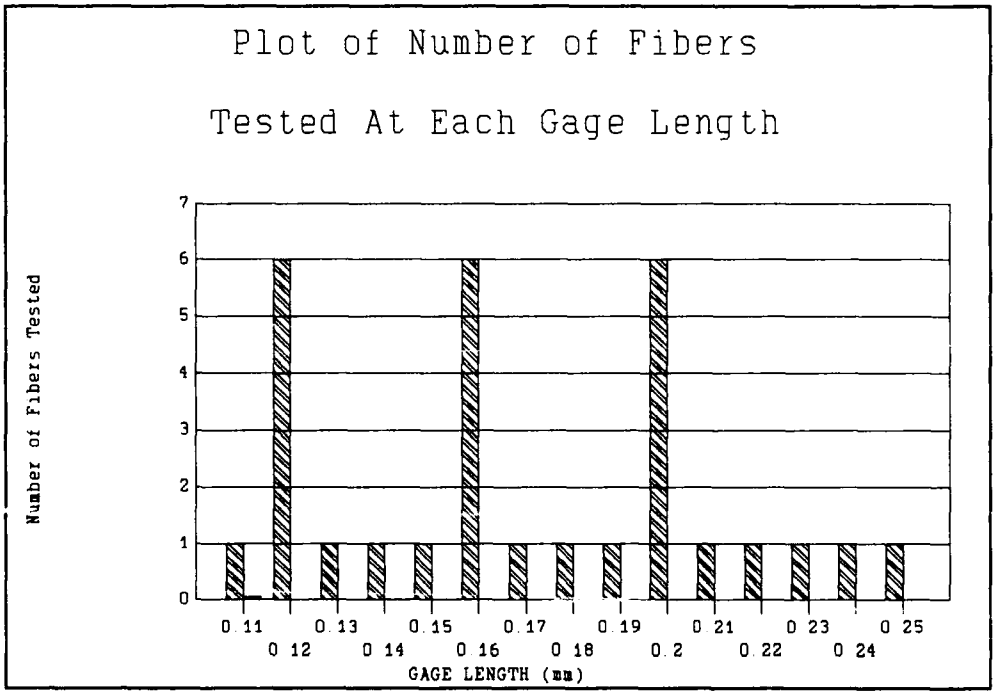

Figure 22 A Plot of the Number of Fibers Tested At Different Gage Lengths

holds for the P55 fiber (see Table X). The regression shows a strong relationship between 1/E and $1/L_f$, however the analysis indicates that the y intercept value should be zero. While the regression fits the data well, as indicated by the F-test value, the relatively small R^2 values indicate that the regression does not account for all the variability in the observed data. This variability is what affects the intercept value, which

should equal 55 Msi. Figure 23 illustrates the variability of the observed data. Again the probable sources of this

Table X The Results Of The Weighted Least Squares Regression Of The P55 Data

WEIGHTED LEAST SQUARES LINEAR REGRESSION OF $1/E_a$

WEIGHTING VARIABLE: L_f^2

PREDICTOR VARIABLES	COEFFICIENT	STD ERROR	STUDENT'S T	P
CONSTANT	-3.3555E-04	6.3008E-03	-0.05	.958
$1/L_f$	1.0375E-02	1.0998E-03	9.43	0.000

CASES INCLUDED	30		
DEGREES OF FREEDOM	28		
OVERALL F	89.00	P VALUE	0.0000
ADJUSTED R SQUARED	0.7521		
R SQUARED	0.7607		
RESID. MEAN SQUARE	1.866E-06		

variation are the same as for the other 2 fibers. However, of all the fibers, the P55 data most clearly shows the variability decreasing with increasing gage length.

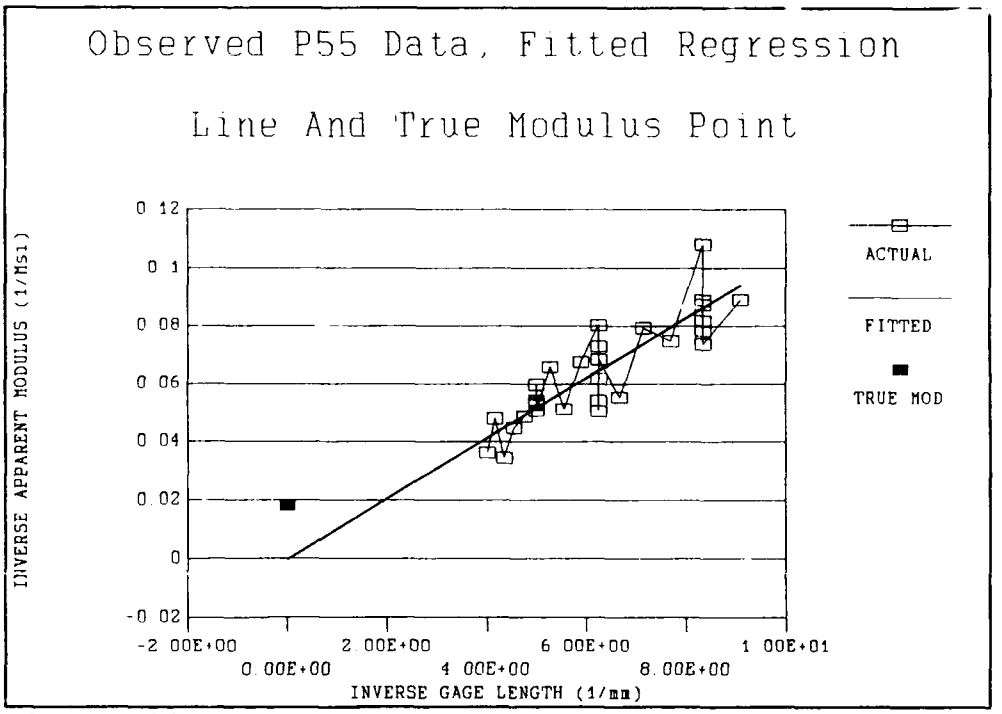

Figure 23 A Plot of The Observed P55 Data, The Regression Line And The True Modulus Point

Summary

Three types of fibers were tested in direct compression with the MTM-8 - the T300, P100 and, P55 fibers. The data variablity observed for all three types of fibers prevented the calculation of the true fiber modulus. The T300 data confirmed the assumption of Euler buckling with clamped (non-rotating) end conditions. The observed P100 strength of 115.9 ksi was much greater than the 70 ksi predicted by the rule of mixtures with P100 composite test data. The P55 observed strength of 112.9

ksi was 8.9% lower than the strength predicted by the rule of mixtures. The apparent tensile and compressive modulus were shown to be the same for all three fiber types. The next chapter will compare how well the results of the different compressive test methods compare to the results predicted from the rule of mixtures for composites.

V. A Comparison of The Fiber Compression Test Methods

Introduction

This chapter will examine how well the observed strengths from the different test methods can be related to the strengths predicted from the rule of mixtures. The different test methods examined are as follows: 1) recoil test; 2) direct compression test; 3) bending test; 4) elastica loop test and; 5) fiber in resin test. The observed strengths were related to the predicted strengths using the least squares regression technique in order to find a linear relationship. Appendix G contains the graphical results of the regression analysis.

Statistical Analysis

The observed strengths from each test method, listed in Table XI, were related to the corresponding predicted strengths by using least squares regression. The following procedure was used for each test method:

1) A check to ascertain if the data can be considered a sample from a normally distributed population

2) A calculation of the unweighted least squares regression and the associated Fitness test and R^2 values for $1/E_a = 1/L_f$

Table XI. A List Of The Predicted And Observed Compressive Strengths (21:4)

LIST OF CPMPRESSIVE STRENGTHS (ksi)

FIBER TYPE	PRED°	RECOIL TEST	DIRECT TEST	BEND TEST	LOOP TEST	RESIN/ FIBER
PBT	38.0	40.0	*	65.0	99.0	40.0
PBT	60.0	40.0	*	75.0	99.0	61.0
PBT	49.0	39.0	*	39.0	*	*
PBT	45.0	40.0	*	44.0	57.0	*
PBT	45.0	60.0	*	*	*	*
PBO	29.0	29.0	43.0	40.0	99.0	*
KEV29	58.0	51.0	30.0	86.0	73.0	63.0
KEV29	68.0	51.0	30.0	86.0	73.0	63.0
KEV49	57.0	53.0	37.0	108.0	107.0	123.0
KEV49	70.0	53.0	47.0	108.0	107.0	123.0
AMP2	33.0	26.0	*	*	*	*
CELL	25.0	25.0	*	*	*	*
T40	400.0	230.0	*	*	*	*
T50	233.0	84.0	*	594.0	*	*
T300	417.0	200.0	*	*	*	*
T300	417.0	189.0	*	*	*	*
AS4	387.0	204.0	*	*	*	1020.0
AS4	390.0	209.0	*	*	*	*
GY70	153.0	60.0	*	*	*	*
P25	167.0	127.0	*	*	*	*
P55	123.0	95.0	112.3[@]	*	*	*
P55	123.0	58.0	*	*	*	*
P75	95.0	81.0	*	390.0	*	62.0
P100	70.0	*	115.9[@]	*	*	*

* DATA NOT AVAILABLE
° DATA FROM RULE OF MIXTURES
@ DATA FROM THIS STUDY

3) A plot of the fitted regression values verses the the residual values to determine data variability and nonlinearity if indicated by step 2 results

4) A recalculation of the least squates regresion with transformed data or a weighting variable as indicated by step 3.

5) A comparison of the regressions for each test method to determine which method "best" fits the predicted strengths.

A plot of the predicted strengths (see Fig. 24) indicates that the fiber population could be separated into two different populations based on fiber types -

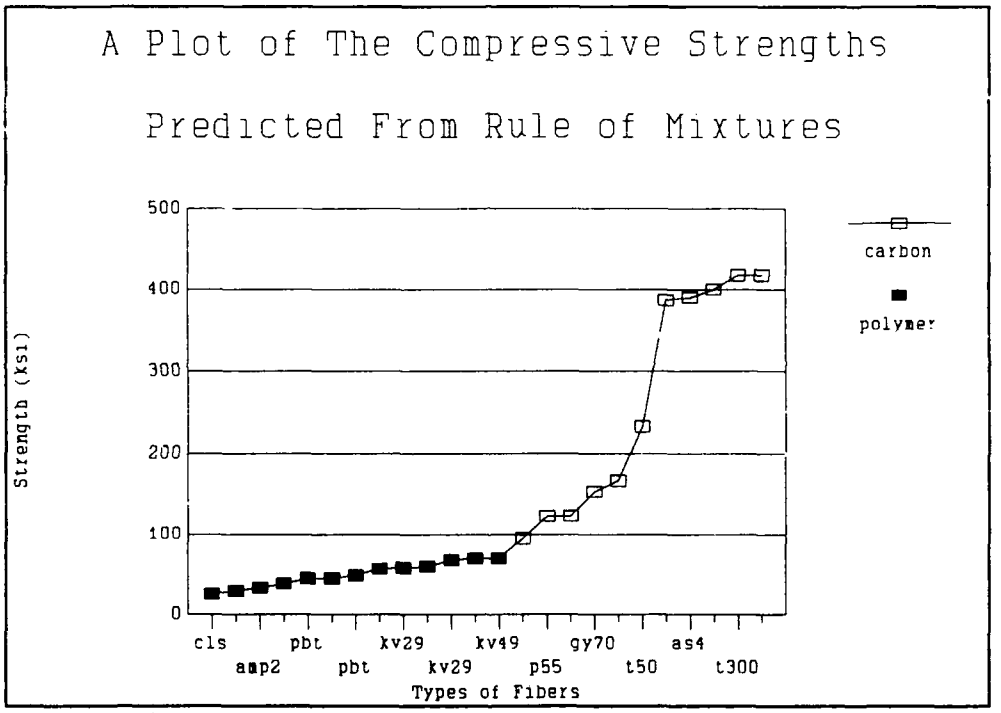

Figure 24. A Plot of The Predicted Compressive Strengths From Rule of Mixtures (21)

polymeric fibers and carbon fibers. Therefore, analysis was performed treating the fiber strength as a single population and as two distinct populations based on fiber type.

A Single Fiber Population

An anlysis of the test methods, regarding the fibers as a single population, was performed because a function relating the observed strengths to the predicted strengths from rule of mixtures of composites regardless of fiber type would be useful to researchers. The first step in the analysis was to determine if the data is normally distributed. A Rankits plot of the predicted data yielded a Wilk-Shapiro number of 0.774. The closer the Wilk-Shapiro number is to 1.0, the stronger the assumption of normality. A value of .774 indicates that the assumption of normality is a valid assumption. Table XII lists the results of unweighted least squares regression for each test method.

All the test methods show excellent overall fitness test (F-test) values and the high R^2 values indicate that the regressions account for a high percentage of the variability in the observed data. The direct test method regression has the closest one-to-one correspondence of the observed strengths with the predicted strengths.

Table XII. The Results of The Unweighted Least Squares Analysis

TEST METHOD	WILKES-SHAPIRO	SAMPLE SIZE	SLOPE	F-TEST NUMBER (P-VALUE)	ADJUSTED R^2
RECOIL	.7965	23	1.8297	536 (.0001)	.9588
DIRECT	.92	7	0.9724	34.03 (.0011)	.8251
BEND	.9269	9	0.68971	165 (.0000)	.9480
LOOP	.8486	8	0.57282	65.46 (.0001)	.8896
RESIN/ FIBER	.7783	8	0.39473	113 (.0000)	.9334

Polymeric Fiber Population

The fiber data was broken into two populations based on fiber type. The Wilk-Shapiro number for the predicted polymeric fiber strengths is .9746 which strongly supports the assumption of normality for this data. Table XIII shows the results of the regression for the polymeric fiber strengths.

Overall, the results of the regressions for the polymeric fibers did not show a dramitic change from the single fiber population regressions. The recoil regression values improved over the recoil regression values of the single fiber population. The slope changed

Table XIII. The Results of The Unweighted Least Squares Analysis For Polymeric Fibers

TEST METHOD	WILKES-SHAPIRO	SAMPLE SIZE	SLOPE	F-TEST NUMBER (P-VALUE)	ADJUSTED R^2
RECOIL	.9352	12	1.1280	299 (.0000)	.9613
DIRECT	.9213	5	1.4426	31.06 (.0051)	.8574
BEND	.9269	9	0.68971	165 (.0000)	.9480
LOOP	.8486	8	0.57282	65.46 (.0001)	.8896
RESIN/ FIBER	.8195	6	0.66041	43.11 (.0000)	.8753

from 1.8297 to 1.128 which is much closer to a one-to-one correspondance. The direct regression slope changed from .9724 to 1.4426. All the results still showed good F-test and R^2 values.

Carbon Fiber Population

The recoil test method was the only method that contained enough data points for a regression analysis of the carbon fibers data. The direct, bend and resin-fiber tests only contained two data points each, which is insufficient to perform a regression analysis and be able to infer any information about the results because a

normality check cannot be performed on the data. The results of the analysis are shown in Table XIV.

Table XIV. The Results of The Unweighted Least Squares Analysis For Carbon Fibers

TEST METHOD	WILKES-SHAPIRO	SAMPLE SIZE	SLOPE	F-TEST NUMBER (P-VALUE)	ADJUSTED R^2
RECOIL	.8894	11	1.8915	364.5 (.0000)	.9706

Again, the the recoil test regression values show an improvement over the single fiber population regression values. Appendix G contains plots showing the results of all the regression analysis.

Summary

All the test methods' results can be related to the predicted strengths with least-squares regression. The recoil test regressions showed the "best" fit, especially when the fiber data was split into two groups based on fiber type. However, discretion must be used intrepreting the results of these regressions. The recoil test data contained more data points than any of the other test methods. Additionally, the recoil, bend,

and loop tests are difficult to perform with high modulus (high stiffness) fibers. The results presented here do indicate that the predicted values from rule of mixtures can be related to the observed strengths from all the test methods.

VI. CONCLUSIONS AND RECOMMENDATIONS

Conclusions

The conclusions drawn from this study can be divided into two categories. The first category concerns the viability of the MTM-8 as a means of determining the compressive strength of composite fibers. The second concerns how the MTM-8 could be used to expand the knowledge base of composite compressive behavior.

The following are the conclusions concerning the viability of the MTM-8:

1. The T300 data supports the assumption of Euler Buckling with clamped end conditions for the experimental set-up used.

2. The apparent modulus varied for any given gage length for all three fiber types. In all three fiber types, this variation increased as the gage length decreased. This data variation renders the inverse apparent modulus - inverse gage length relationship inadeguate as a means of determining the true modulus because the variation causes the y-intercept to be different than the inverse of the true modulus. The causes for this variation include machine compliance,

poor glue bonding to either the fiber or the anvil and, gage length measurement error.

3. The MTM-8 can be used to show that the apparent tensile and compressive moduli for gage lengths below 0.2 mm are the same. Therefore, the true tensile modulus may be substituted for the true compressive modulus in any subsequent numerical analysis.

4. The MTM-8 is a viable means of testing in direct compression fibers with diameters as small as approximately 10 micrometers. The results of this testing relate almost one-to-one with the strengths predicted by rule of mixtures, according to a least-squares analysis.

The following are conclusions concerning the fiber data collected in this study.

1. The compressive strength of the T300 fiber cannot be measured with the current set-up of the MTM-8 because the thermoplastic glue cannot hold the fiber. The reasons for the glue failure could be poor glue-fiber bonding, poor glue-anvil bonding, and the small diameter of the fiber acting as a stress concentration in the glue.

2. The compressive strength of the P100 fiber was found to be 115.9 ksi, which is larger than the 70 ksi predicted from the rule of mixtures.

3. The compressive strength of the P55 fiber was found to be 112.3, which is smaller than the 123 ksi predicted by the rule of mixtures.

4. The carbon and polymeric fiber strengths determined by the MTM-8 can be related to the predicted fiber strengths with a least squares regression. Although all the different test methods can be related to the predicted strengths from the rule of mixtures for composites, the MTM-8 data is the data that most closely relates to the rule of mixtures data one-to-one.

Recommendations

The recommendations are also split into two categories. The first category addresses improvements in the MTM-8. The second addresses experimental methodologies for determining an empirical relationship between fiber strength and composite strength.

The following are the recommendations for improving the MTM-8.

1. Change the fiber mounting technique so that small diameter fibers, such as the T300 fiber, can be tested. The mounting glue could be changed or possibly some other mechanical clamping device could be devised.

2. Improve the optics on the MTM-8 so that magnifications of greater than 100X can be achieved. The current 100X magnification is not large enough to distinguish kinkbands or other deformations in the fiber itself. One possible option is a fiber optic system that produces a digitized image that can be computer enhanced.

The following recommendations address how the MTM-8 might be used to increase our knowledge of composite compressive behavior.

1. Test more fiber types. Only 5 fibers types have been tested with the MTM-8 to date. The MTM-8 has demonstrated its ability to test both polymeric and carbon fibers. In addition, the MTM-8 data can be related to the predicted rule of mixtures strengths by multiplying by .9724.

2. A minimum of thirty samples of a given fiber type should be tested in order to characterize the fiber's statistical population.

3. Incorporate fiber compressive testing with composite sample compressive sample testing. For example, test P55 and P100 fibers while simultaneously testing composite specimens fabricated with these fibers. Appendix H describes, in detail, a research effort that incorporates experimental design based on response surface methodology concepts.

Appendix A: MTM-8 Test Procedures

Compression testing of carbon fibers in the MTM-8 requires patience and practice. Over 20 hours were spent practicing mounting fibers before any data were collected. Figures 25 - 30 are photographs of the mounting equipment, the MTM-8, and the photography equipment. The following are the step-by-step procedures that evolved for testing the fibers:

1) Ensure the anvils are free of glue, the fine strain micrometer is set at 10.0 and the load micrometer is set on 9.0.

2) Randomly select a fiber and cut to a length of approximately 1 cm.

3) Touch the sticky end of the mounting arm to one end of the 1 cm long fiber.

4) Place the mounting arm onto the mounting tripod and adjust the arm so the free end of the fiber is in the groove of the right anvil.

5) Place a small quantity of the powdered glue over the fiber on the right anvil. Melt the glue by placing the tip of the heat probe under the right anvil.

6) After the glue solidifies (5 - 10 sec.), cut the fiber close to the mounting arm and remove the mounting tripod from in front of the MTM-8.

7) Move the left anvil towards the right anvil until the left end of the fiber is in the groove of the left anvil. Leave a gap of about 0.5 cm between the anvils so that grains of glue cannot bridge the gap between the anvils.

8) Place powdered glue over the fiber on the left anvil and melt with the heat probe.

9) Check alignment with the traveling microscope. Remelt the glue under the appropriate anvil as required and adjust the placement of the left anvil to align the fibers. The left anvil position can be adjusted in three dimensions.

10) Add glue onto each anvil until the fiber portions in the grooves cannot be seen through the glue. Melt and remelt the glue to relieve residual stresses.

11) Melt the glue on the left anvil and then set the zero load point (the point where the imaging mirror is balanced on two wires) with the load micrometer. For this study the zero load point was set at 7.05 on the load micrometer. Caution - once the zero load is set,

the MTM-8 becomes very sensitive to vibrations. Be careful not to touch the right anvil because it will be sensitive to any motion and the fine wires balancing the imaging mirrors can be damaged.

12) Measure the desired gage length from the edge of the right anvil with the traveling microscope. Melt the glue on the left anvil and move the left anvil with the coarse strain micrometer until the desired gage length is set.

13) Allow the glue to set for approximately 5 minutes to allow thermal stresses to dissipate. Align the mirror generated images in the telescope.

14) Apply loads with the load micrometer and re-align the mirror images with the fine strain micrometer. Record the loads and associated displacements until fiber failure.

15) After fiber failure, separate the anvils, set the load back to 9.0 on the load micrometer and evaporate the glue off the anvils with the heat probe. Go back to step 1.

The MTM-8 is a delicate mechanism. At one point, the machine was accidentally jarred and the fine wires balancing imaging the mirrors broke. Repairs lasted 8

hours and required extensive disassembly of the MTM-8. While the MTM-8 has a few shortcomings (primarily limited magnification in the optics), this machine is capable of testing fibers with diameters on the order of tens of micrometers in tension or compression.

Figure 25 A Picture of MTM-8 With Fiber Mounting Equipment

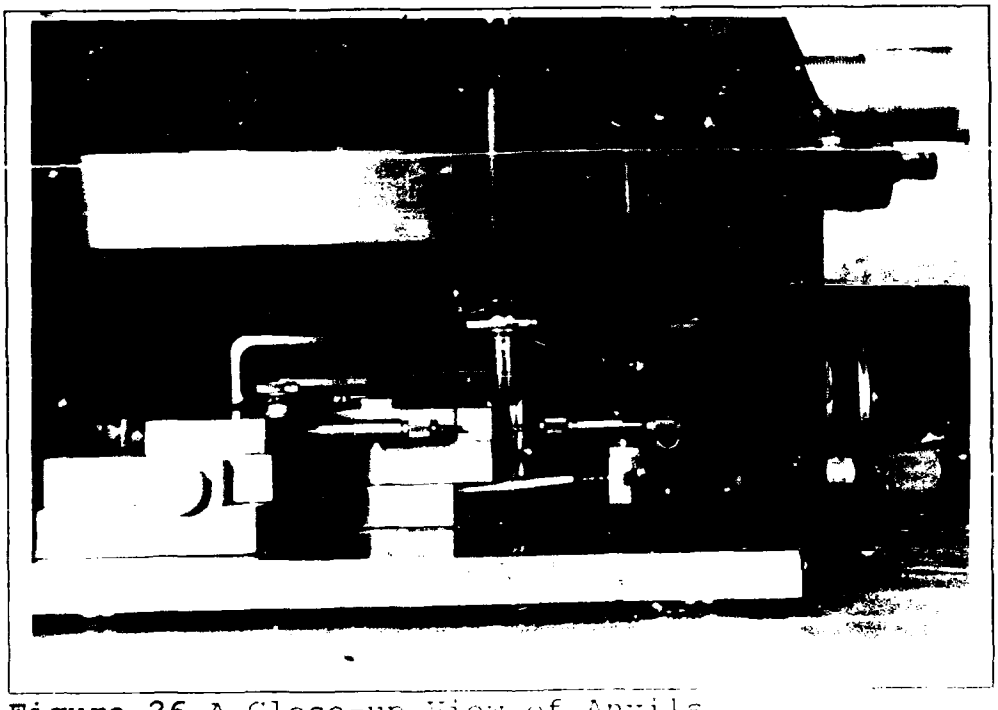

Figure 26 A Close-up View of Anvils

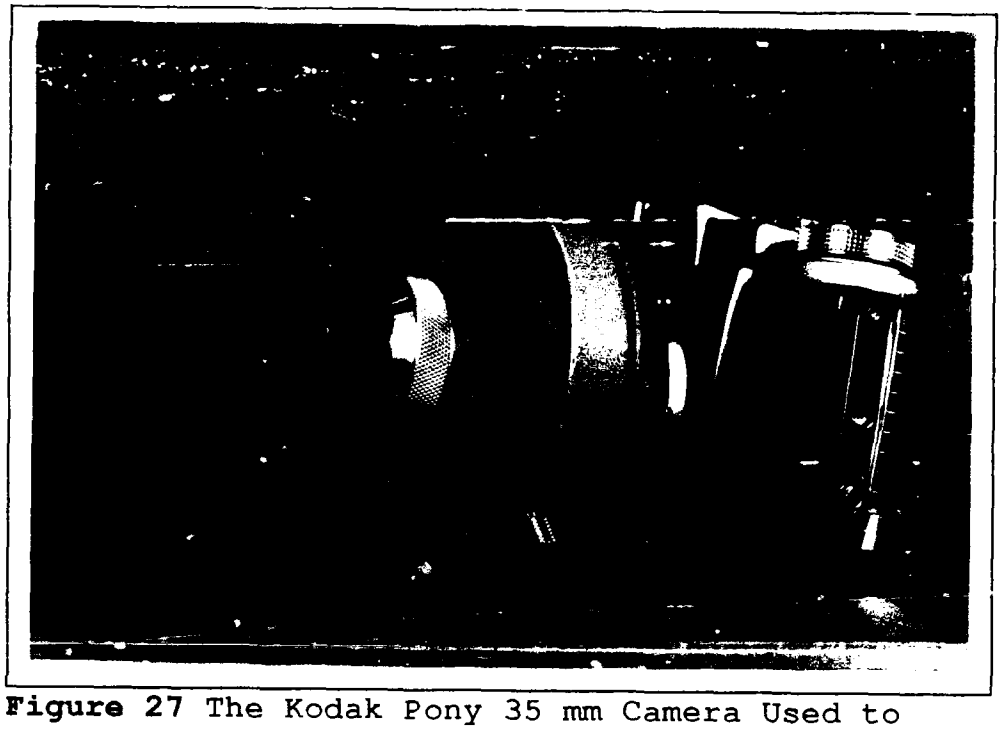

Figure 27 The Kodak Pony 35 mm Camera Used to Photograph the Fibers

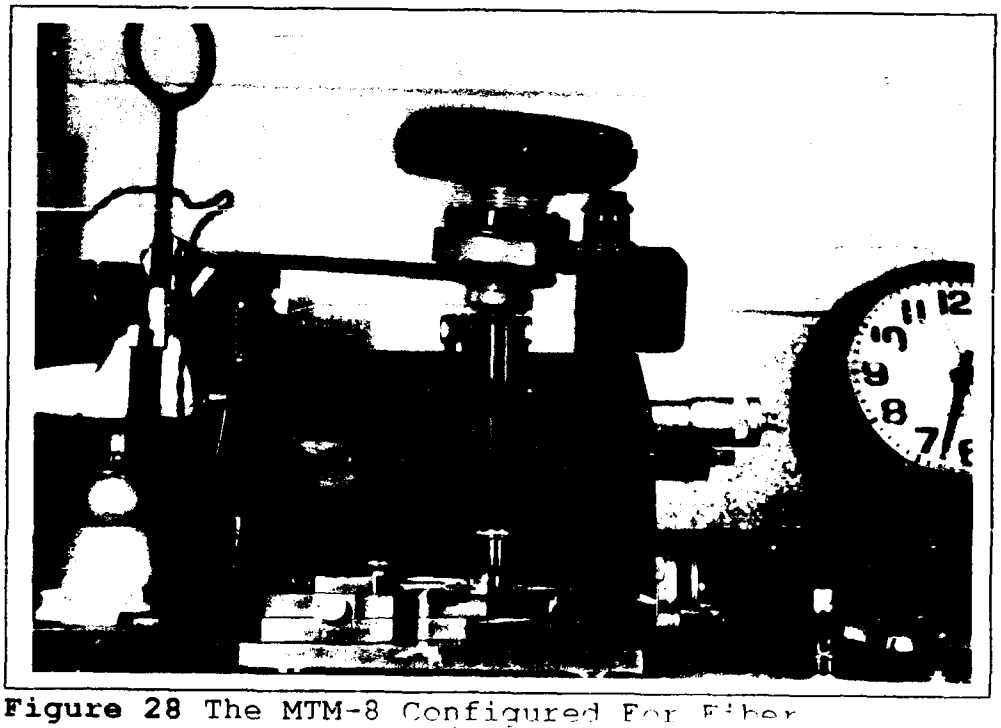

Figure 28 The MTM-8 Configured For Fiber Photography

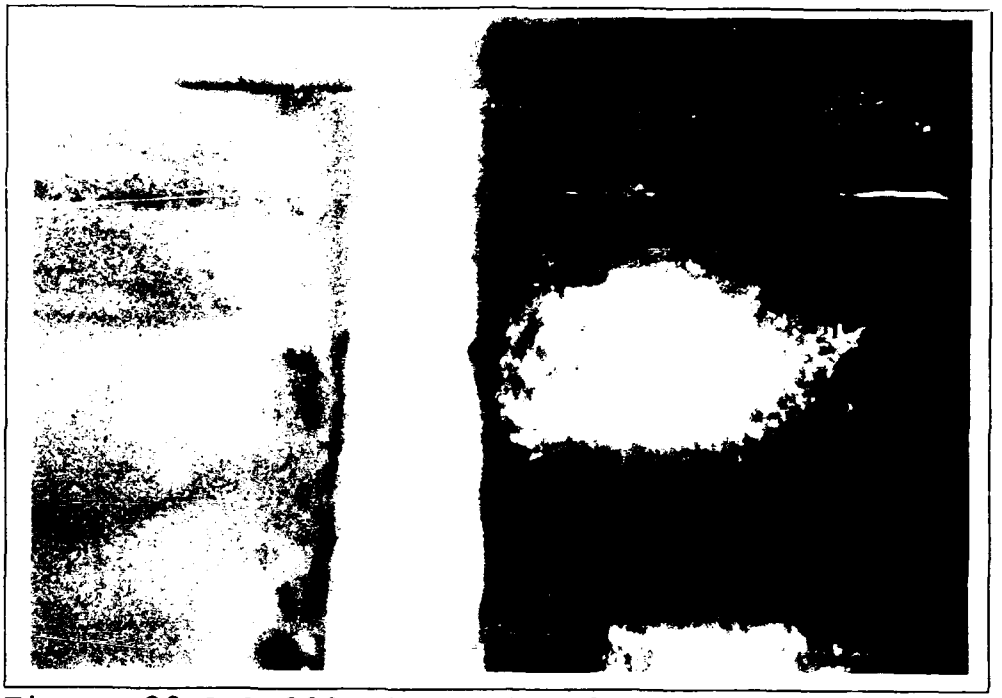

Figure 29 A T-300 Fiber of .16 mm Gage Length Mounted in MTM-8, Approximately 100X Magnification

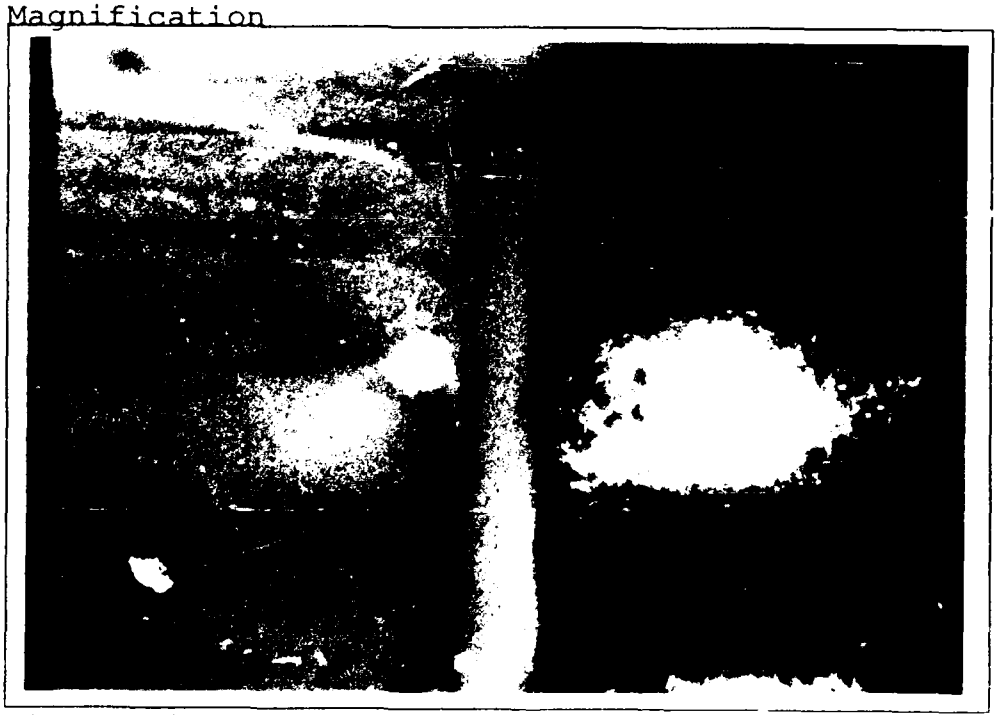

Figure 30 A Mounted T300 Fiber After Failure, Approximately 100X Magnification

Appendix B: Test Equipment List

Compression Testing

Micro-Tensile Testing Machine
Model: MTM-8
Techne (Princeton) Limited, 1968
Eye piece from Bausch-Lomb magnification 10X

Kodak 35 mm Camera
Model: Pony
Lens: .75 inch diameter magnification approx. 10X
manufacturer unknown
Film: Polariod Auto-processing, High-contrast, Black and White, 400 ASA

Computers, Software and Related Equipment

Commodore Personal Computer
Model: PC10C/PC20C Serial # CA1016975
Operating System: MS-DOS 3.2.1

Zenith Personal Computer
Model: Z248 Serial # ZVM1380
Operating System: MS-DOS 3.3

Quattro
Type: Spreadsheet
Borland International, copyright 1987

Statistix, version 2.0
Type: Interactive statistical analysis program
NH Analytical Software, copyright 198-

Wordperfect, version 5.0
Type: word processor
Wordperfect Corporation, copyright 1988

Script Printer
Model: EK-LNO3R-SP001 Serial # RI78281
Digital Corporation
Note: Used with the Zenith 248 PC

APPENDIX C: Statistical Analysis

Introduction

This appendix discusses the use of statistics in this study. This discussion will be divided into two sections - statistical theory and data analysis. The theory section discusses the different analytical methods used in this study and the data analysis section details the application of the theory to collected data.

Statistical Theory

The following statistical methodologies were used in this study: 1) a two tailed, one sample t-test; 2) a two sample t-test; 3) paired t-test and; 4) least squares regression. The tests are labeled as t-tests because the t distribution is used to define the test statistic. The t distribution is used to characterize the distribution of a small sized (typically $n<30$) sample of a normally distributed distribution. The t distribution provides a more accurate description of the data variation typical of small sample sizes than does the normal distribution. As the sample size increases,

the t distribution curve conforms ever more closely to the normal distribution curve (5:267).

Two tailed, one sample t-test (5:296-298). This test was used to determine if the observed mean strengths of the fibers equaled the predicted strengths from both the Euler buckling equation and the rule of mixtures for composites. The test is constructed as follows, when applied to this study:

Null hypothesis: $\sigma_{pred} = \sigma_{obs}$

Alternate hypothesis: $\sigma_{pred} \neq \sigma_{obs}$

Test statistic: $$t = \frac{\sigma_{pred} - \sigma_{obs}}{s/[n]^{.5}}$$

where

σ_{pred} = mean observed strength
σ_{obs} = predicted strength
by Euler buckling with T300
by rule of mixtures for P100 and P55
s = standard deviation calculated with STATISTIX
n = sample size

Null hypothesis rejection region for a confidence level of $1-\alpha$:

$$t \geq t_{\alpha/2,n-1} \quad \text{or} \quad -t_{\alpha/2,n-1} \geq t$$

The reject region can also be defined by comparing the p-value (the area under the tail of the t curve) to $\alpha/2$ as follows:

$$\alpha/2 \geq \text{p-value}(t)$$

Table XV lists the results of the two tailed t-tests performed on the data collected on the 3 fiber types.

Table XV The Results From Two Tailed, One Sample T-Tests For Observed vs. Predicted Fiber Strengths

T-Test with a 98% Confidence Level : $\alpha/2 = .01$

Fiber	Sample Size	Test Statistic P-Value	Decision
T300	10	0.305	accept null
P100	22	0.000	reject null
P55	30	0.000	reject null

The results are discussed in Chapter 4.

Two sample t-test (5:334-341). This test is very similar to the one sample t-test, however this test is to check for equality of means between two samples. This test follows the same basic procedures as the one sample test, except that the test statistic is calculated differently. The two sample t-test as applied to the T300 data is as follows:

Null hypothesis: $\sigma_1 - \sigma_2 = 0$

Alternate hypothesis: $\sigma_1 - \sigma_2 \neq 0$

where

σ_1 = mean strength of the fibers mounted with the old glue

σ_2 = mean strength of the fibers mounted with the new glue

If the samples have equal variances then the test statistic is calculated:

$$t = \frac{\sigma_1 - \sigma_2}{s_p[1/m + 1/n]^{.5}}$$

where

m = sample size of fibers mounted with the old glue

n = sample size of fibers mounted with the new glue

s_p = pooled estimator of the common variance

$$= \frac{(m-1)s_1^2 + (n-1)s_2^2}{m + n - 2}$$

where

s_1 = sample variance for fibers mounted with the old glue

s_2 = sample variance for fibers mounted with the new glue

If the samples have unequal variances then the test statistic is calculated:

$$t = \frac{\sigma_1 - \sigma_2}{[s_1^2/m + s_2^2/n]^{.5}}$$

Null hypothesis rejection region for a confidence level of $1-\alpha$:

$$t \geq t_{\alpha/2,n-1} \quad \text{or} \quad -t_{\alpha/2,n-1} \geq t$$

The reject region can also be defined by comparing the p-value (the area under the tail of the t curve) to $\alpha/2$ as follows:

$$\alpha/2 \geq \text{p-value}(t)$$

STATISTIX automatically performs all of the calculations for this test and the results are discussed in Chapter 4.

Paired t-test (5:345-346). This test is used when two observations are made on each object in the a sample. This test was used to determine if the tensile and compressive moduli for the fibers were equal. Again, this test follows the same basic steps as the other tests. This test was applied to the fiber data as follows:

Null hypothesis: $E_t - E_c = 0$

Alternate hypothesis: $E_t - E_c \neq 0$

where

E_t = apparent tensile modulus
E_c = apparent compressive modulus

Test statistic:

$$t = \frac{E(d)}{s_d / [n]^{.5}}$$

where

$E(d)$ = mean value of the d_i's
$d_i = E_t - E_c$ for the i^{th} fiber
s_d = standard deviation of the d_i's
n = sample size

The null hypothesis rejection region for a confidence level of $1-\alpha$:

$$t \geq t_{\alpha/2,n-1} \quad \text{or} \quad -t_{\alpha/2,n-1} \geq t$$

The reject region can also be defined by comparing the p-value (the area under the tail of the t curve) to $\alpha/2$ as follows:

$$\alpha/2 \geq \text{p-value}(t)$$

The results of the paired t-tests are listed in Table XVI. STATISTIX was used to perform the calculations.

Table XVI Results Of Paired T-Test For $E_t = E_c$

Fiber	Sample Size	P-Value	Confidence of $E_t = E_c$
T300	9	.084	91.6%
P100	4	.288	71.2%
P55	7	.018	98.2%

For both the T300 and the P55 fibers, the test indicates that the moduli can be considered equal. The P100 test does not give as strong an indication, but three of the four samples varied by less than 10%. For a higher confidence, three more P100 fibers were tested. The values in Msi for the fibers (E_t , E_c) were (41.9,27.6), (61.41,54.6) and, (44.21,45.26) respectively. The p-value for the paired t-test dropped to .064, therefore, the apparrent E_t and E_c for P100 may be considered equal with 93.6% confidence.

Least squares regression (14:31-40). Least squares regression is a method of "fitting" a straight line to observed data where the following sum is minimized:

$$f(b_o, b_1) = \Sigma [y_i - (b_o + b_1 x_i)]^2$$

where

$$b_1 = \frac{n\Sigma(x_i y_i) - (\Sigma x_i)(\Sigma y_i)}{n\Sigma(x^2_i) - (\Sigma x_i)^2}$$

$$b_o = \frac{\Sigma y_i - b_1 \Sigma x_i}{n}$$

where for this study

$y_i = 1/E_a$ or the compressive strengths predicted by the rule of mixtures

$x_i = 1/L_f$ or observed compressive strengths

STATISTIX was used to compute the least squares regressions for this study. STATISTIX automatically performs a two tail, one sample t-test to indicate whether or not b_o or b_1 should equal zero. In addition, STATISTIX performs an overall fitness test, which is a measure of how well the regression fits the data. The smaller the F-test p-value, the better the regression fits the data. Finally, STATISTIX computes R^2 values which are a measure of the amount of data variability accounted for by the regression. The closer the R^2 values are to 1.0, the more the regression accounts for data variability.

Data Analysis

The data analysis employed in this study utilized the following algorithm: 1) a data normality check; 2) a data bias check; 3) a calculation of the means and standard deviations; 4) and a calculation of the appropriate least squares regression. The software program STATISTIX was used to perform the calculations.

Normality check. The data must be checked to ascertain whether or not it can be considered to be a sample from a normally distributed population. This check is important because the statistical tests and the least square regression assume the data is normally distributed.

Wilk-Shapiro/Rankits plots were calculated with STATISTIX for each set of fiber data. Table XVII lists the Wilk-Shapiro (W-S) numbers for the fiber data. A W-S number ranges from 0 to 1. Discretion must be used in interpreting the W-S numbers. Typically, the range of .8 to 1.0, indicates that the assumption of normality can be considered highly valid. In the range of .7 to .8, the assumption of normality can be considered valid and below .7 the assumption of normality is suspect.

Table XVII W-S Numbers For All The Fiber Data Analysis

Fiber	Strength Data	Inverse Modulus Data
T300 - all fibers	.9807	*
old glue	.8665	*
new glue	.9390	.9056
P100 - all fibers	.9788	*
1st group	.9217	*
2nd group	.9888	.9082
P55 - all fibers	.9730	.9595

Based on the W-S numbers, all the different combinations of fiber data used in this study may be assumed to be from a normally distributed population.

Data Bias. Bias is systematic error and is to be avoided. A simple method of detecting bias is to plot the data in the order it was collected. Each set of fiber data was plotted in this manner.

Figure 31 shows the plot of the T300 fiber data in the order it was collected. The plot shows a grouping of data. The stars mark the strengths of the first 16 fibers, which were mounted with the old glue, while the x marks the fibers mounted with the new glue. This

grouping led to the two sample t-test performed in Chapter 4.

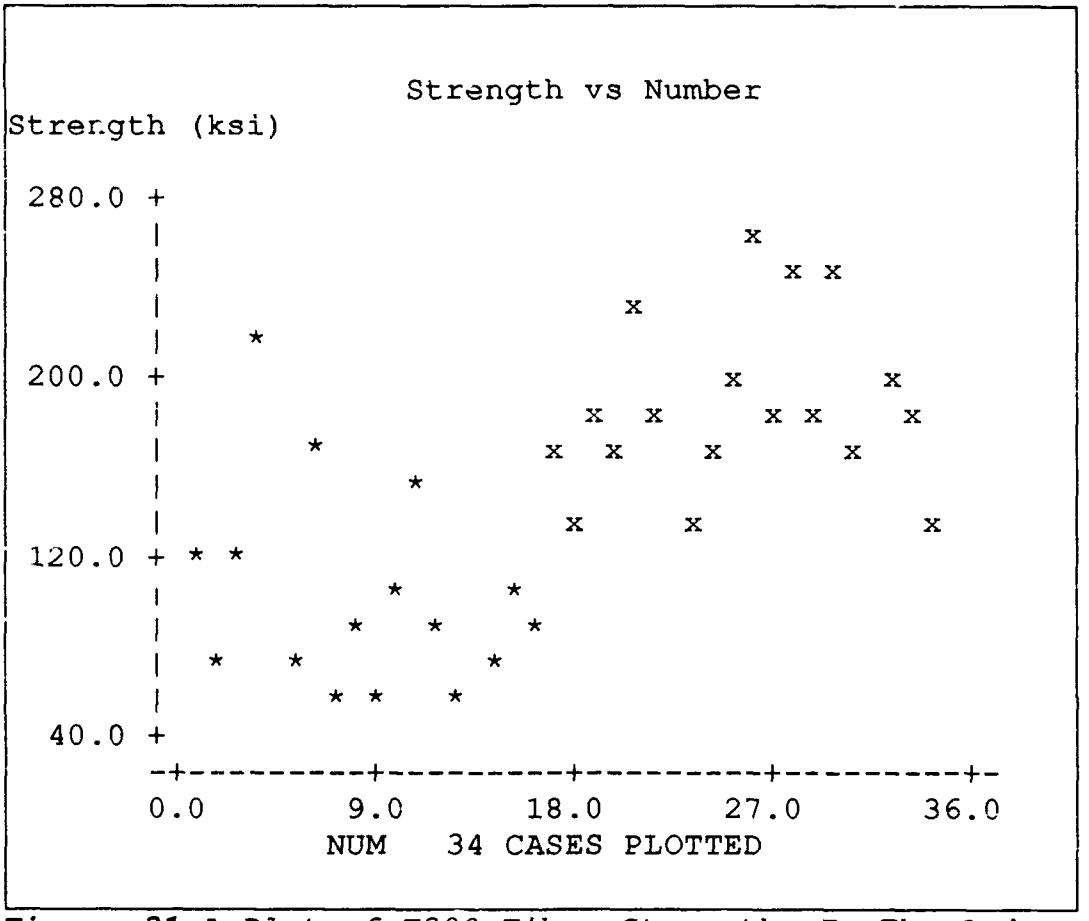

Figure 31 A Plot of T300 Fiber Strengths In The Order of Collection

Figure 32 shows the plot of the P100 fiber data. An upward trend is evident in the first thirteen fibers. This trend led to a two sample t-test to determine if the mean strength of the first thirteen fibers was significantly different than the mean strength of the remaining fibers. The results of the t-test are listed

in Table XIX. The small p-value indicates that the sample means maybe considered different with 99% confidence.

Figure 33 shows the plot of all the P55 fibers in the order they were tested. The plot shows no sign of bias. The plots of gage length verses strength (Figures 34 -36) for all three fibers do not show any data bias due to gage length. This indicates that the stress due to end effects is not a factor.

Least squares regression. An unweighted least squares regression for $1/E_s = 1/L_f$ was performed for every fiber data set. Table XVIII summarizes the results. Plots of the observed data, coupled with small R^2 values, led to the recalculation of the regressions with a weighting variable to eliminate the data variability. The weighted least squares regressions are presented in Chapter 4.

Table XVIII The Results Of The Unweigthed Least Squares Regressions

	T300	P100	P55
Constant, b_0 P-value	.8571	.1392	.8116
Slope, b_1 P-value	.1288	.0097	.0000
F-test P-value	.1288	.0097	.0000
Adjusted R^2	.0843	.2548	.7524

Table XIX A Two Sample T-Test For The P100 Fiber Data

TWO SAMPLE T TESTS FOR OLD STRENGTH VS NEW STRENGTH

VARIABLE	MEAN	SAMPLE SIZE	S.D.	S.E.
OS	80.41	13	25.02	6.940
NS	115.0	23	31.22	6.511

	T	DF	P
EQUAL VARIANCES	-3.42	34	0.0017
UNEQUAL VARIANCES	-3.64	29.8	0.0010

	F	NUM DF	DEN DF	P
TESTS FOR EQUALITY OF VARIANCES	1.56	22	12	0.2153

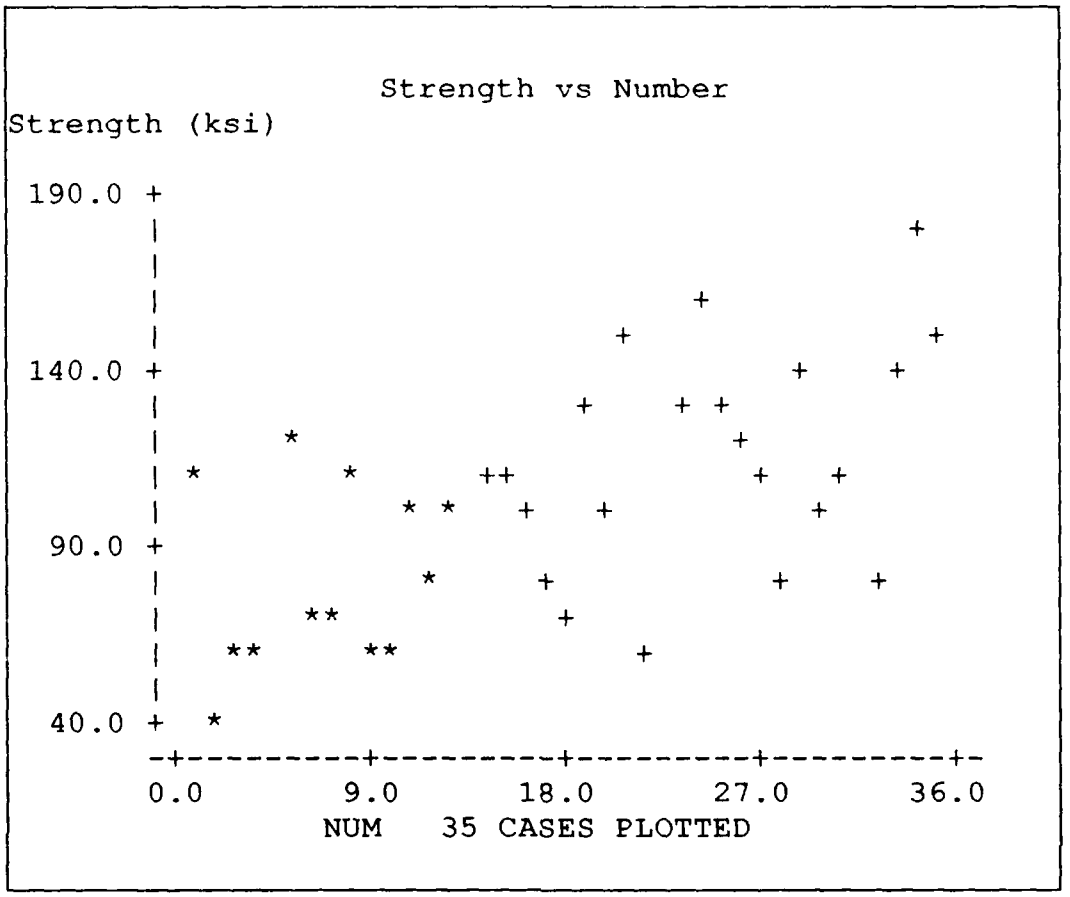

Figure 32 A Plot Of P100 Fiber Strengths In the Order of Collection

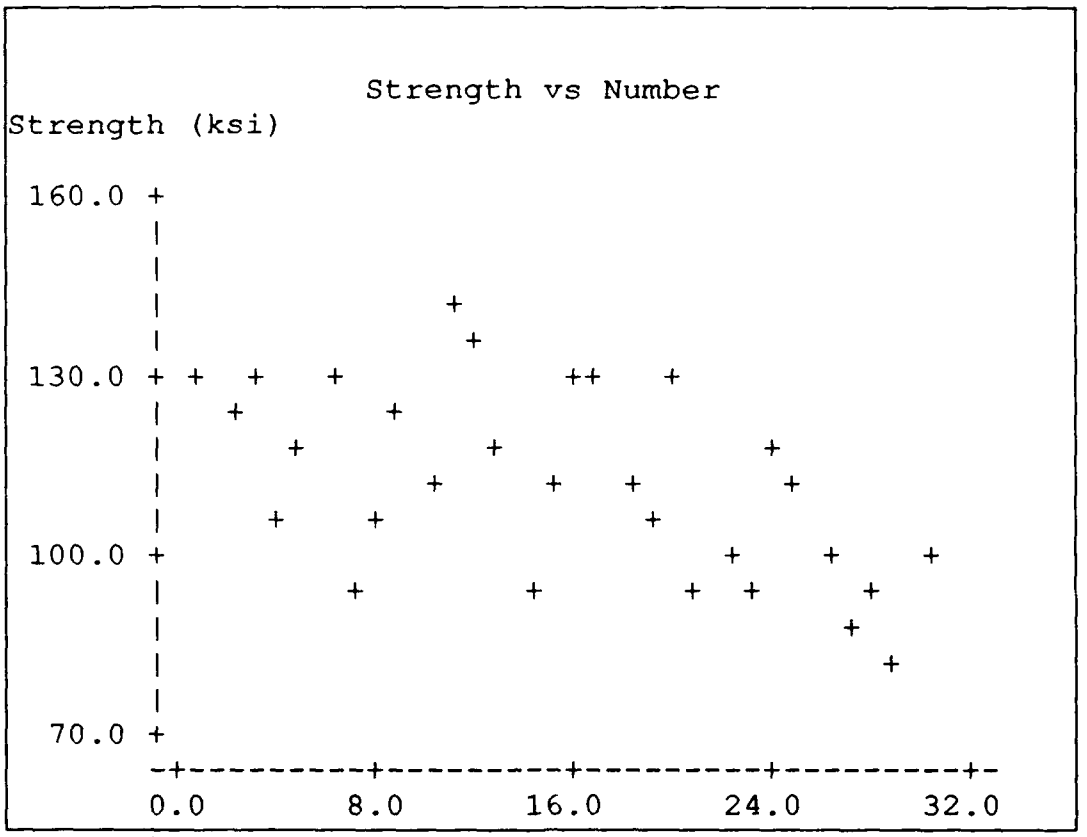

Figure 33 A Plot of The P55 Fiber Data In The Order of Collection

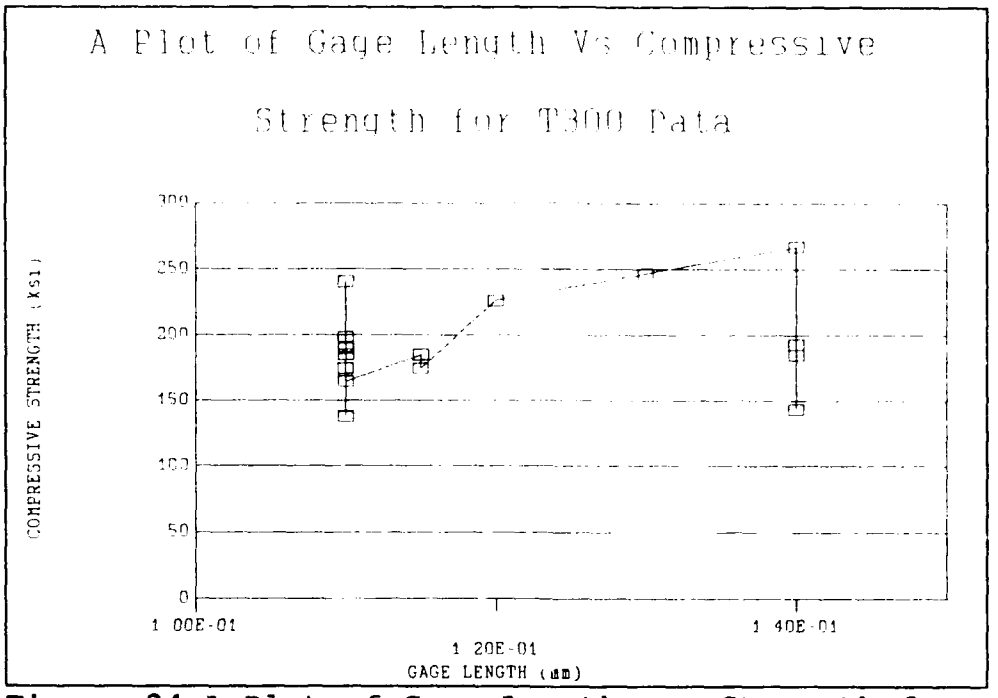

Figure 34 A Plot of Gage Length vs. Strength for T300 Data

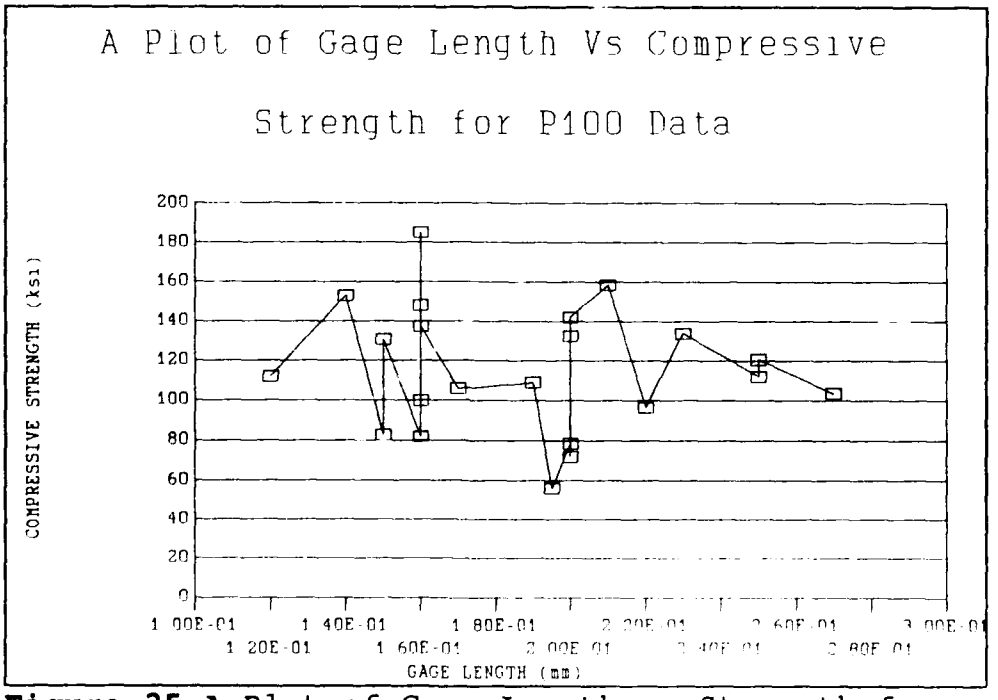

Figure 35 A Plot of Gage Length vs Strength for P100 Data

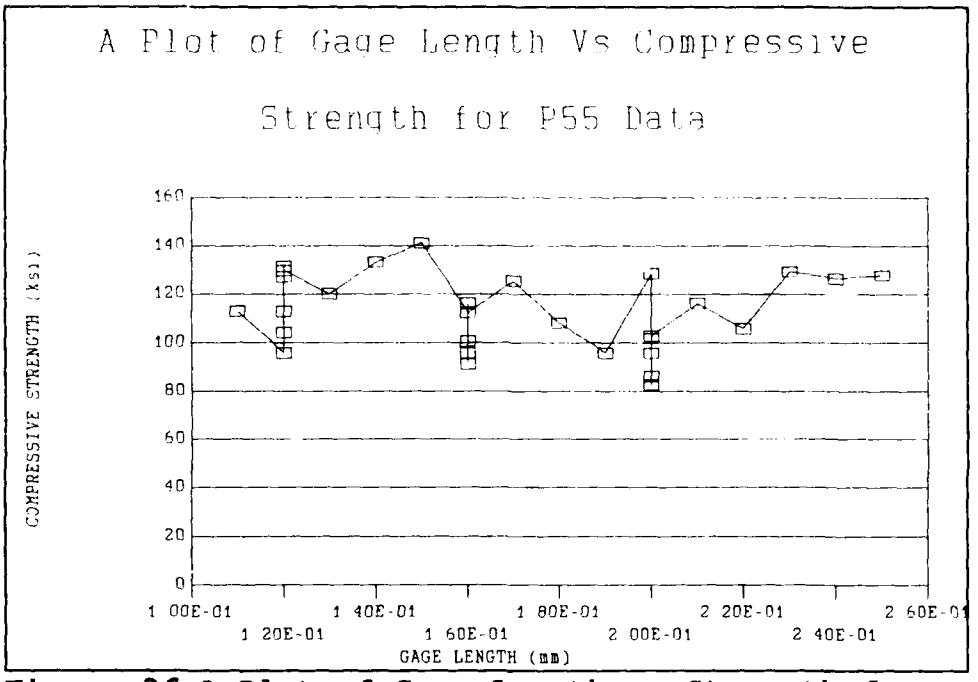

Figure 36 A Plot of Gage Length vs Strength for P55 Data

Appendix D: T300 Data

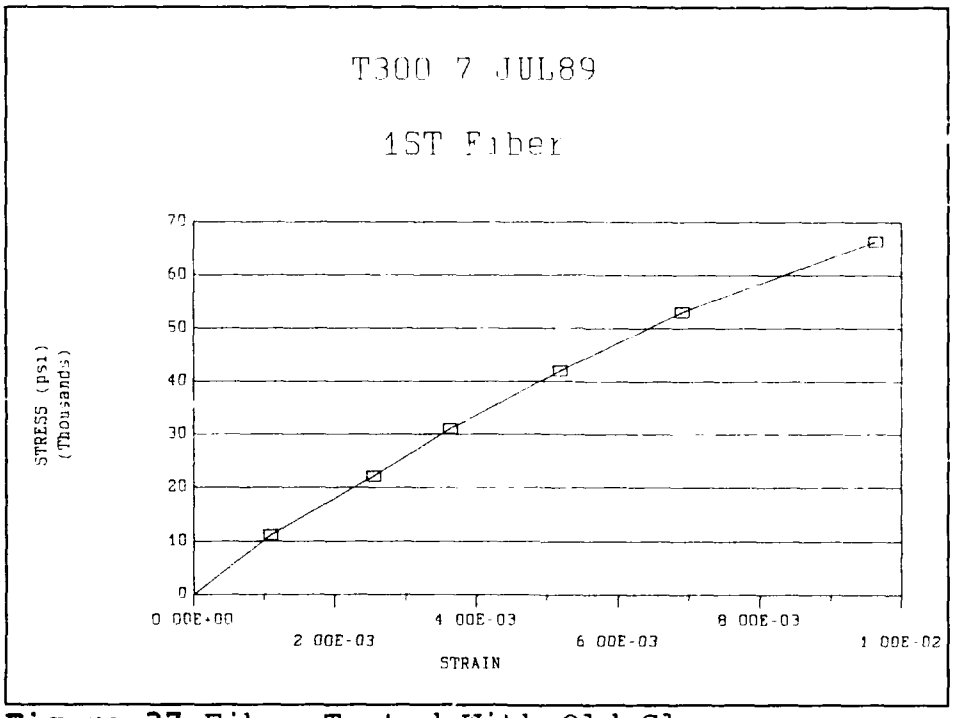

Figure 37 Fiber Tested With Old Glue

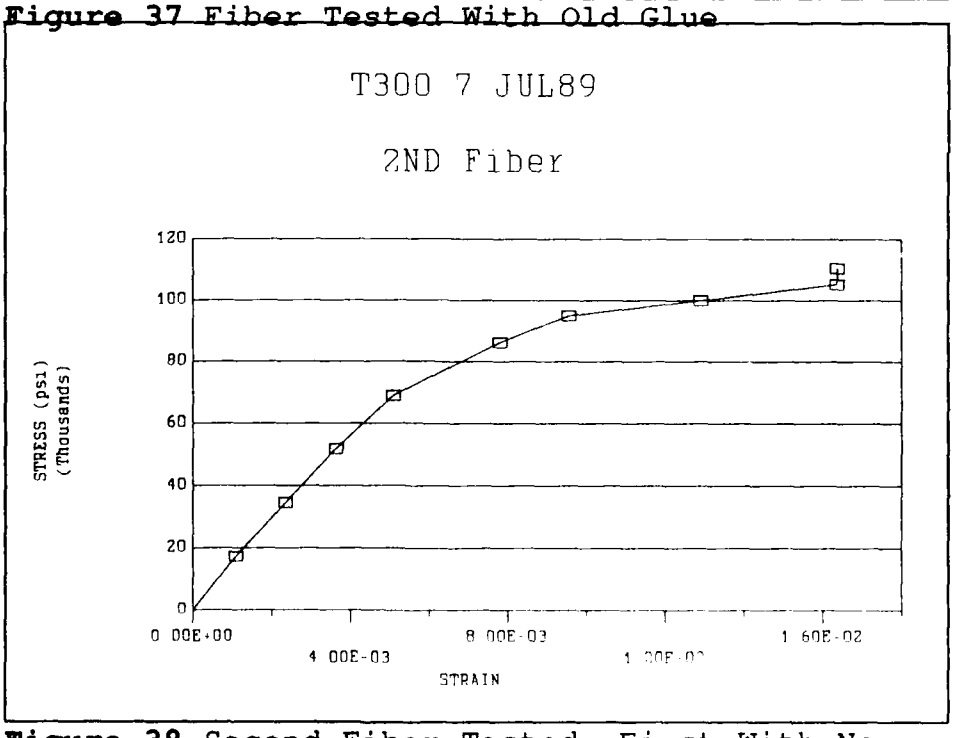

Figure 38 Second Fiber Tested, First With New Glue

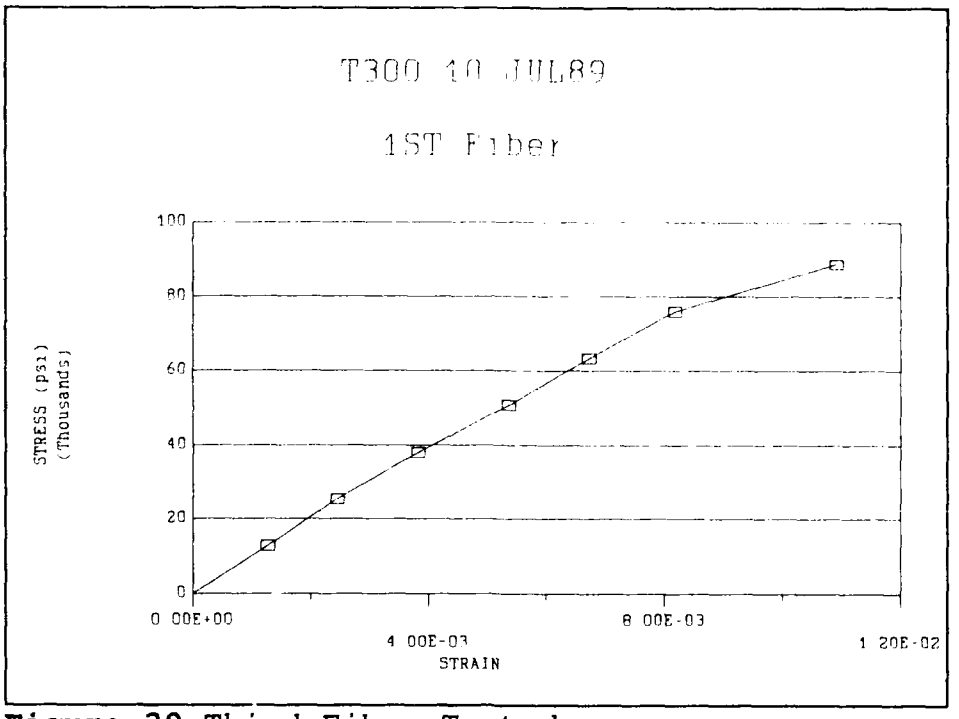

Figure 39 Third Fiber Tested

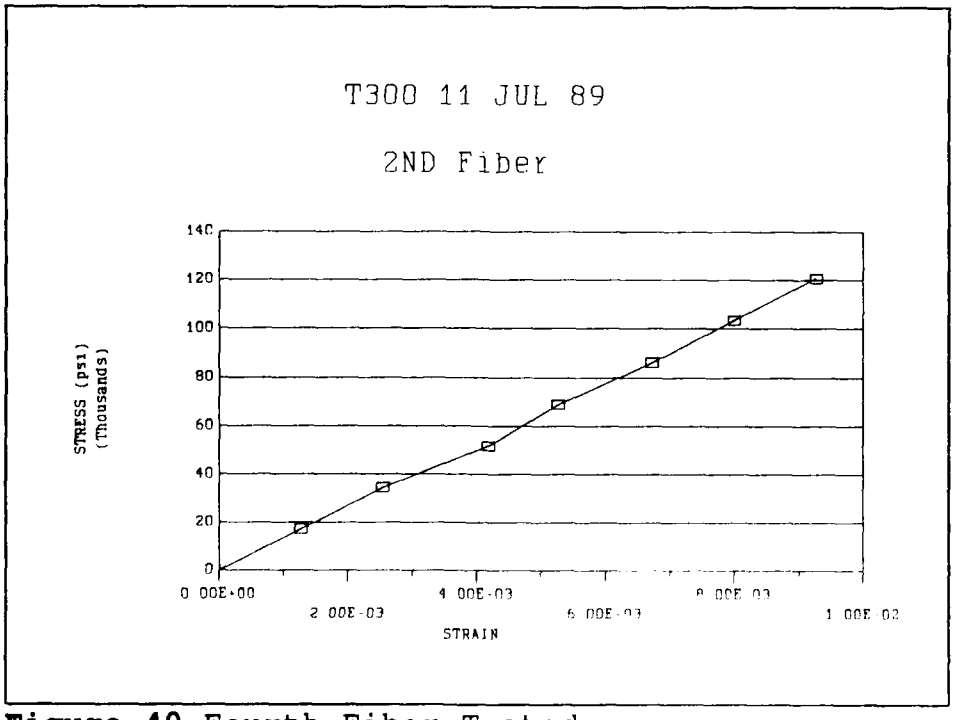

Figure 40 Fourth Fiber Tested

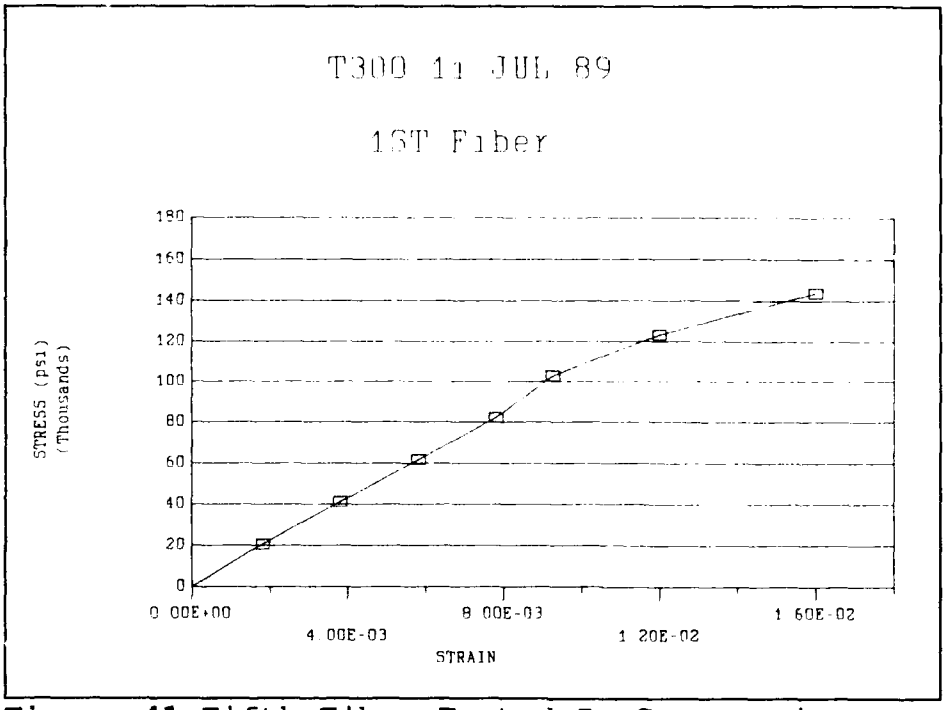

Figure 41 Fifth Fiber Tested In Compression

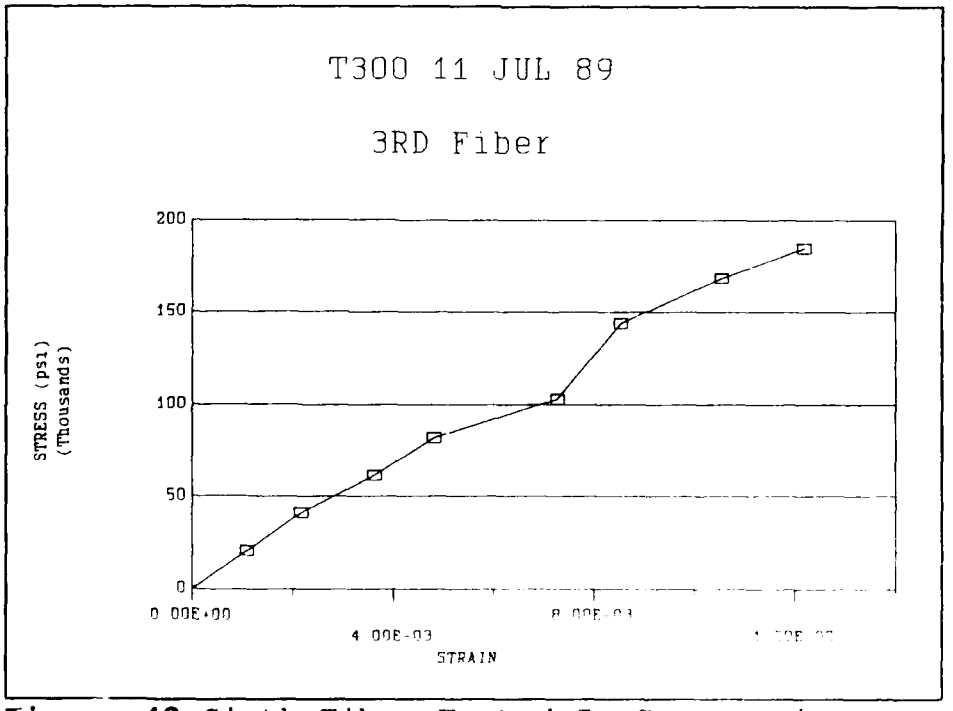

Figure 42 Sixth Fiber Tested In Compression

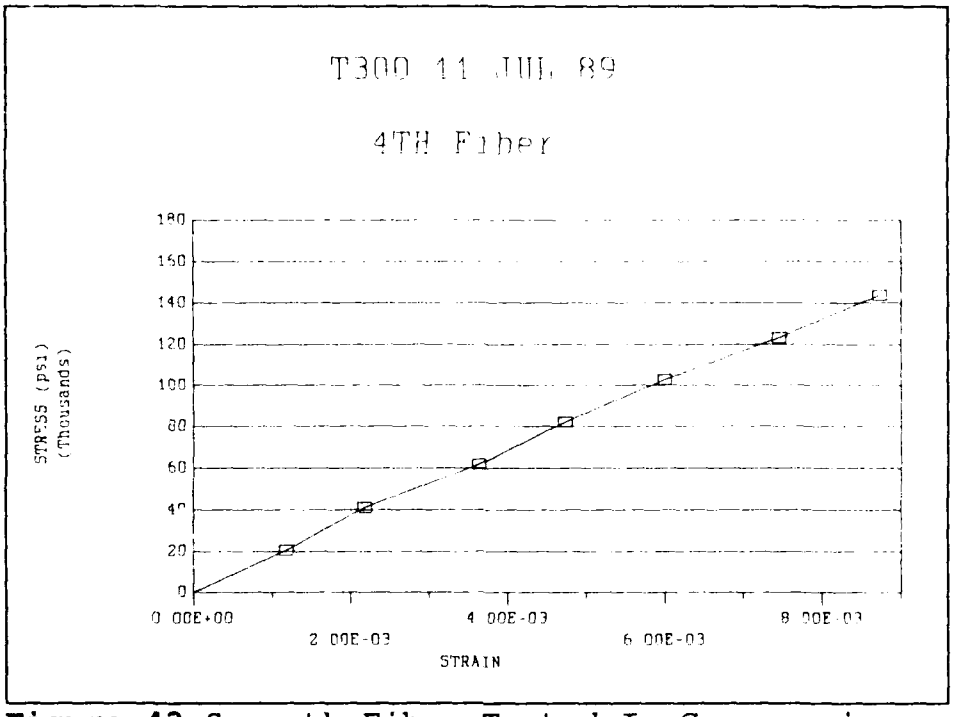

Figure 43 Seventh Fiber Tested In Compression

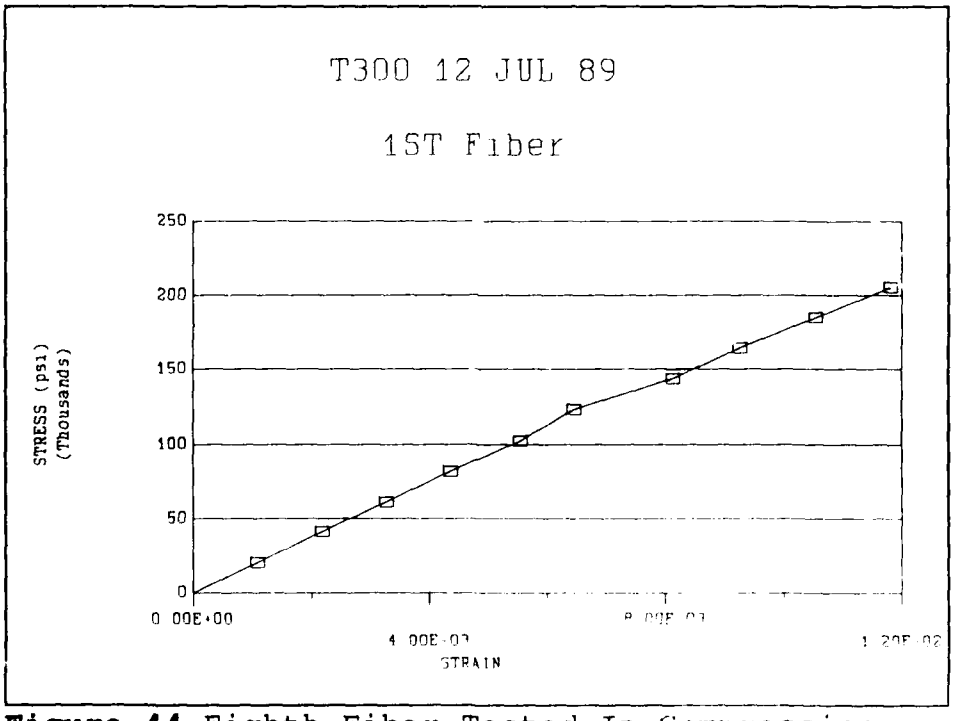

Figure 44 Eighth Fiber Tested In Compression

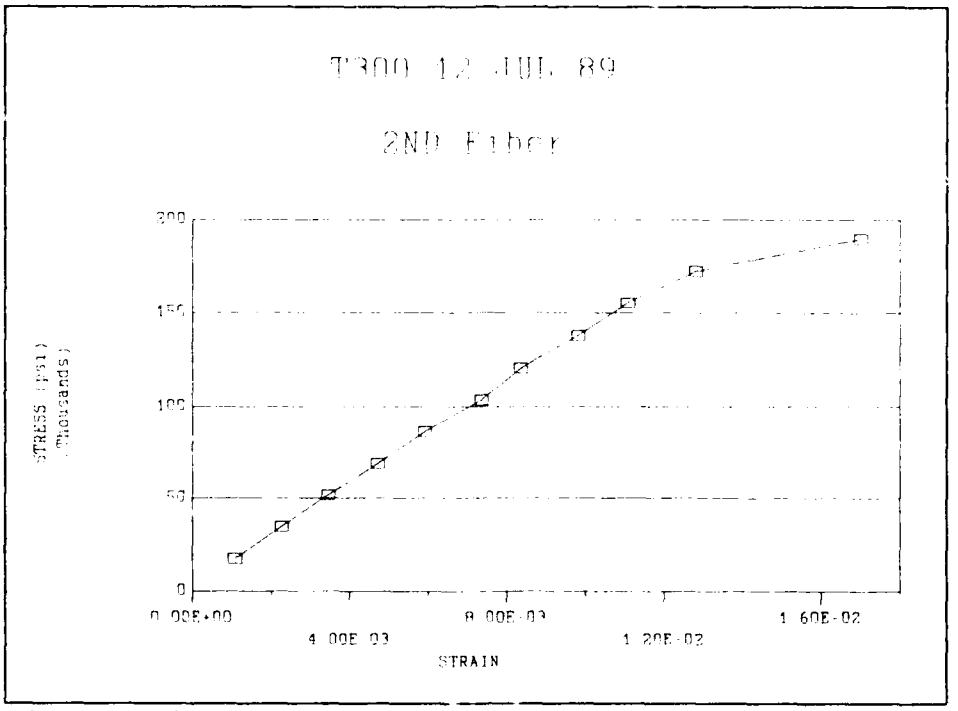

Figure 45 Ninth Fiber Tested In Compression

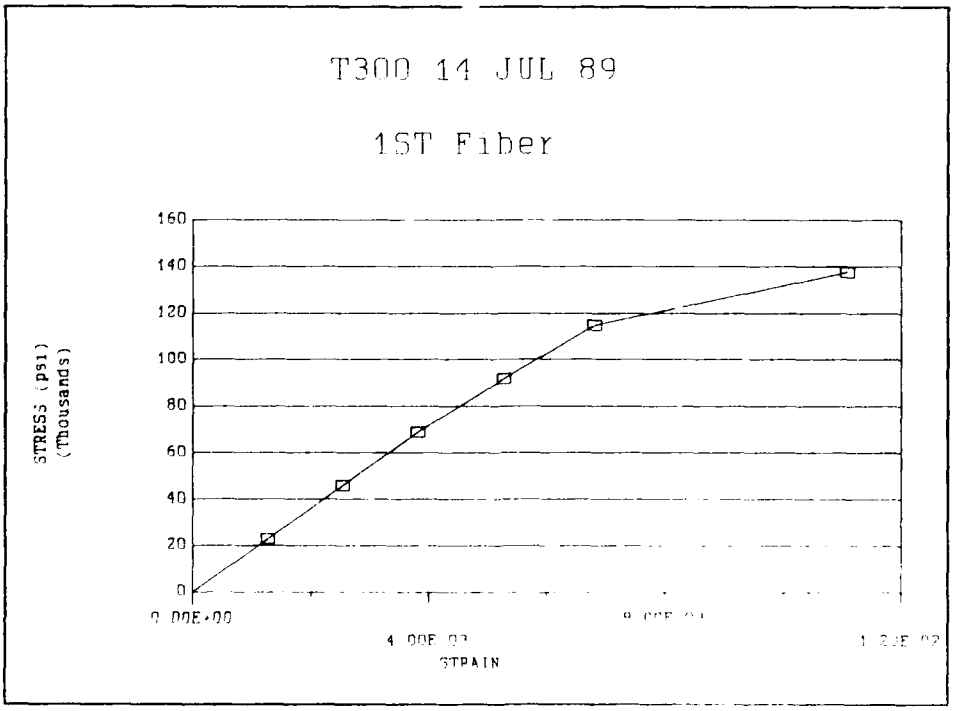

Figure 46 Tenth Fiber Tested In Compression

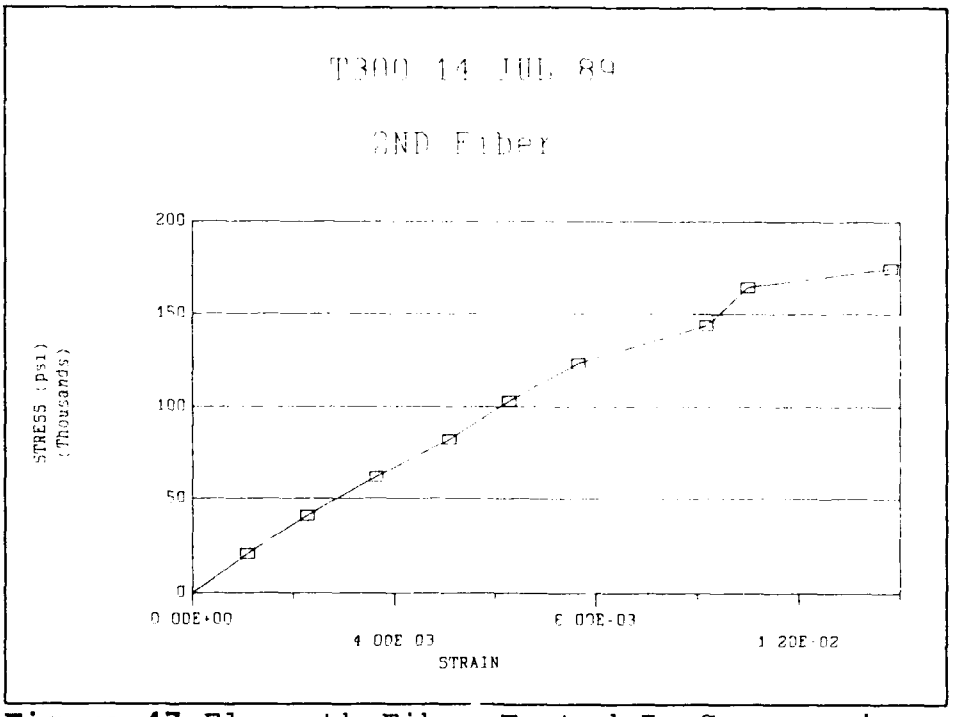

Figure 47 Eleventh Fiber Tested In Compression

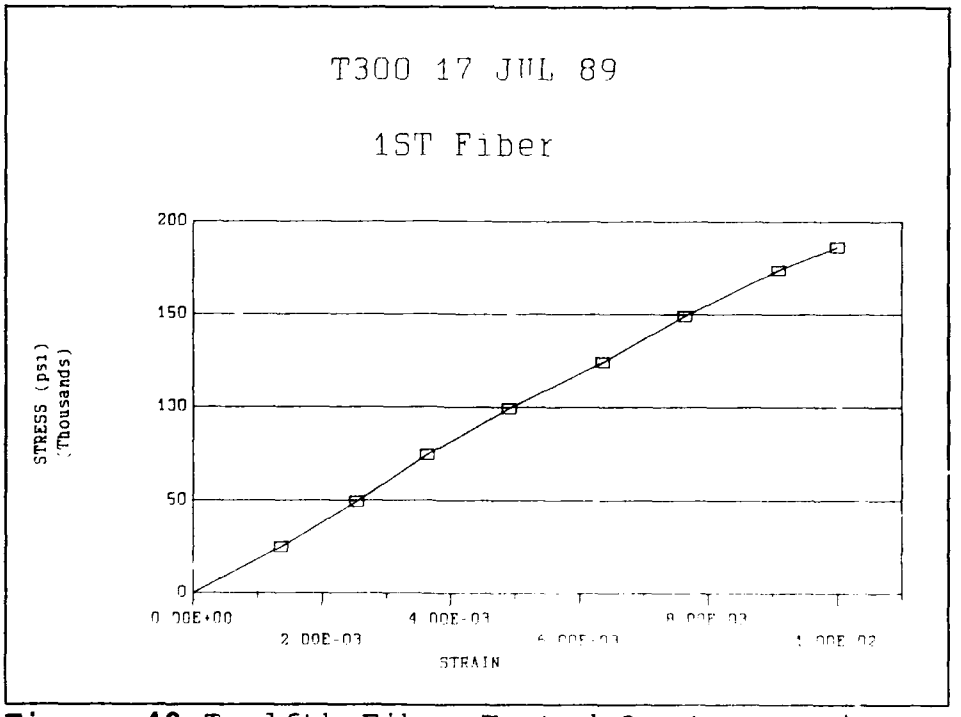

Figure 48 Twelfth Fiber Tested In Compression

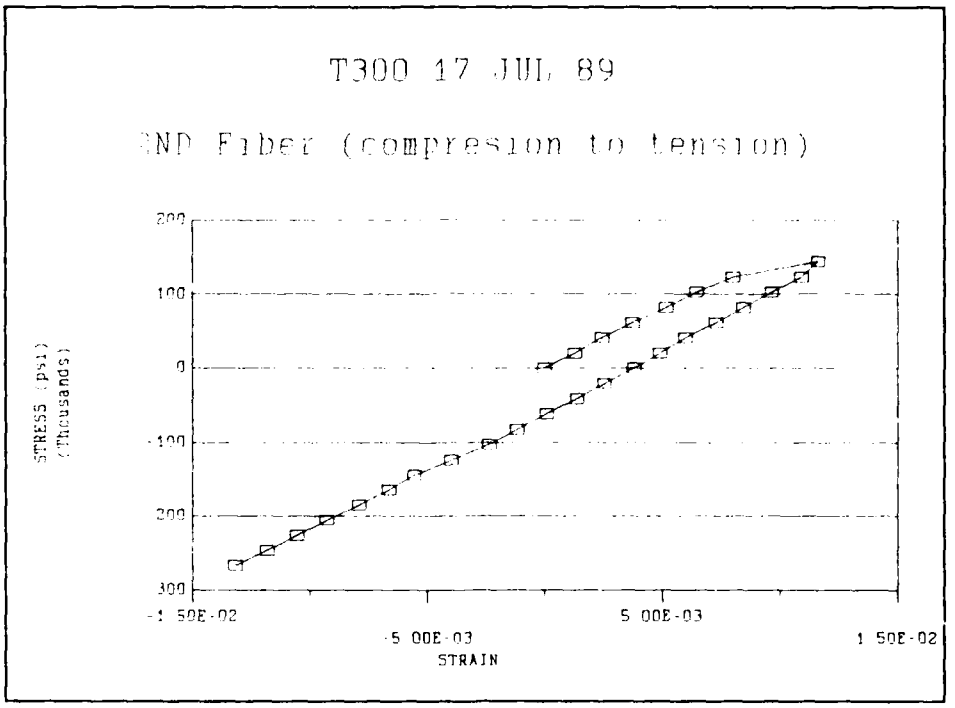

Figure 49 Thirteenth Fiber Tested In Compression

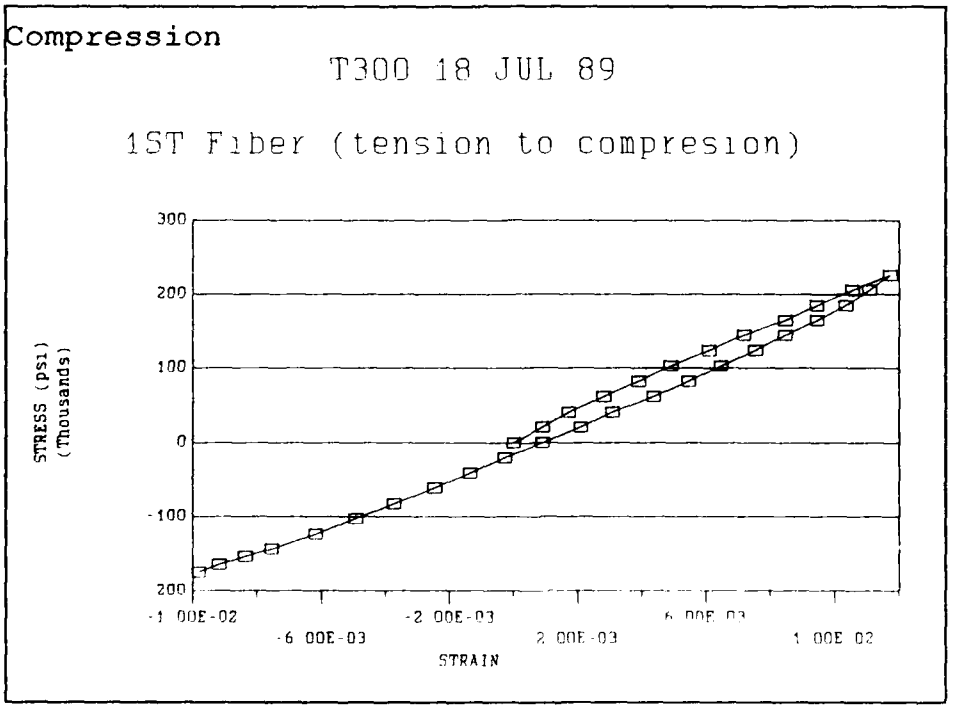

Figure 50 Fourteenth Fiber Tested In Compression

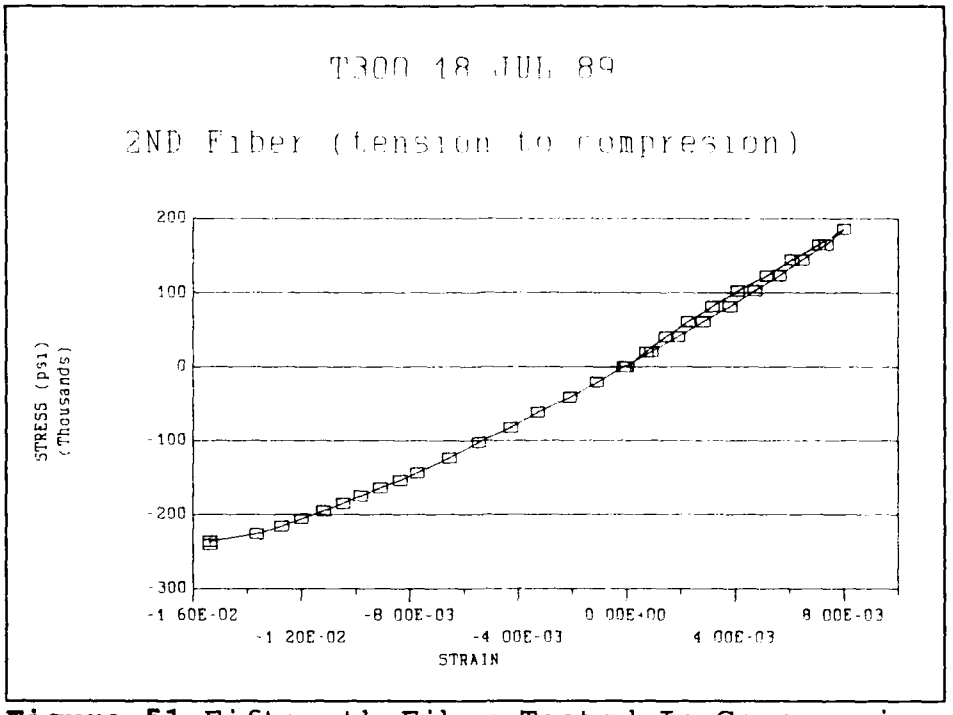

Figure 51 Fifteenth Fiber Tested In Compression

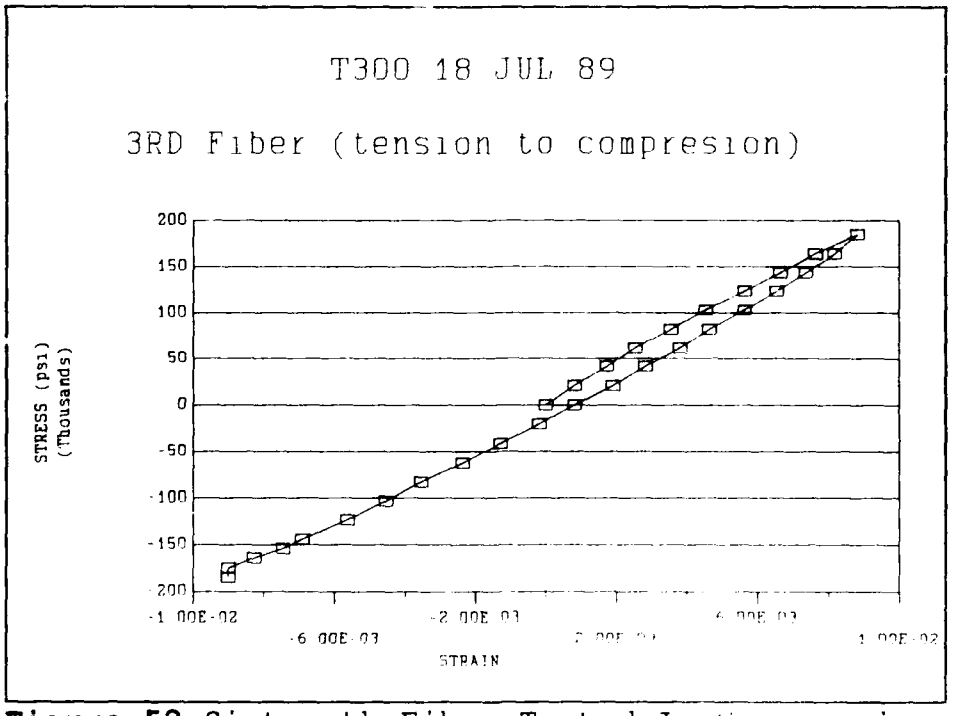

Figure 52 Sixteenth Fiber Tested In Compression

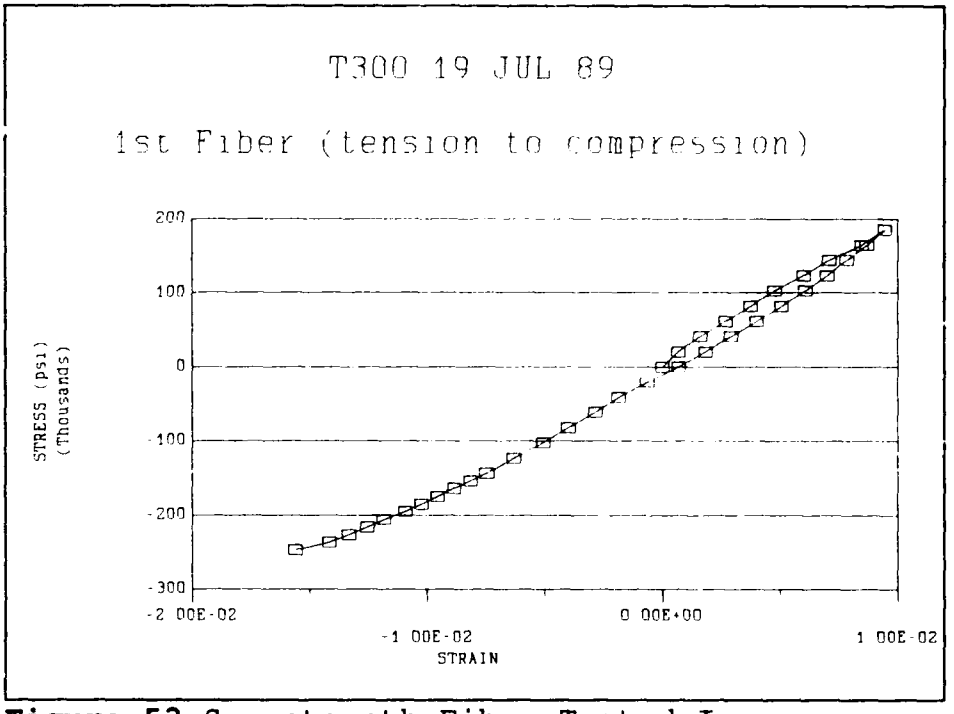

Figure 53 Seventeenth Fiber Tested In Compression

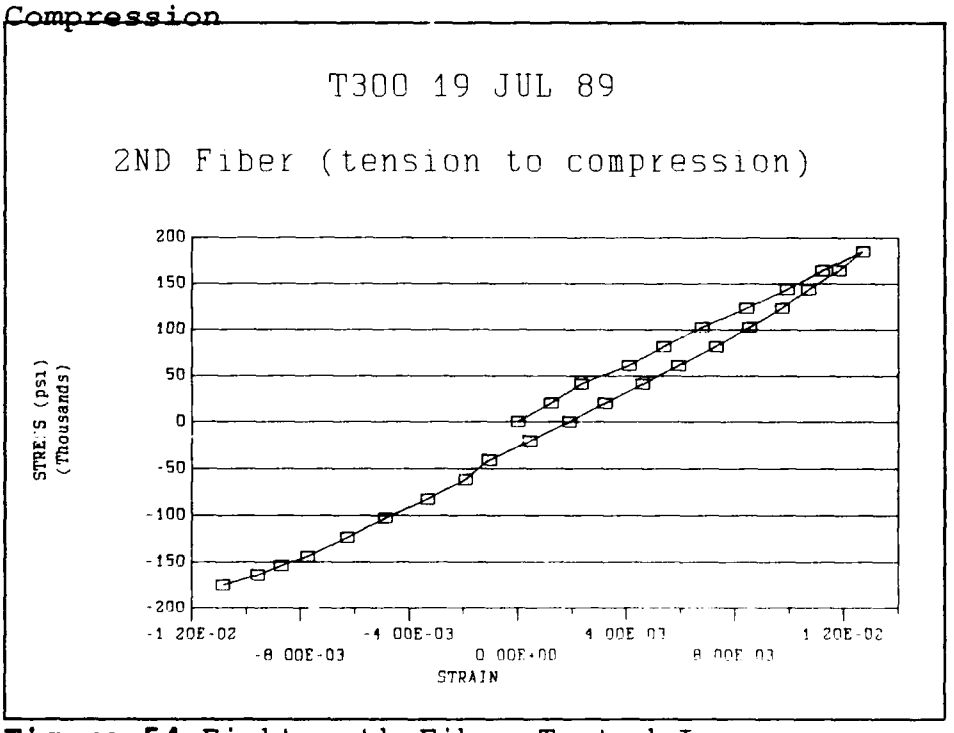

Figure 54 Eighteenth Fiber Tested In Compression

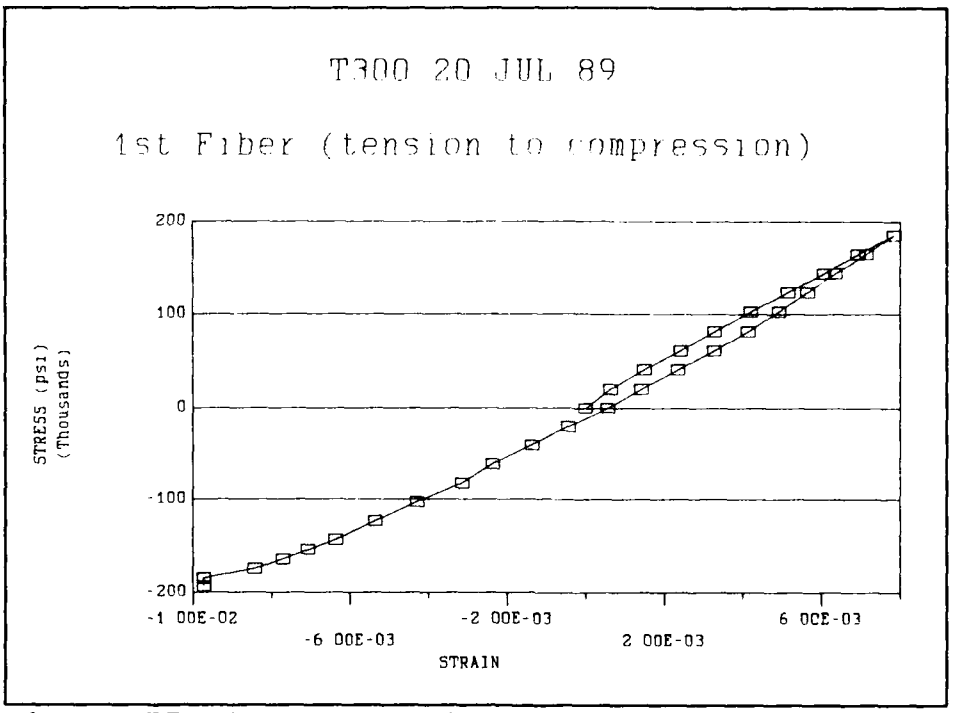

Figure 55 Nineteenth Fiber Tested In Compression

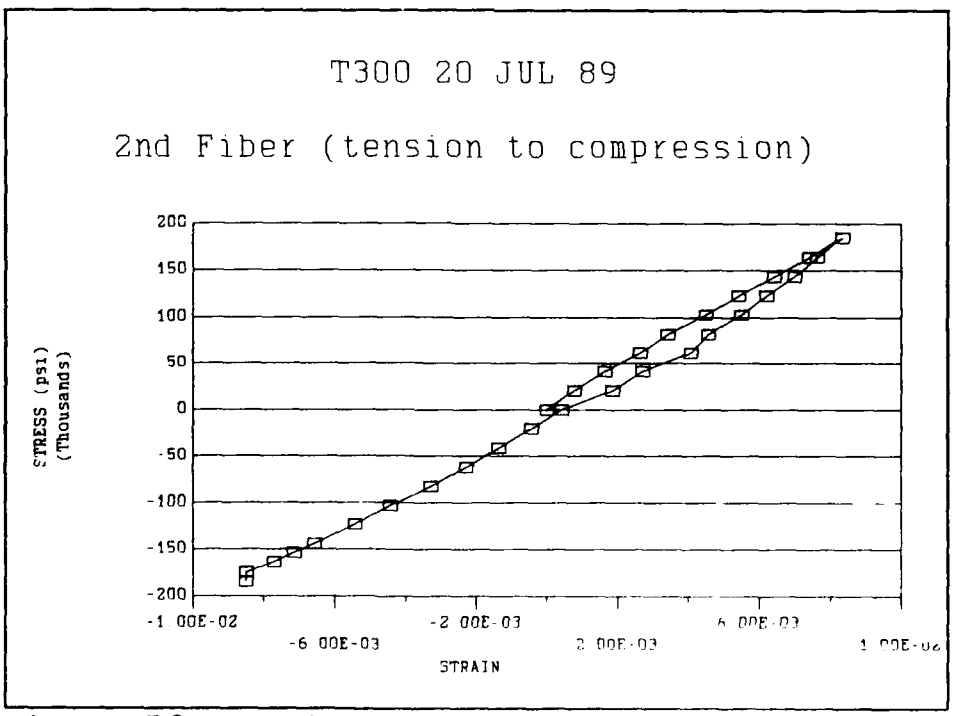

Figure 56 Twentieth Fiber Tested In Compression

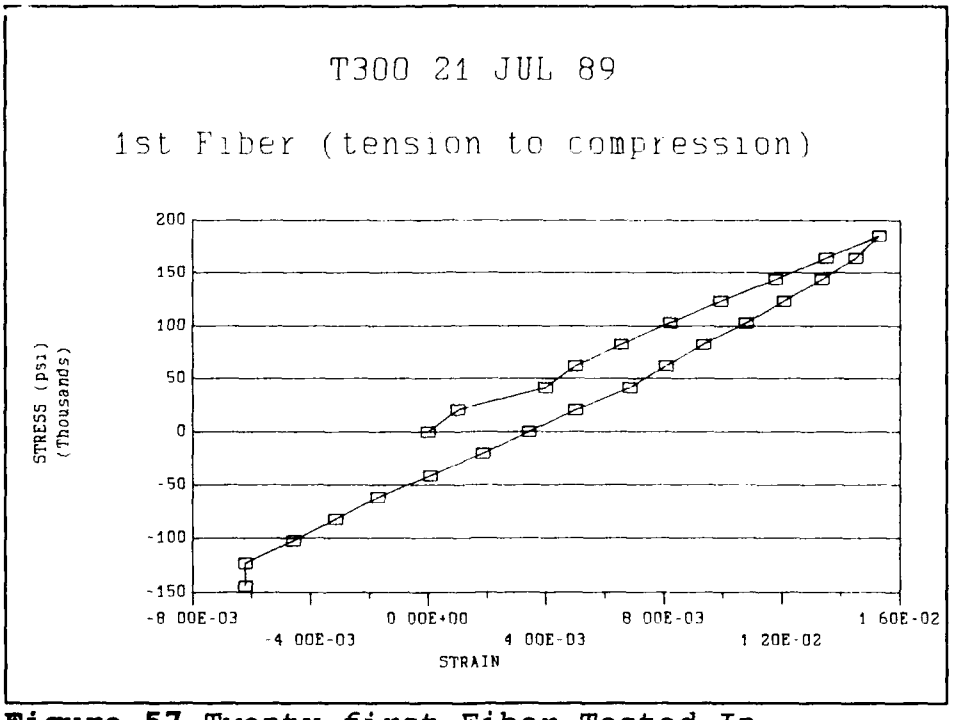

Figure 57 Twenty-first Fiber Tested In Compression

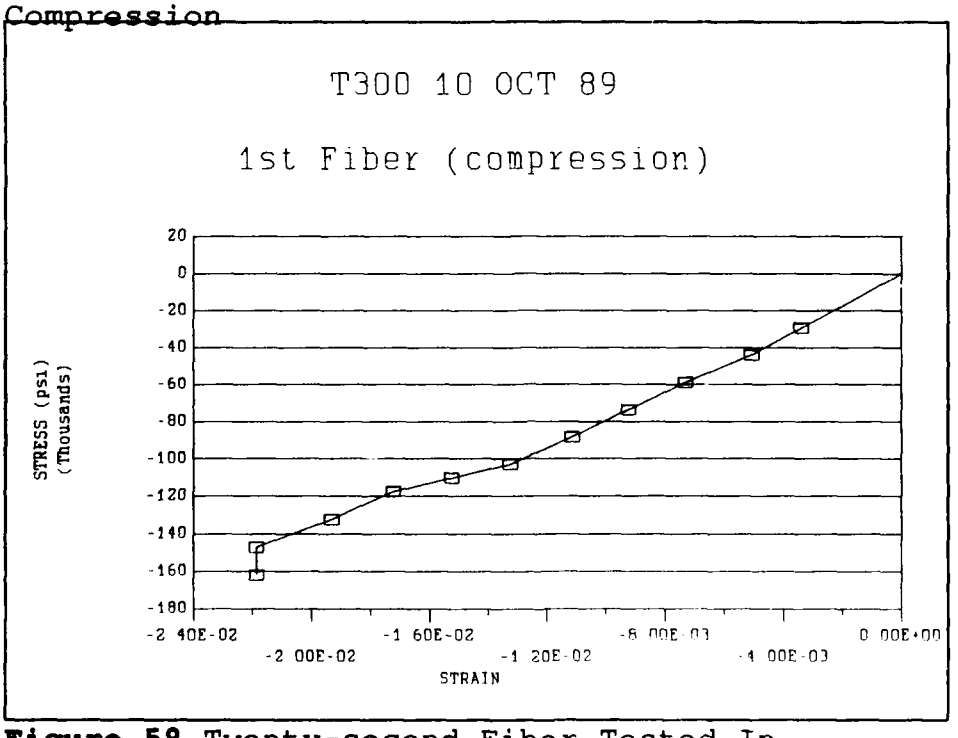

Figure 58 Twenty-second Fiber Tested In Compression

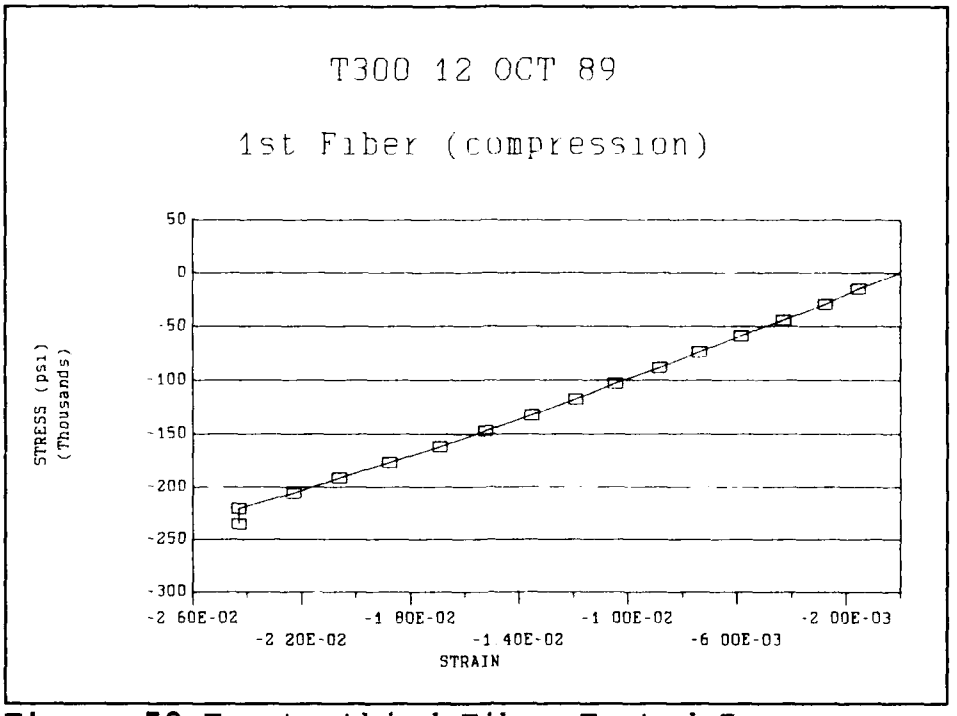

Figure 59 Twenty-third Fiber Tested In Compression

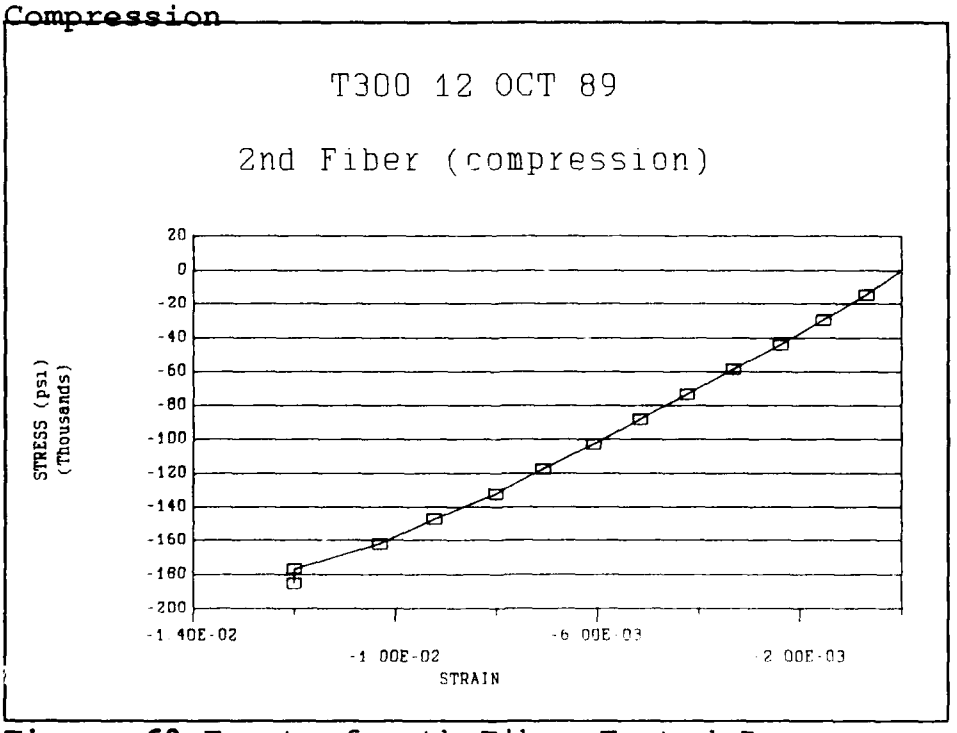

Figure 60 Twenty-fourth Fiber Tested In Compression

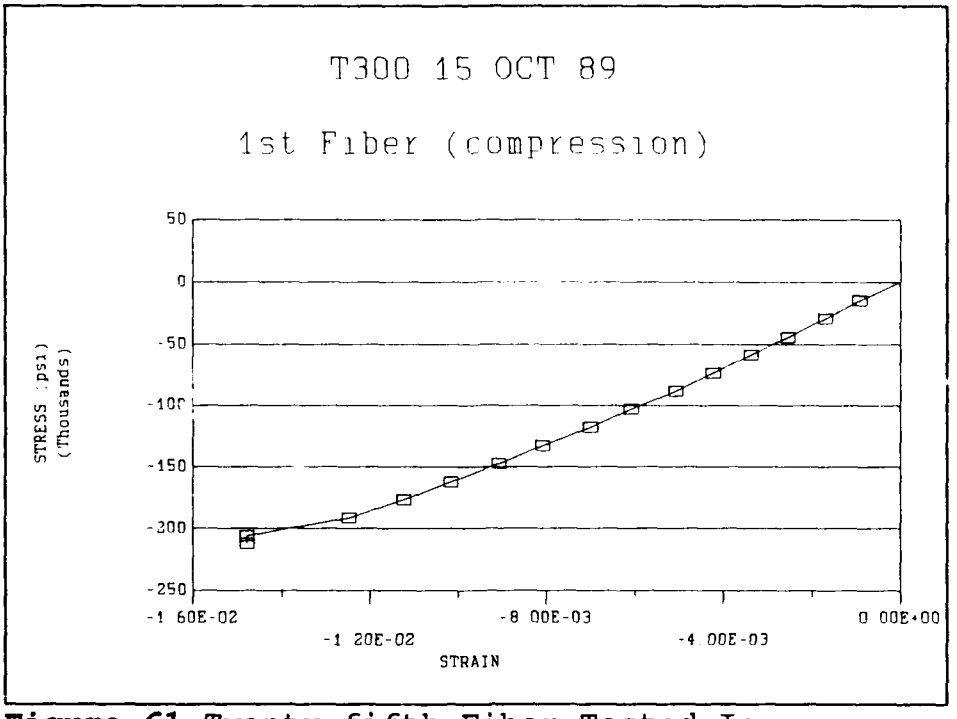

Figure 61 Twenty-fifth Fiber Tested In Compression

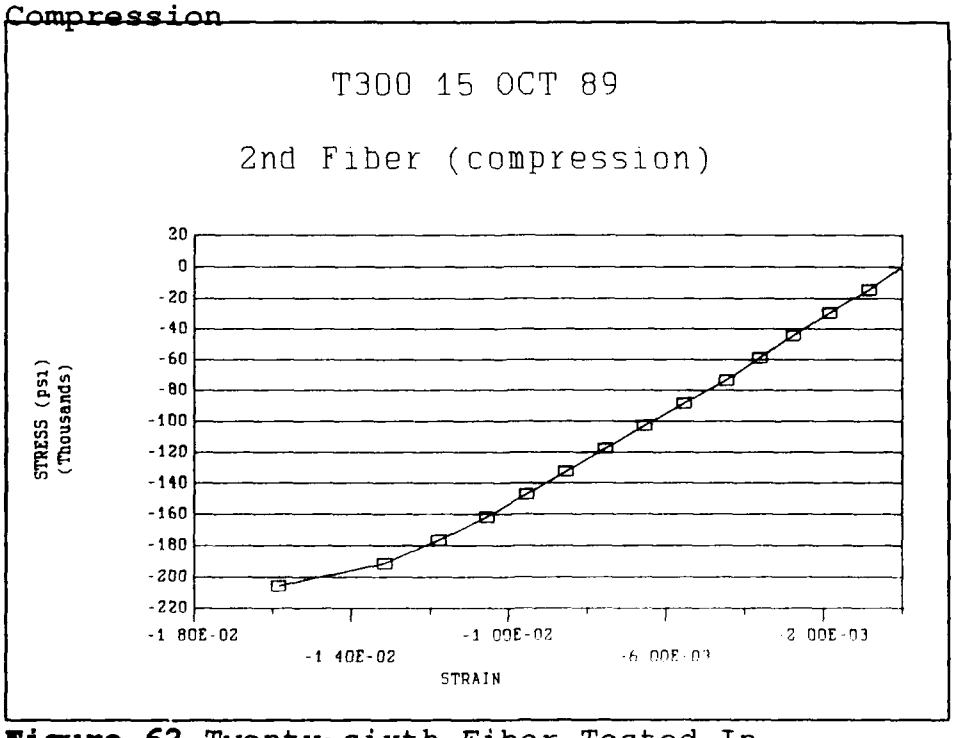

Figure 62 Twenty-sixth Fiber Tested In Compression

Table XX Table Of The T300 Fiber Data

#	DIAM μm	L_t mm	σ MPa	σ ksi	E_t Mpsi	E_t Mpsi
1	8.89	0.11	803.1	116.47	*	*
2	6.10	0.11	483.3	70.090	*	*
3	6.10	0.11	824.0	119.50	*	*
4	6.10	0.11	1478	214.30	*	*
5	6.67	0.11	523.1	75.87	*	*
6	6.67	0.11	1158	168.00	*	*
7	7.78	0.11	410.7	59.560	*	*
8	6.67	0.11	594.4	86.210	*	*
9	7.78	0.11	438.5	63.600	*	*
10	6.67	0.11	689.5	100.00	*	*
11	5.55	0.11	1048.	152.00	*	*
12	6.67	0.11	653.6	94.800	*	*
13	7.22	0.11	426.1	61.800	*	*
14	8.33	0.11	457.3	66.330	*	*
15	6.67	0.11	758.4	110.00	*	*
16	7.78	0.11	611.7	88.710	8.9	*
17	6.11	0.11	1133	164.38	9.9	*
18	6.67	0.11	951.1	137.94	12.9	*
19	6.11	0.11	1318	191.10	15.75	*
20	6.11	0.11	1133	164.39	16.79	*
21	6.11	0.12	1558	226.03	19.44	*
22	6.67	0.11	1308	189.67	14.00	*
23	5.25	0.11	949.9	137.77	14.56	*
24	6.11	0.11	1204	174.66	14.37	*
25	5.56	0.11	1369	198.50	19.20	*
26	6.11	0.14	1842	267.12	20.40	20.43
27	6.11	0.11	1275	184.93	18.80	19.40
28	6.11	0.11	1658	240.41	18.50	23.70
29	6.11	0.115	1275	184.98	20.70	21.70
30	6.11	0.13	1700	246.60	17.25	20.10
31	6.11	0.115	1204	174.60	14.80	14.72
32	6.11	0.14	1331	193.00	22.54	23.92
33	6.11	0.14	1275	184.90	22.23	22.40
34	6.11	0.14	991.5	143.80	12.77	12.29
35	7.22	0.065	1116	161.87	7.95	*
36	7.22	0.065	1623	235.45	9.43	*
37	7.22	0.065	1278	185.42	16.40	*
38	7.22	0.065	1461	211.90	11.19	*

Appendix E: P100 Data

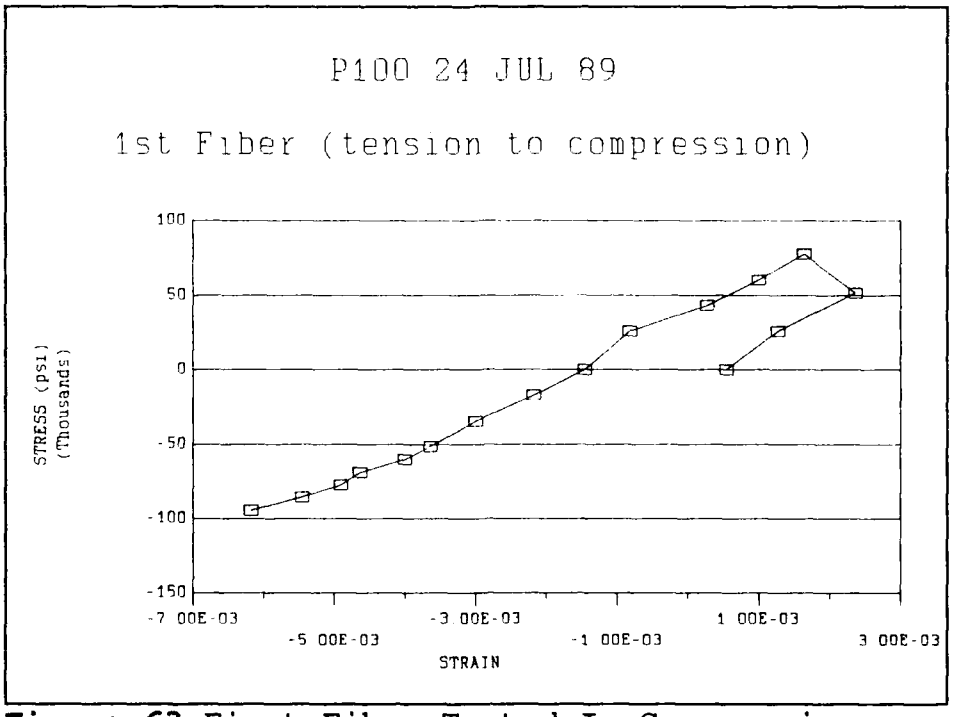

Figure 63 First Fiber Tested In Compression

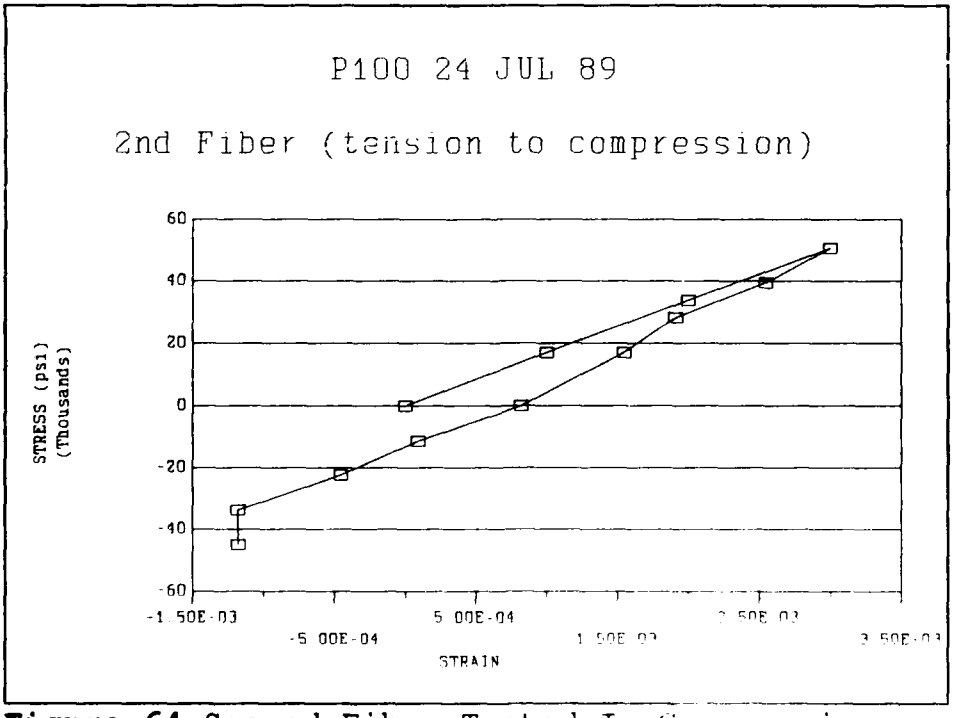

Figure 64 Second Fiber Tested In Compression

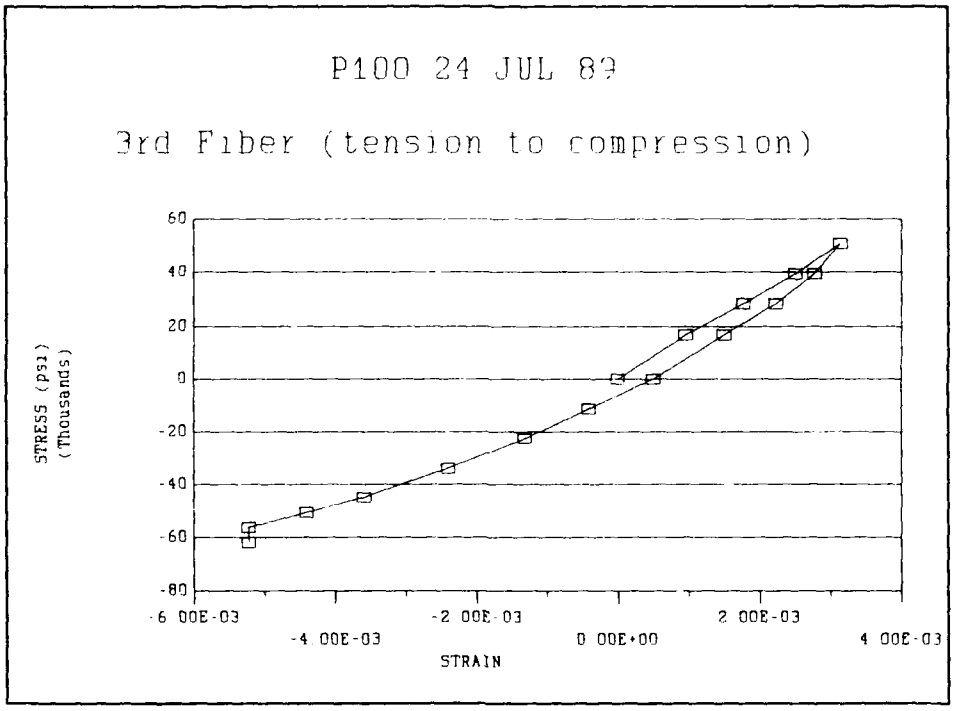

Figure 65 Third Fiber Tested In Compression

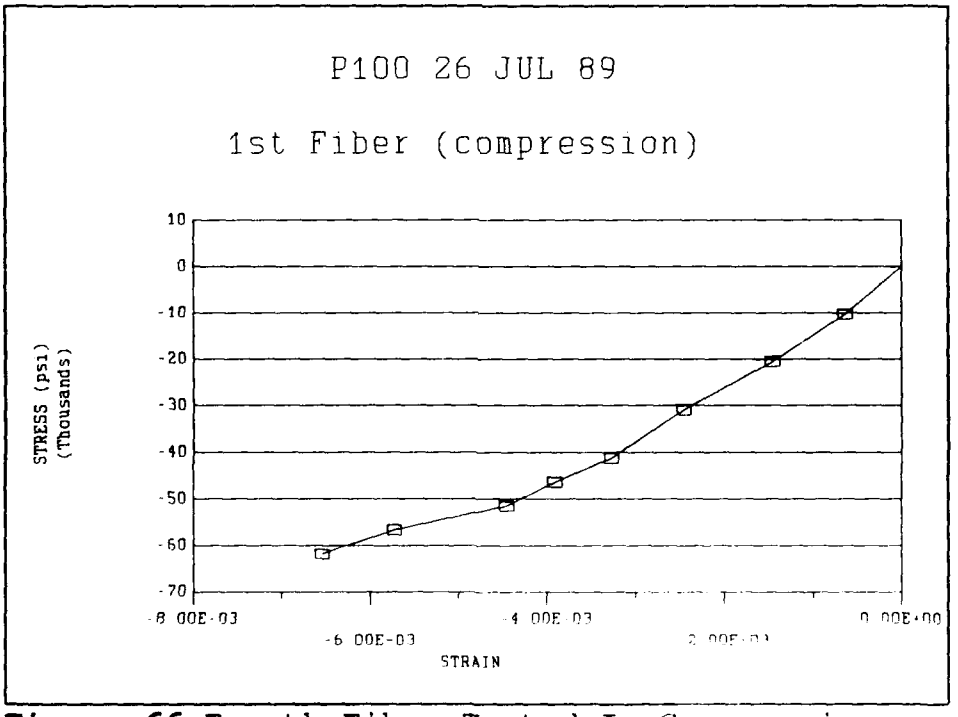

Figure 66 Fourth Fiber Tested In Compression

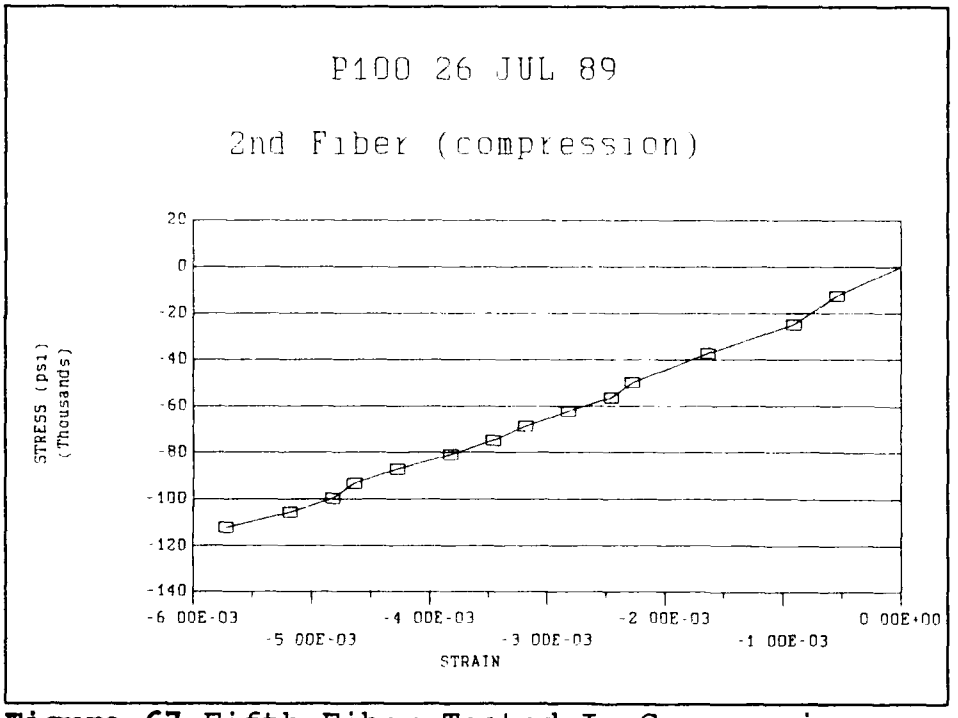

Figure 67 Fifth Fiber Tested In Compression

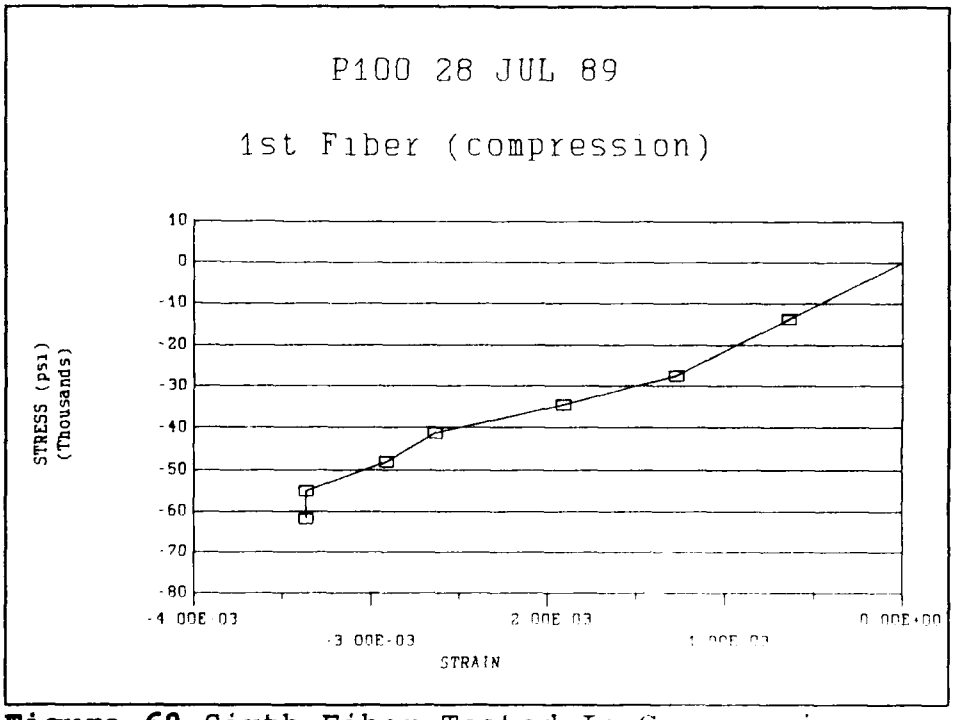

Figure 68 Sixth Fiber Tested In Compression

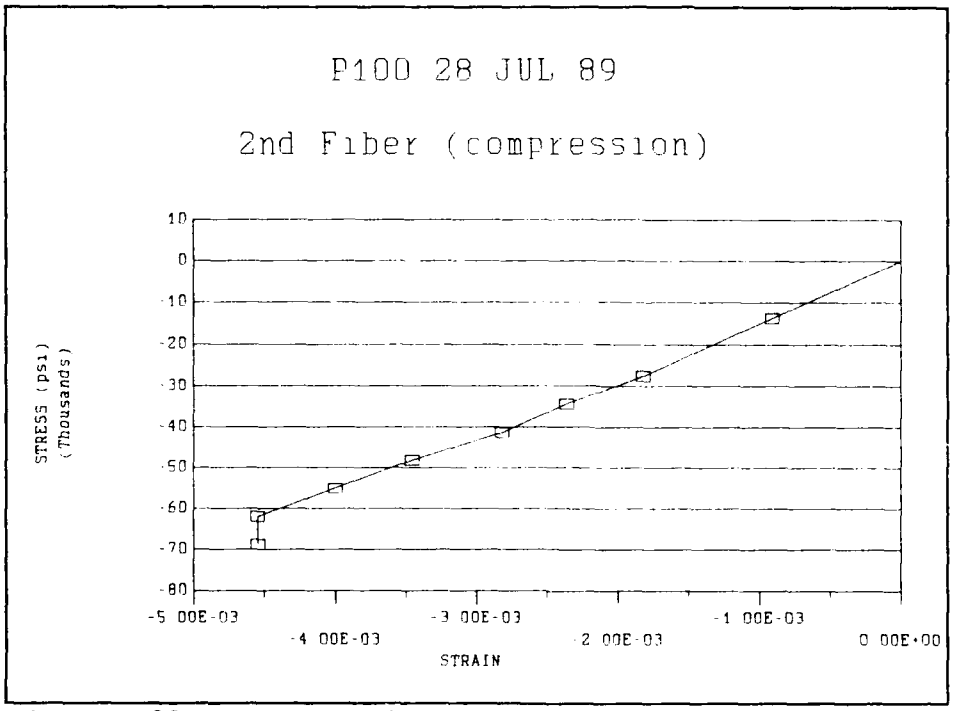

Figure 69 Seventh Fiber Tested In Compression

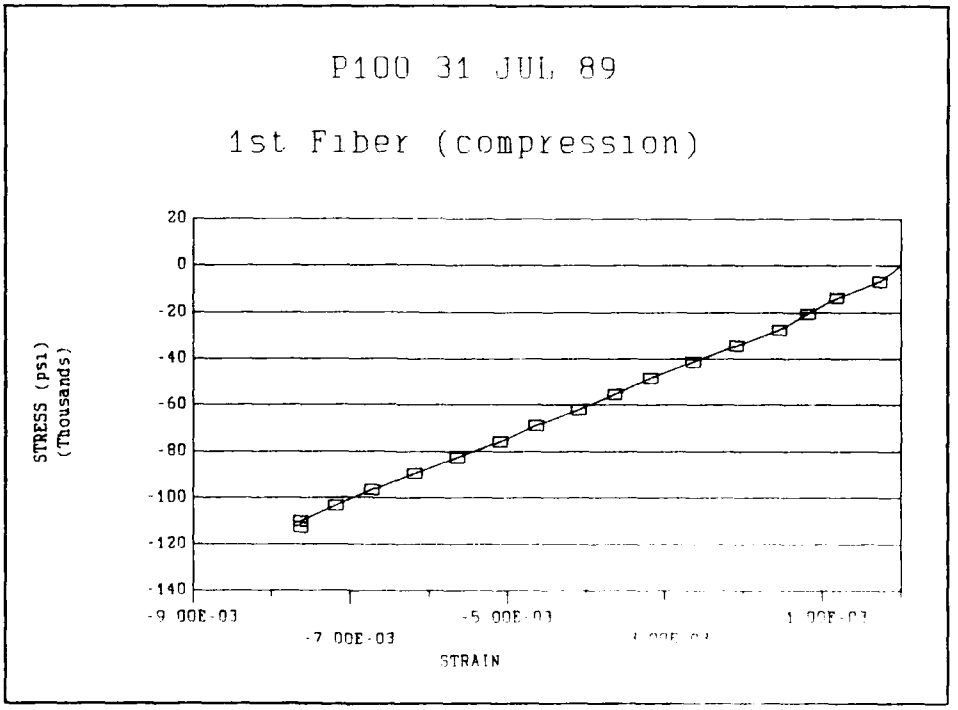

Figure 70 Eighth Fiber Tested In Compression

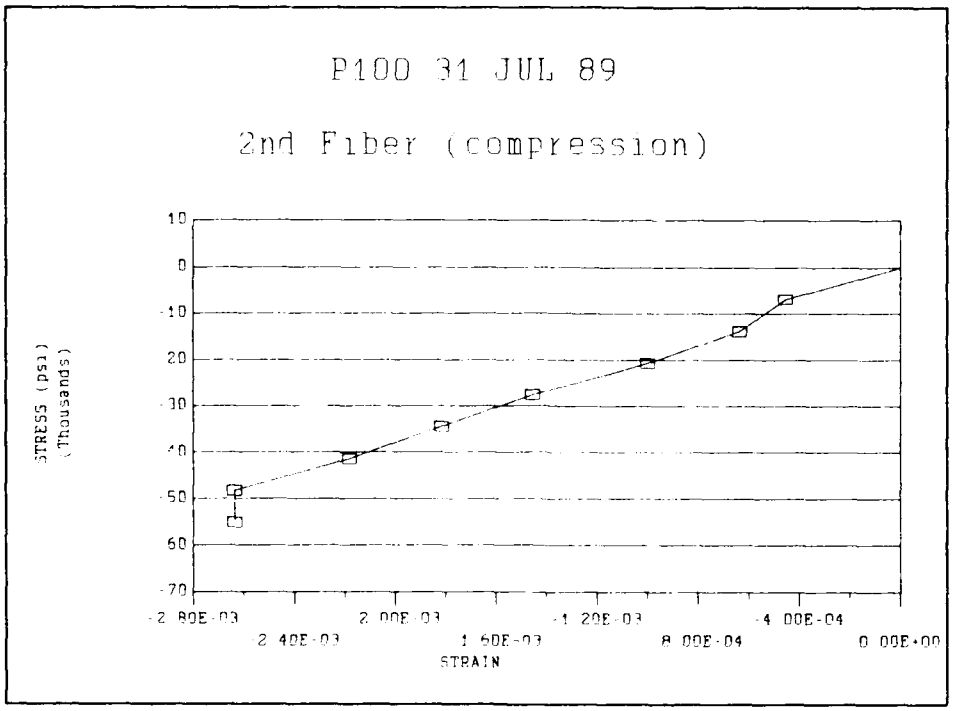

Figure 71 Nineth Fiber Tested In Compression

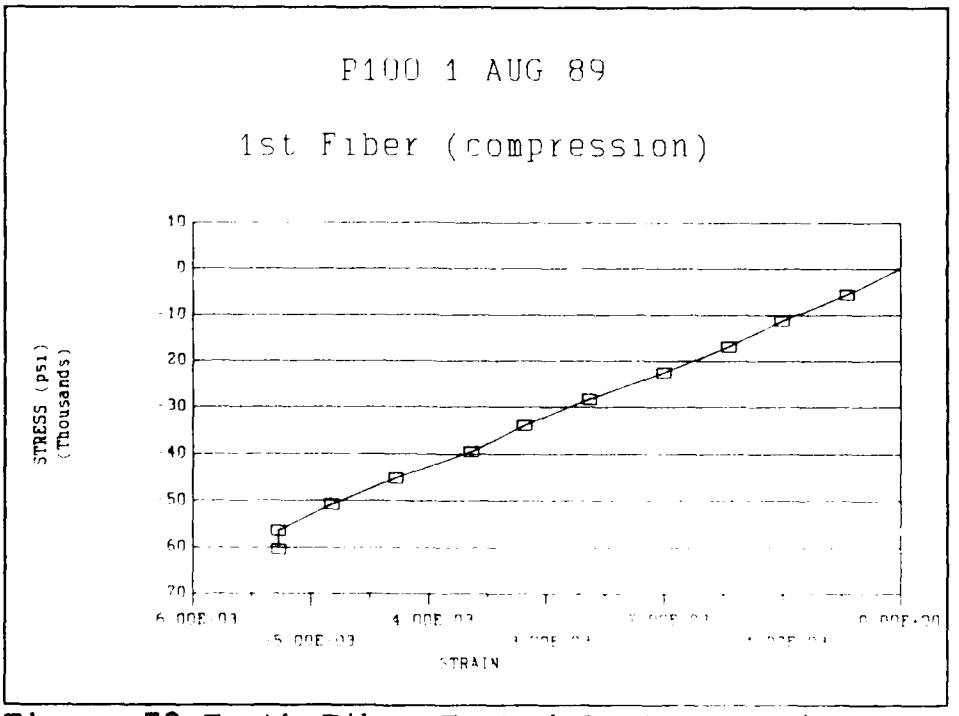

Figure 72 Tenth Fiber Tested In Compression

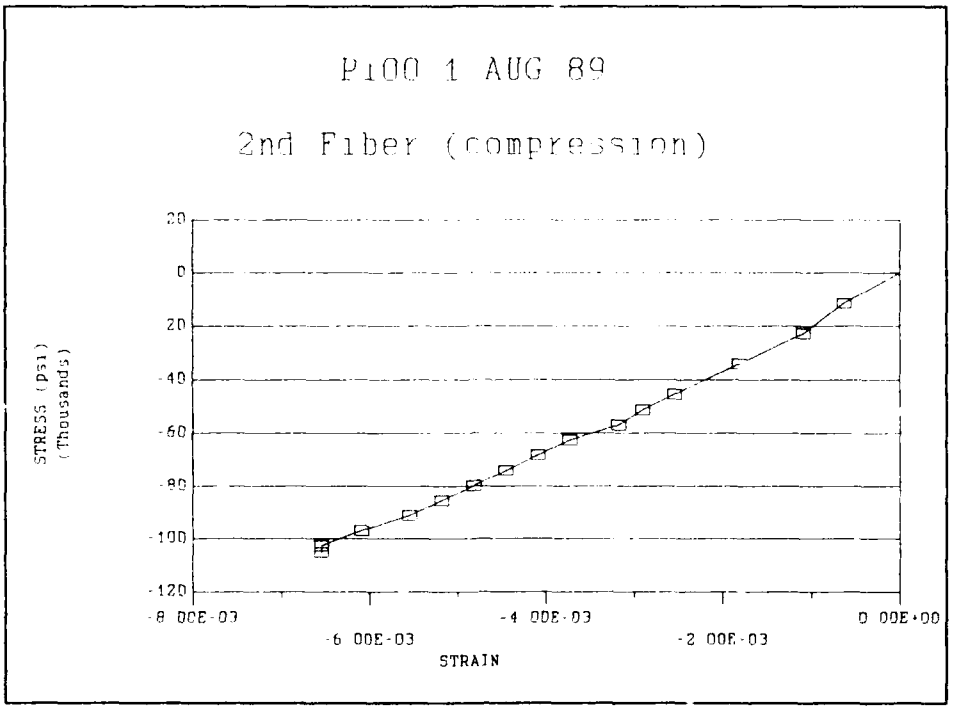

Figure 73 Eleventh Fiber Tested In Compression

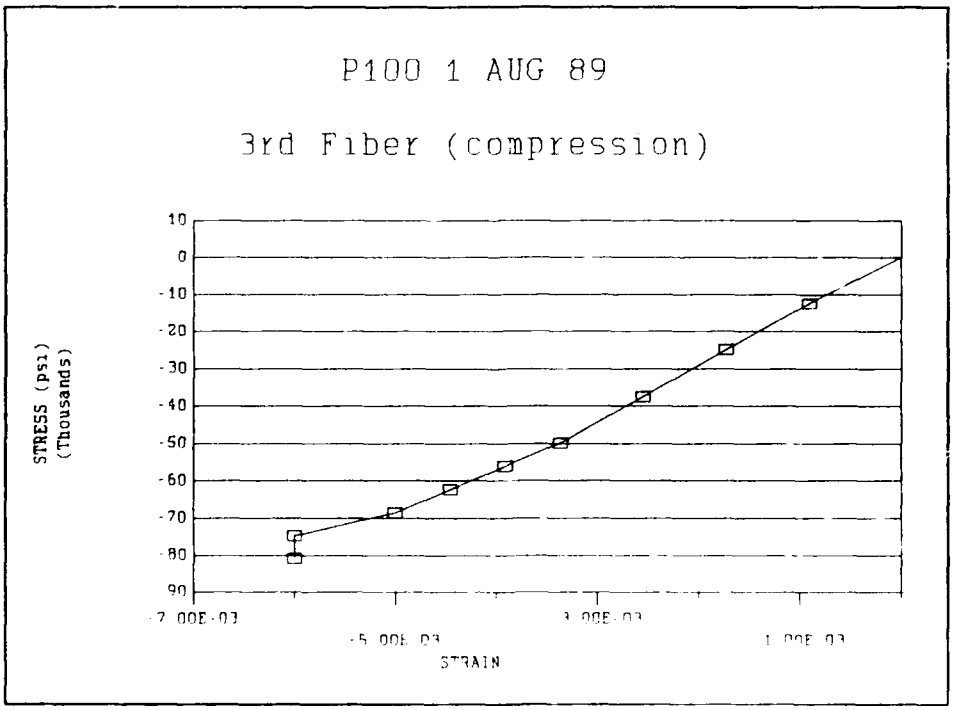

Figure 74 Twelfth Fiber Tested In Compression

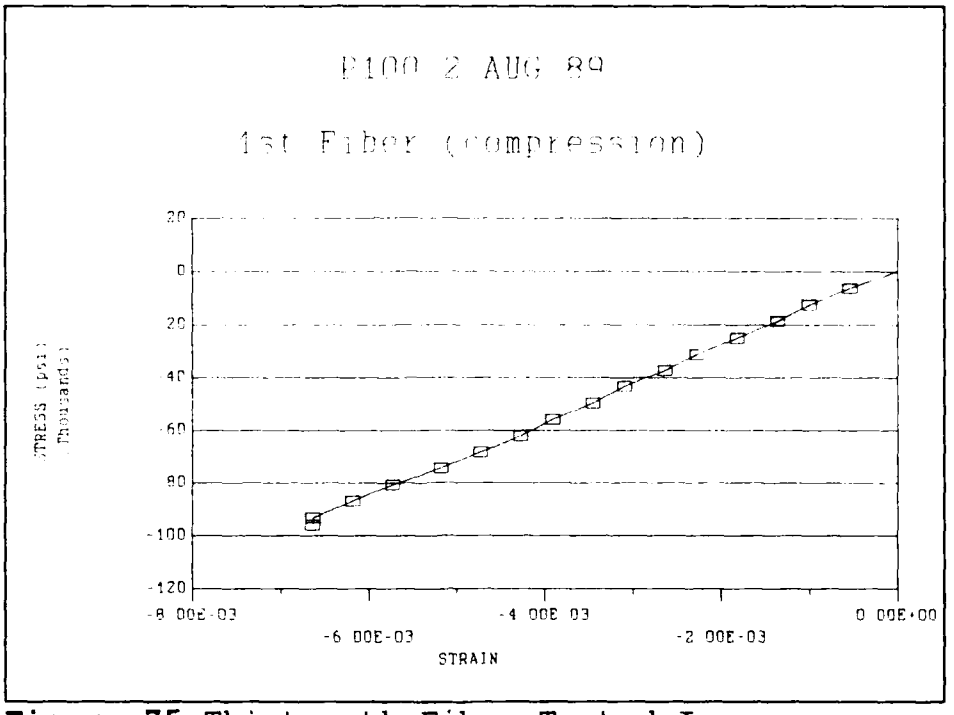

Figure 75 Thirteenth Fiber Tested In Compression

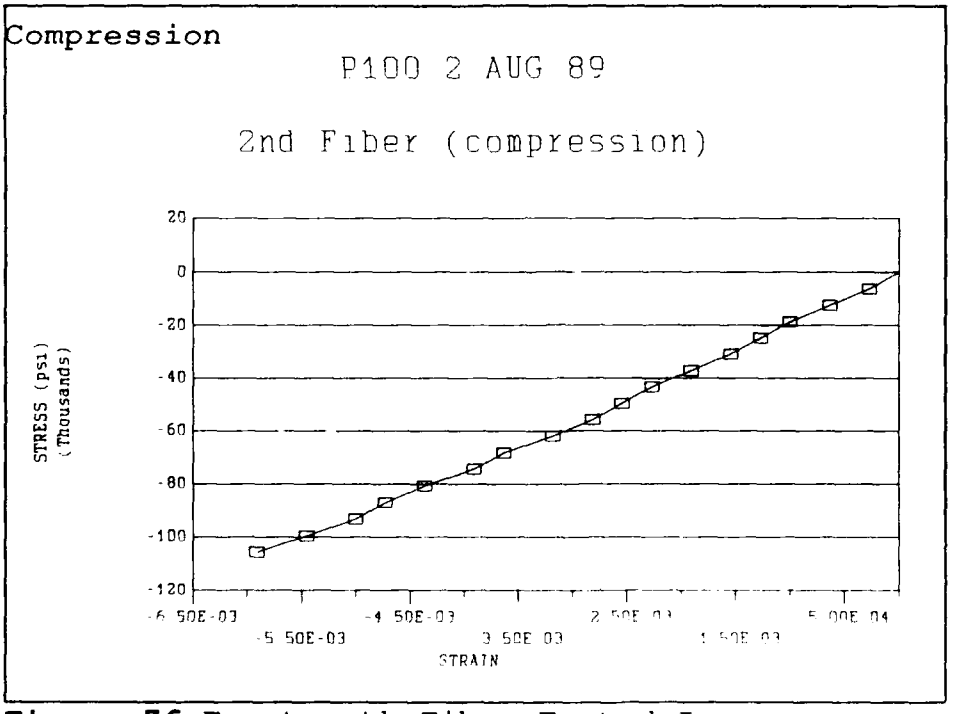

Figure 76 Fourteenth Fiber Tested In Compression

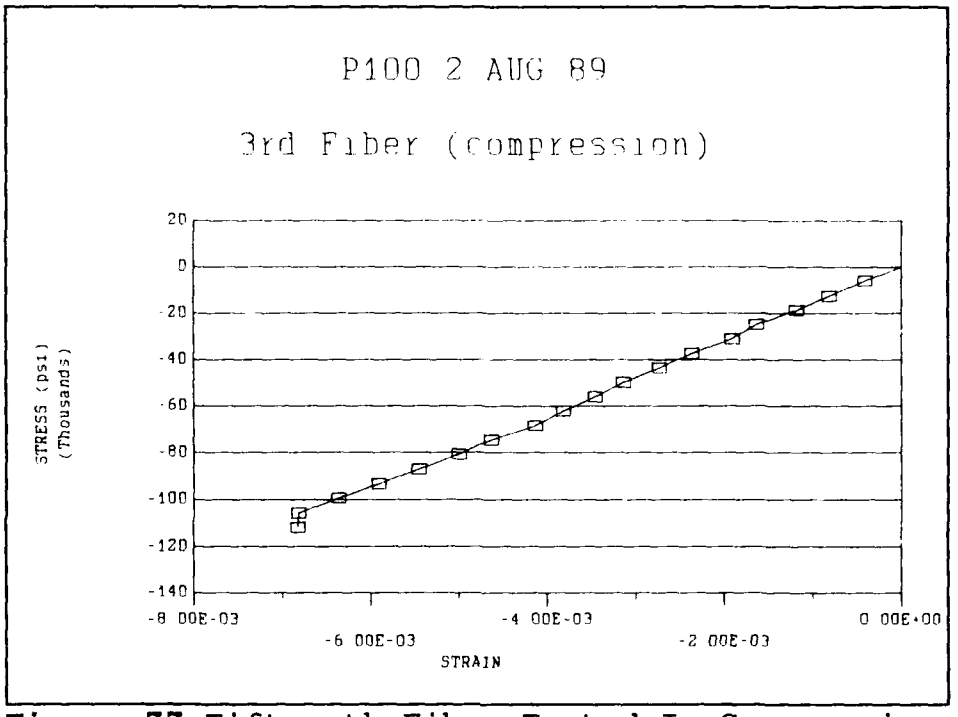

Figure 77 Fifteenth Fiber Tested In Compression

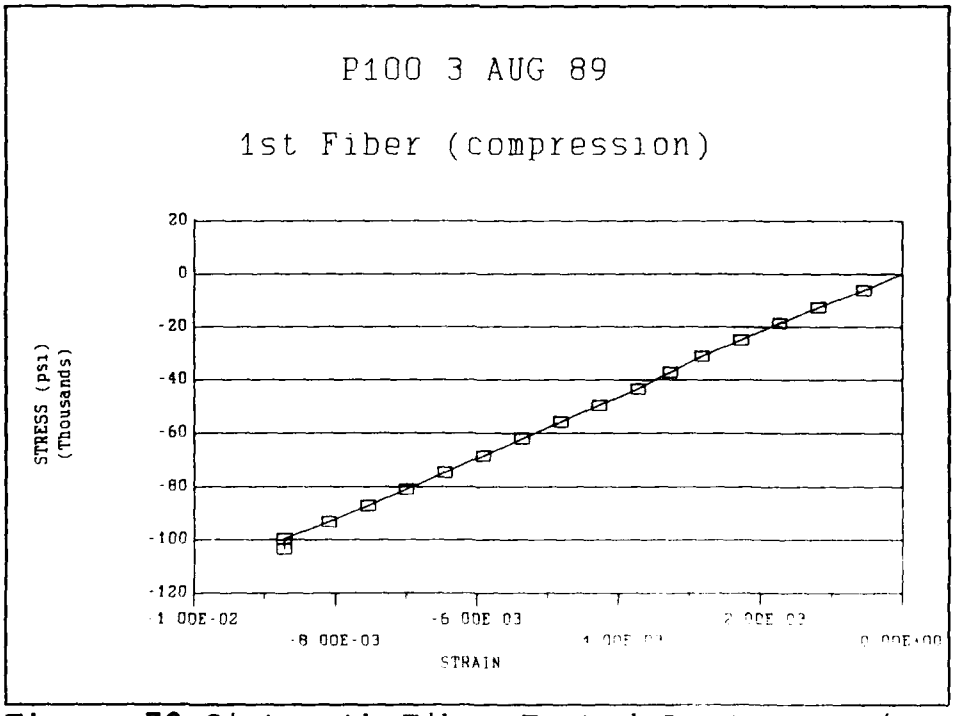

Figure 78 Sixteenth Fiber Tested In Compression

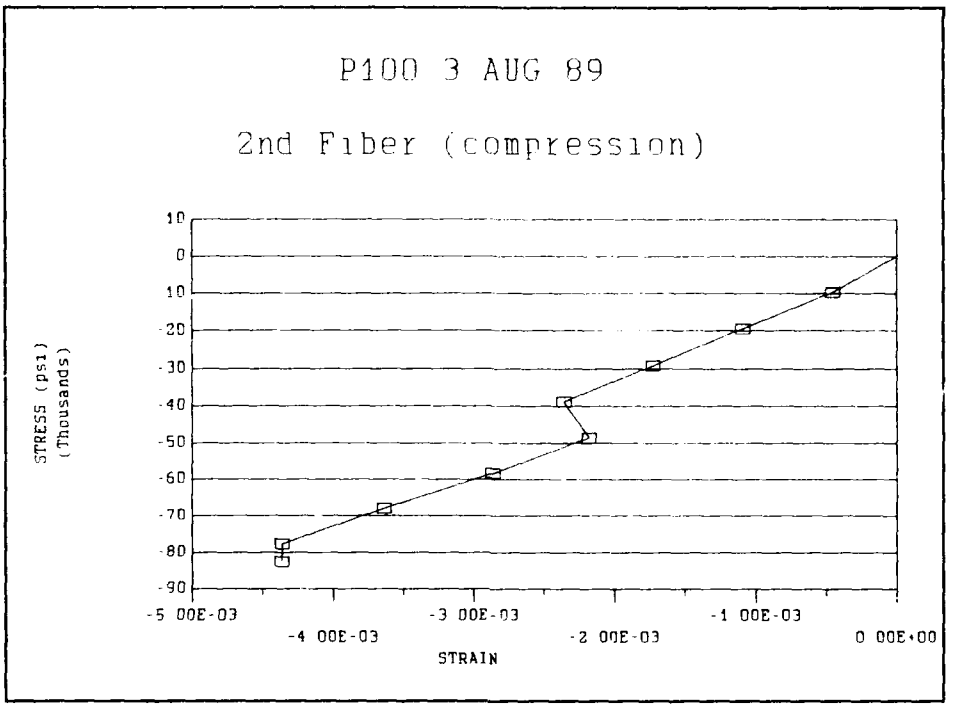

Figure 79 Seventeenth Fiber Tested In Compression

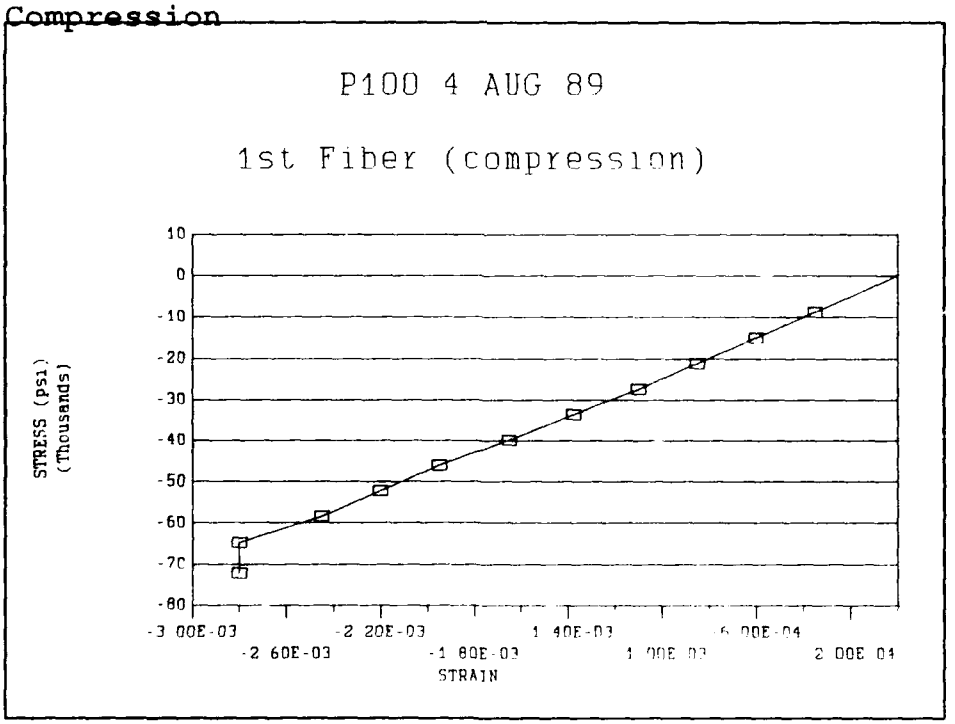

Figure 80 Eighteenth Fiber Tested In Compression

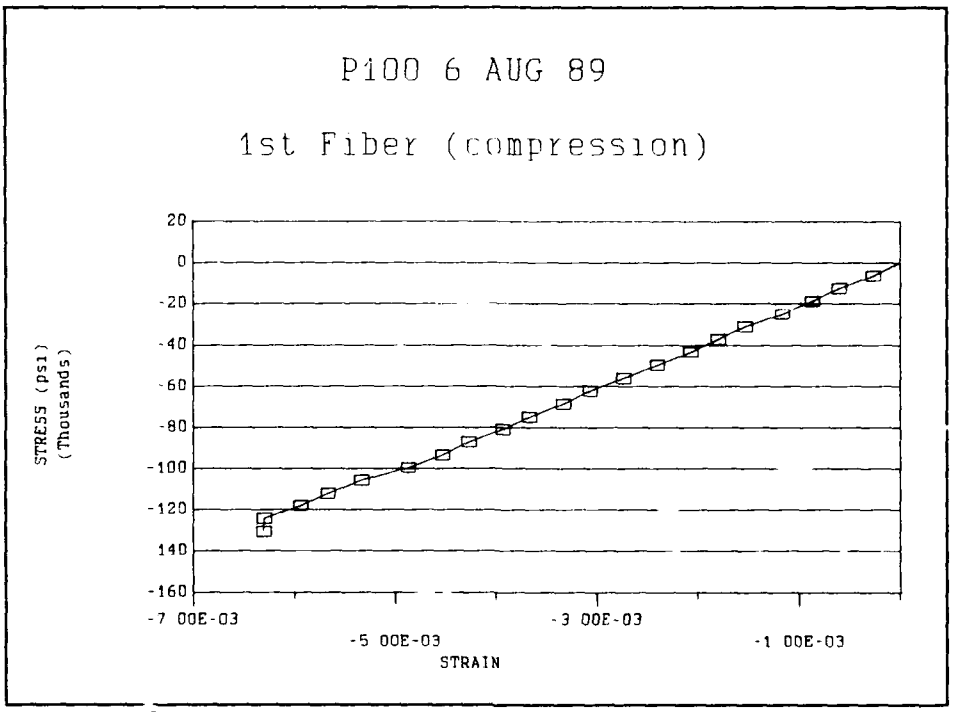

Figure 81 Nineteenth Fiber Tested In Compression

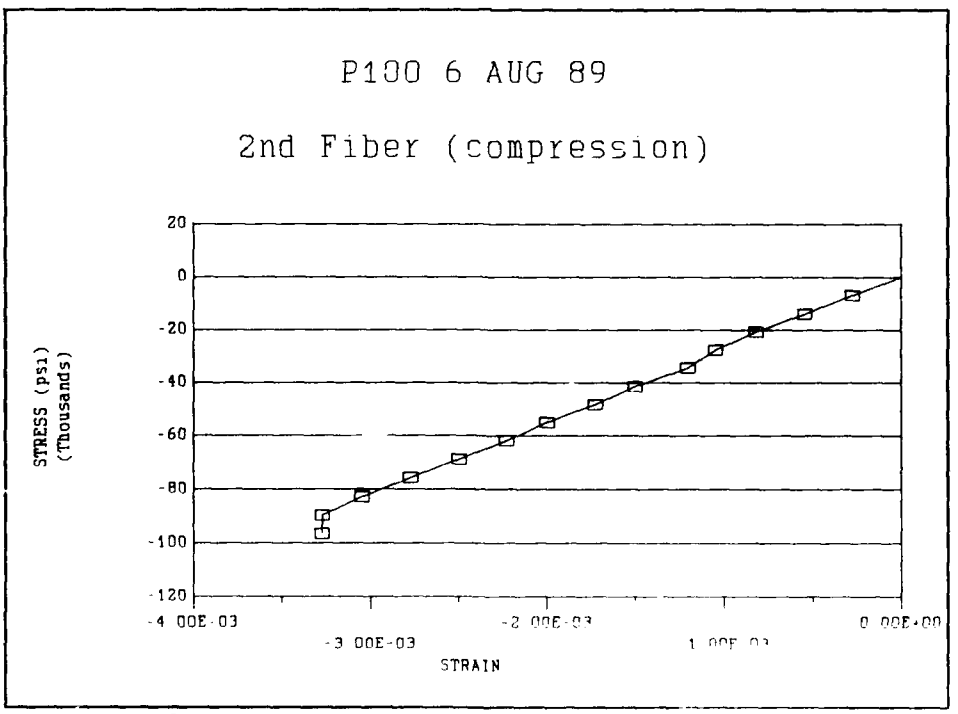

Figure 82 Twentieth Fiber Tested In Compression

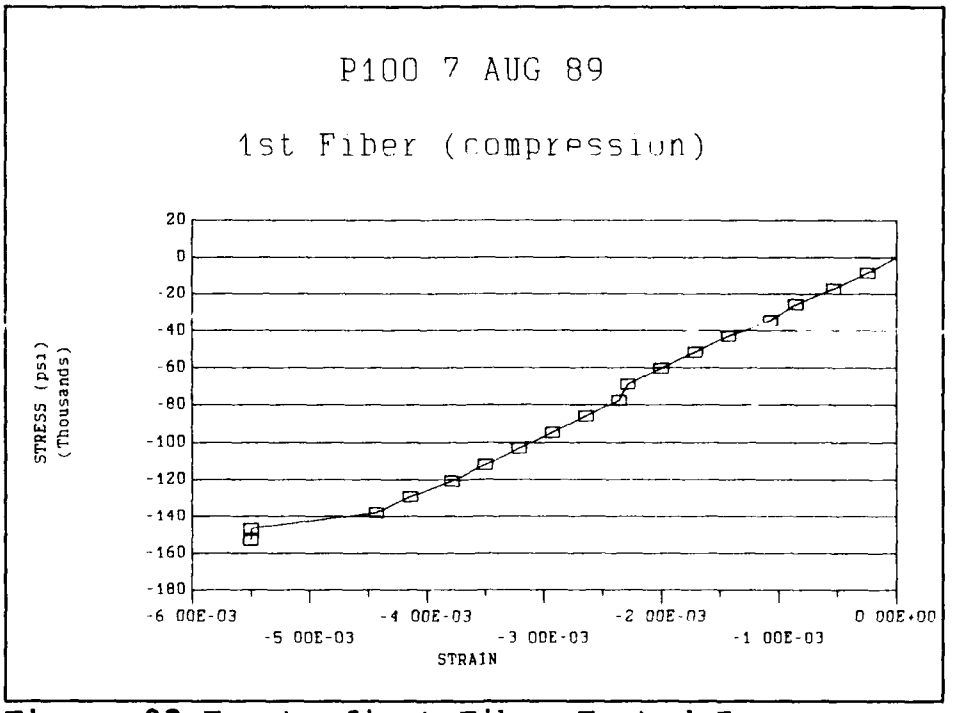

Figure 83 Twenty-first Fiber Tested In Compression

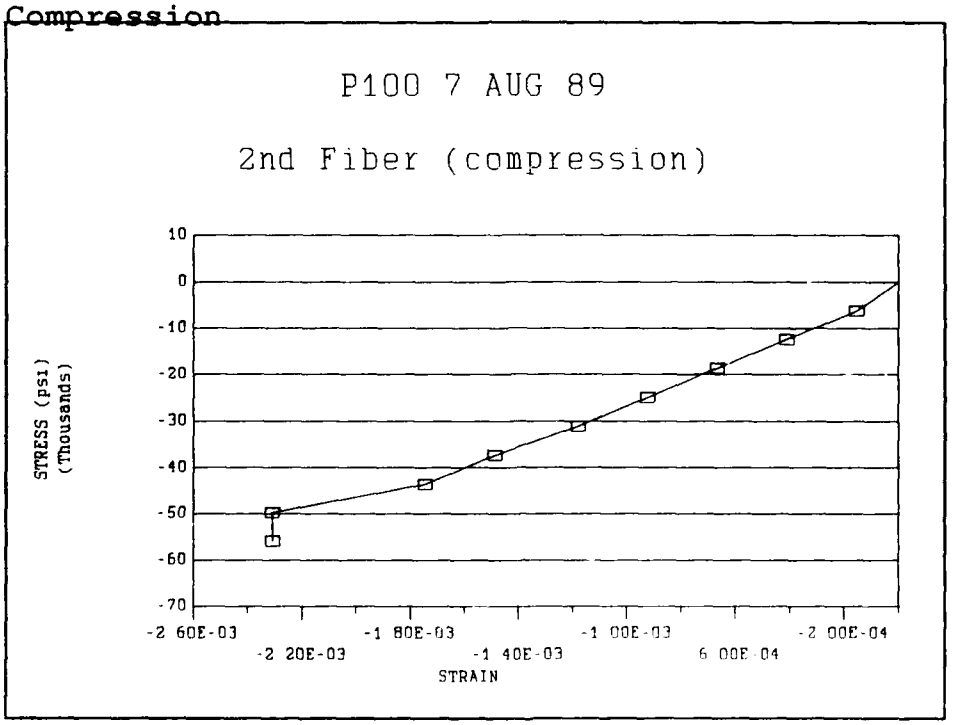

Figure 84 Twenty-second Fiber Tested In Compression

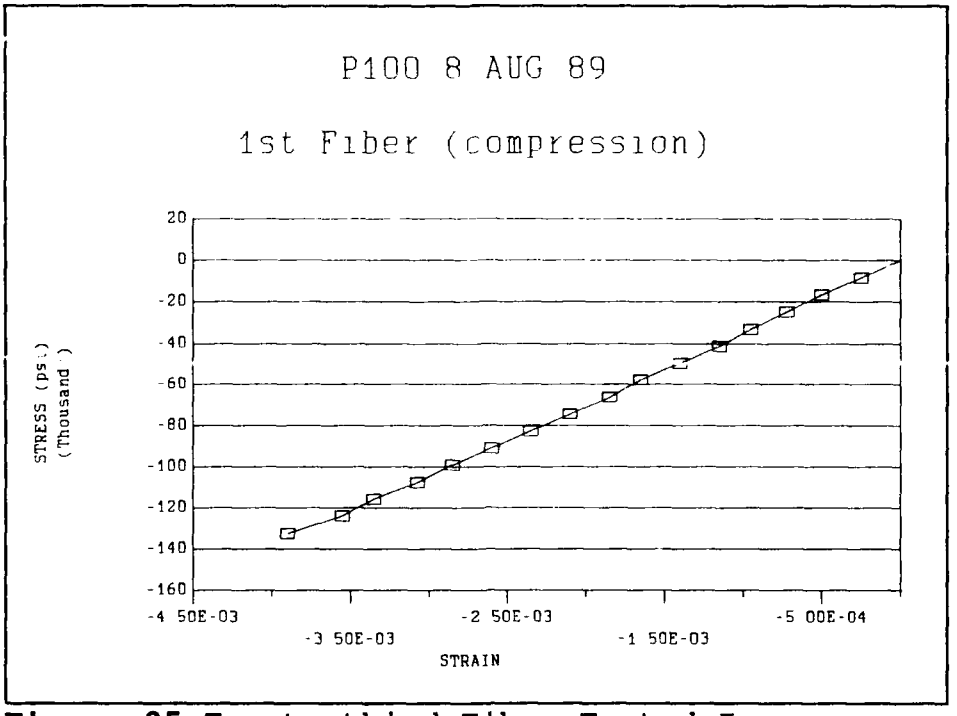

Figure 85 Twenty-third Fiber Tested In Compression

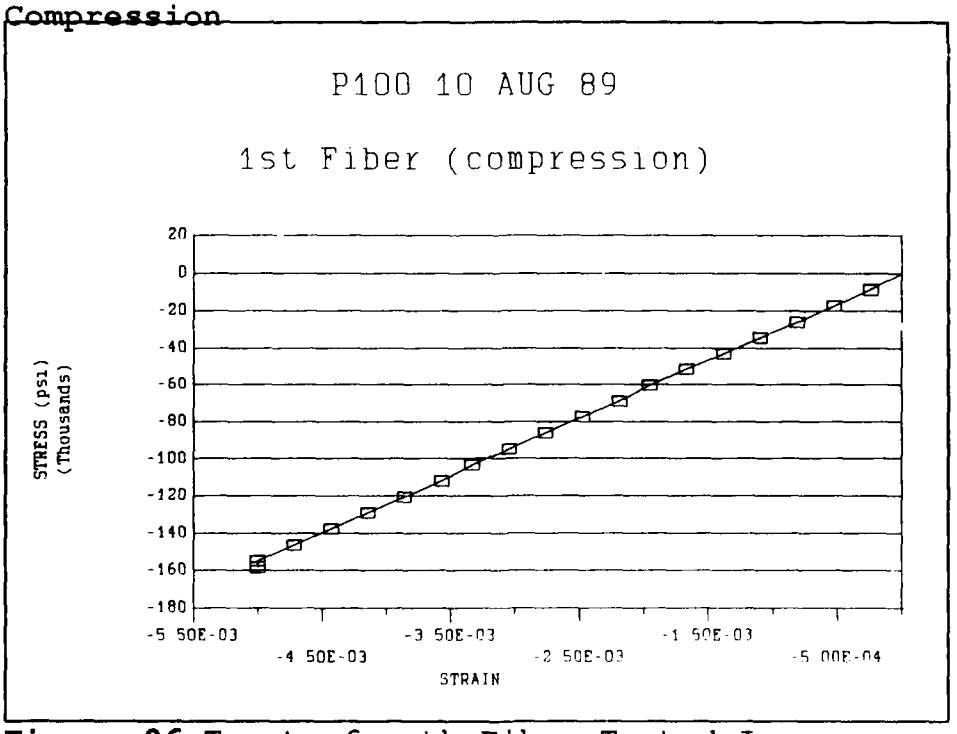

Figure 86 Twenty-fourth Fiber Tested In Compression

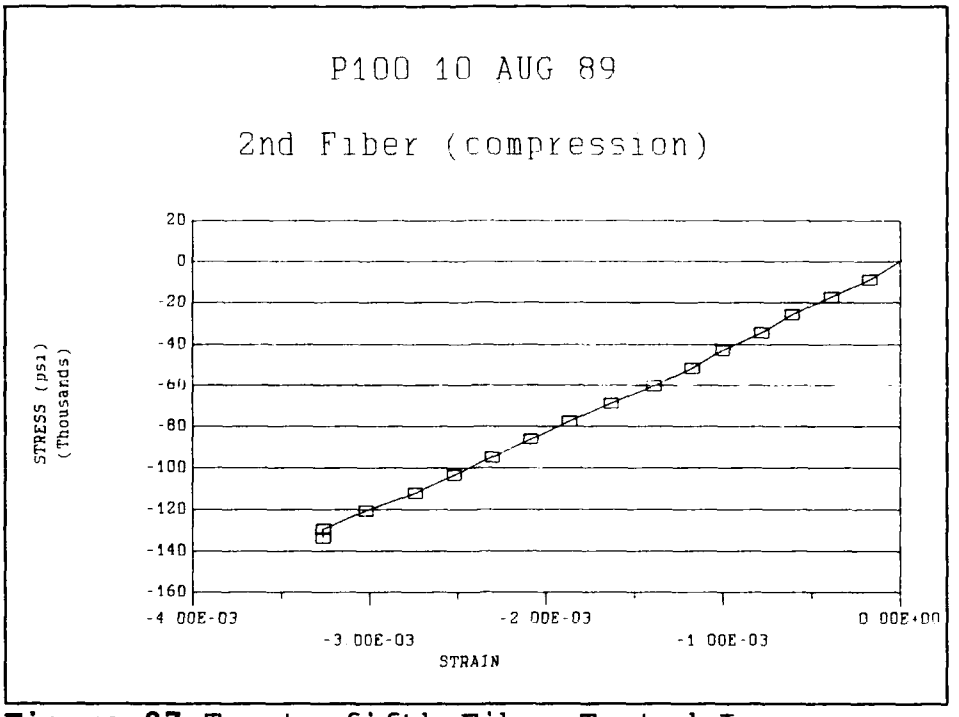

Figure 87 Twenty-fifth Fiber Tested In Compression

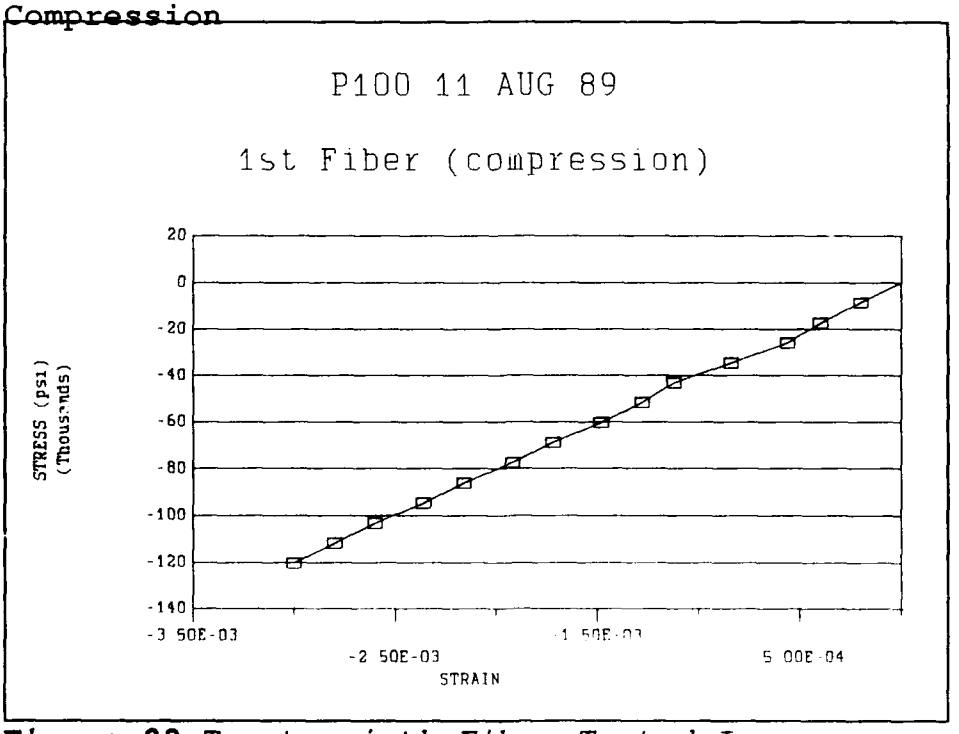

Figure 88 Twenty-sixth Fiber Tested In Compression

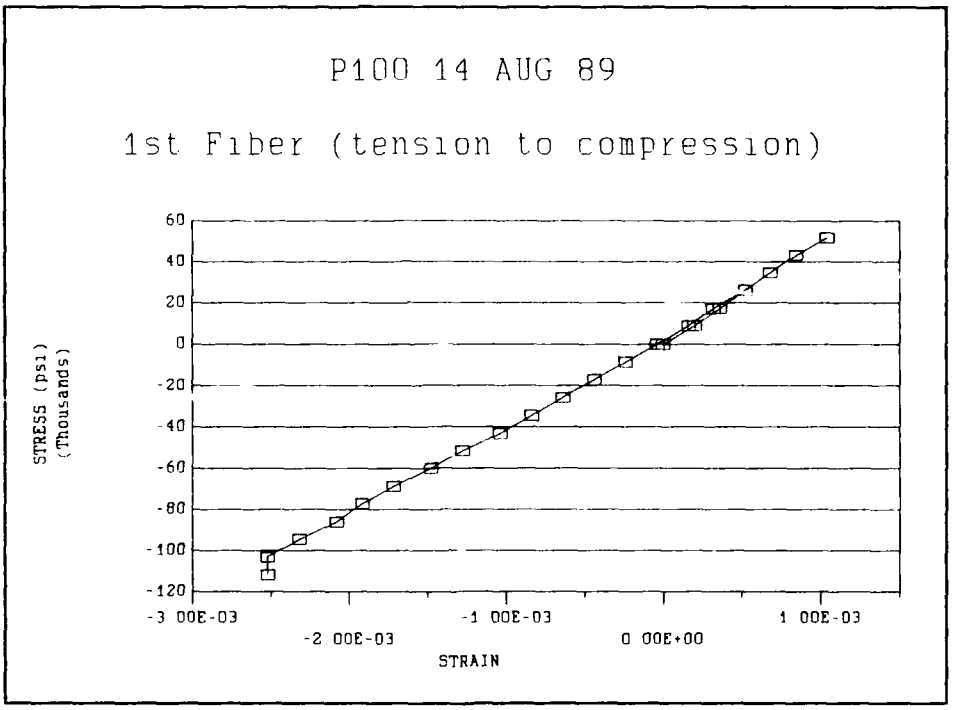

Figure 89 Twenty-seventh Fiber Tested In Compression

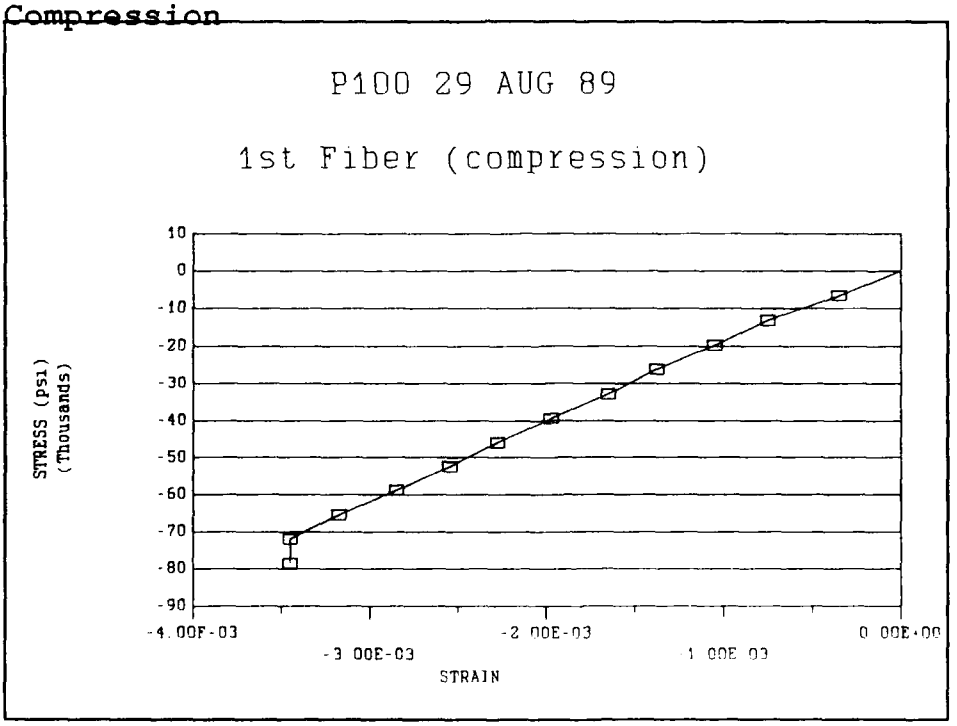

Figure 90 Twenty-eighth Fiber Tested In Compression

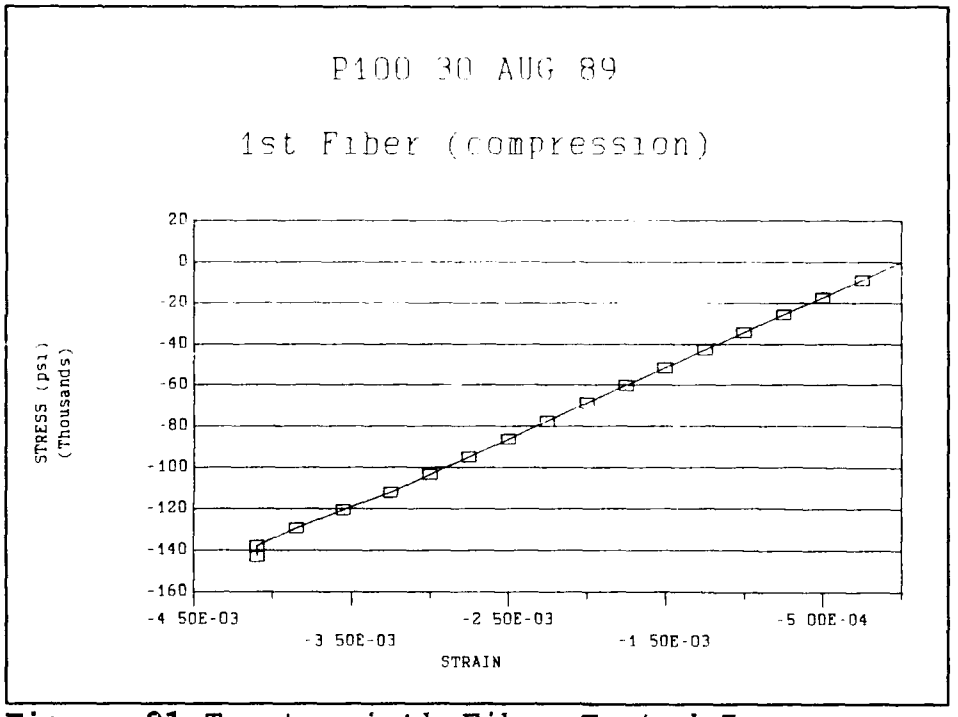

Figure 91 Twenty-ninth Fiber Tested In Compression

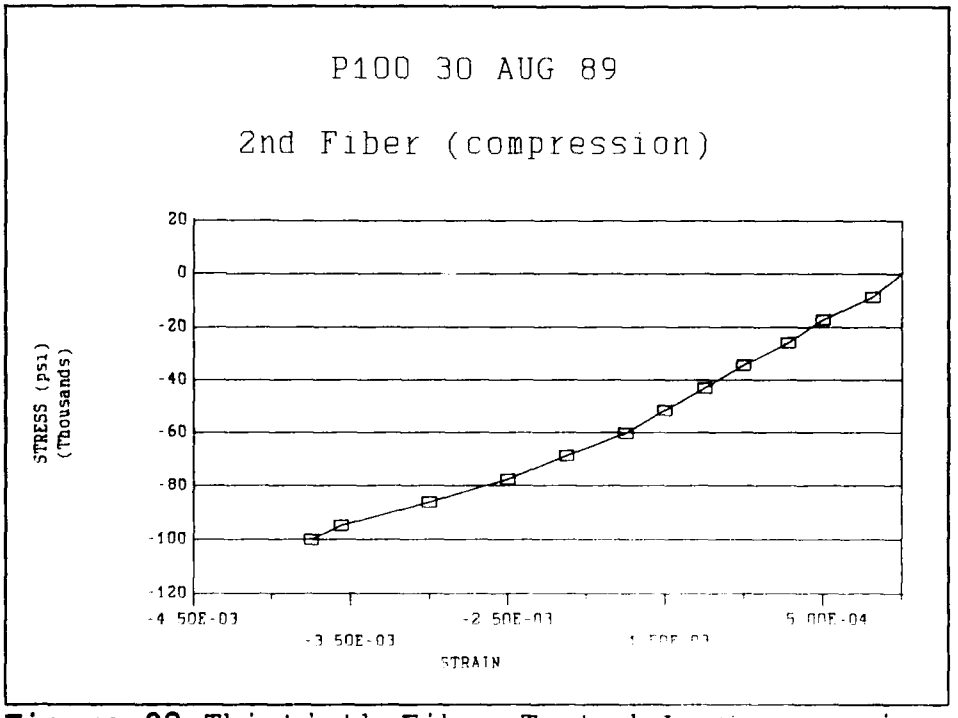

Figure 92 Thirtieth Fiber Tested In Compression

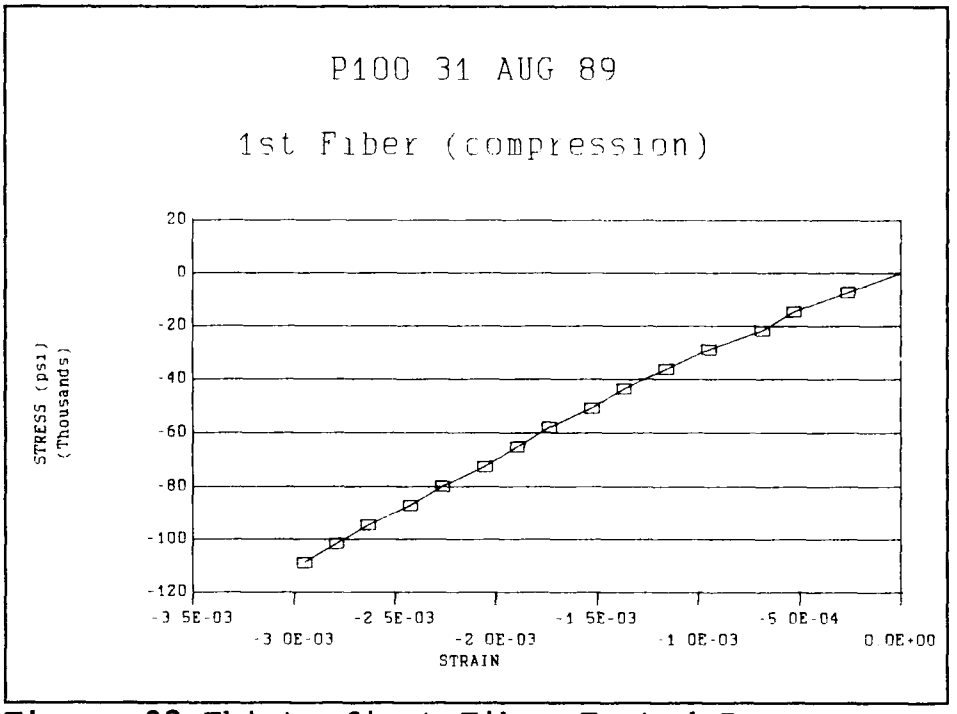

Figure 93 Thirty-first Fiber Tested In Compression

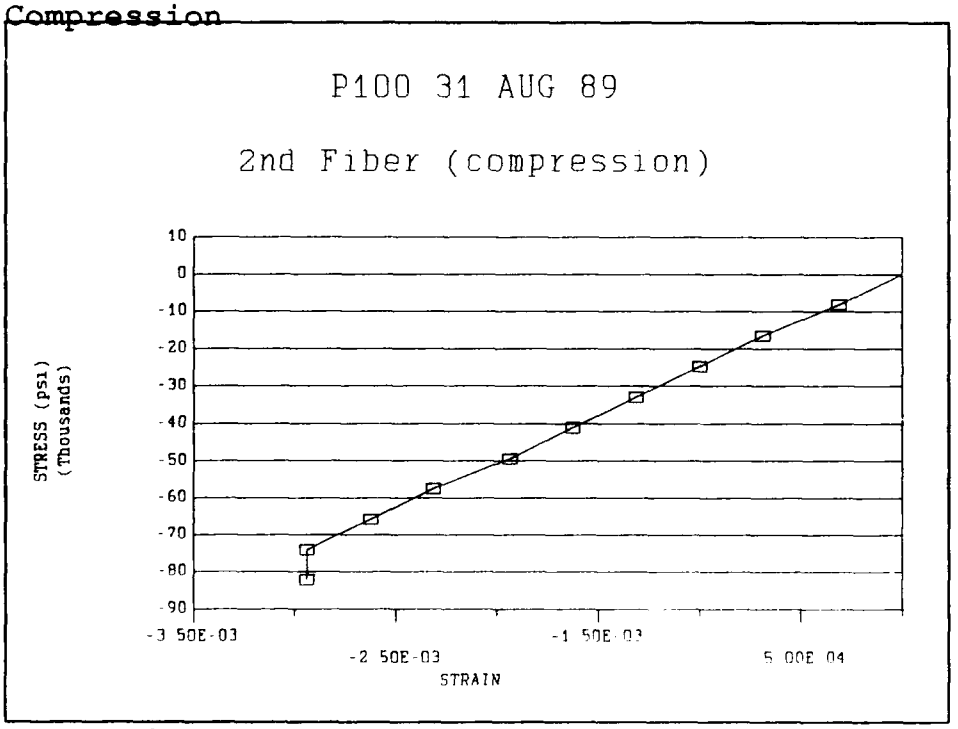

Figure 94 Thirty-second Fiber Tested In Compression

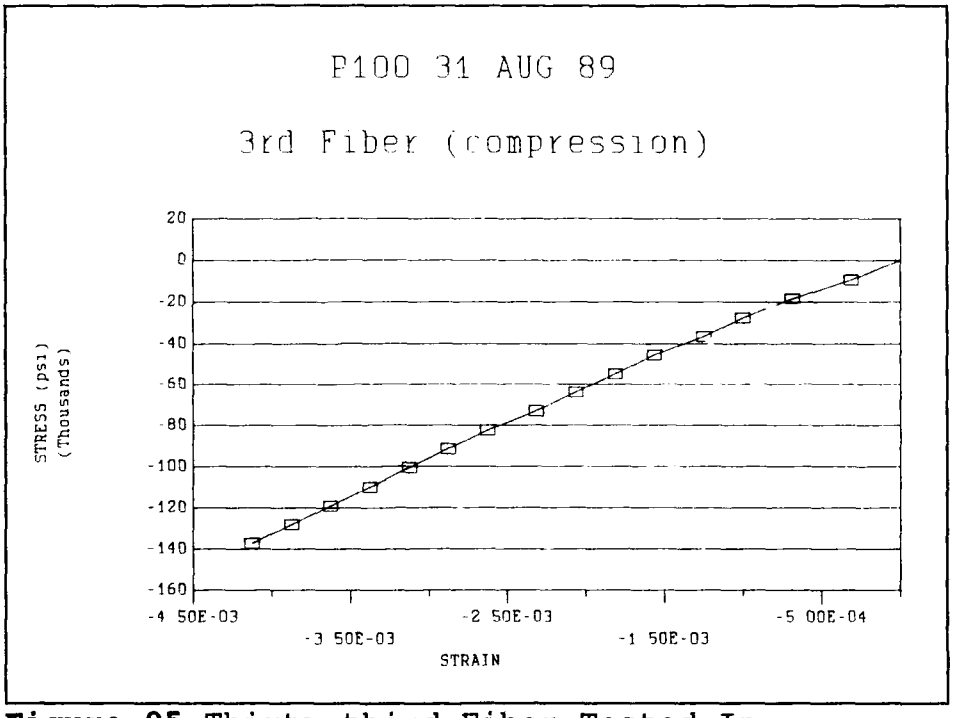

Figure 95 Thirty-third Fiber Tested In Compression

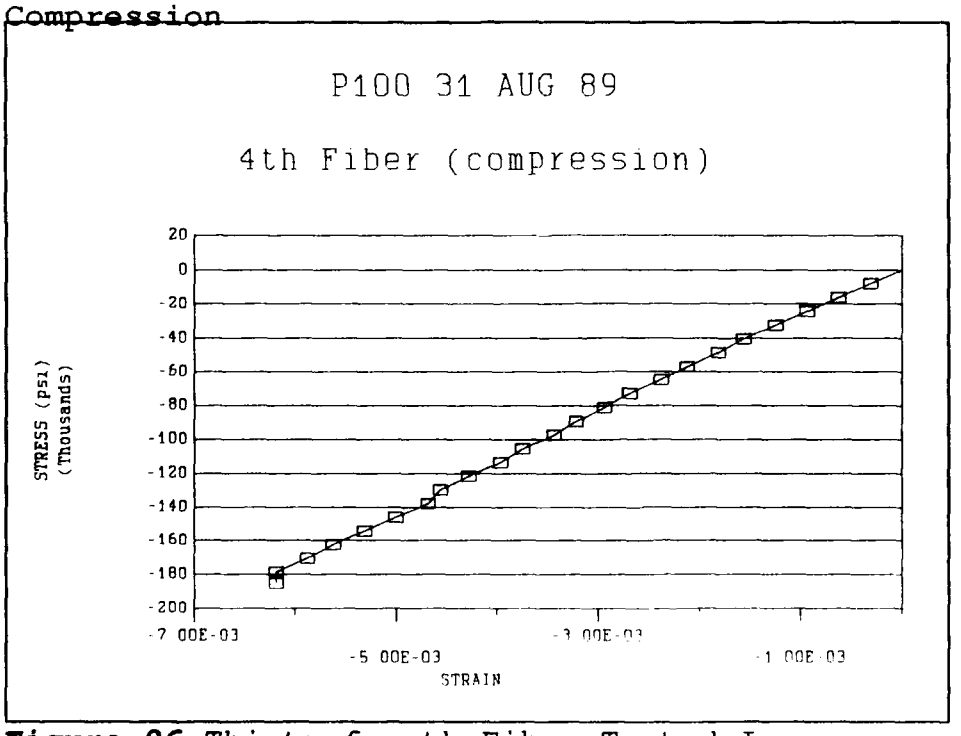

Figure 96 Thirty-fourth Fiber Tested In Compression

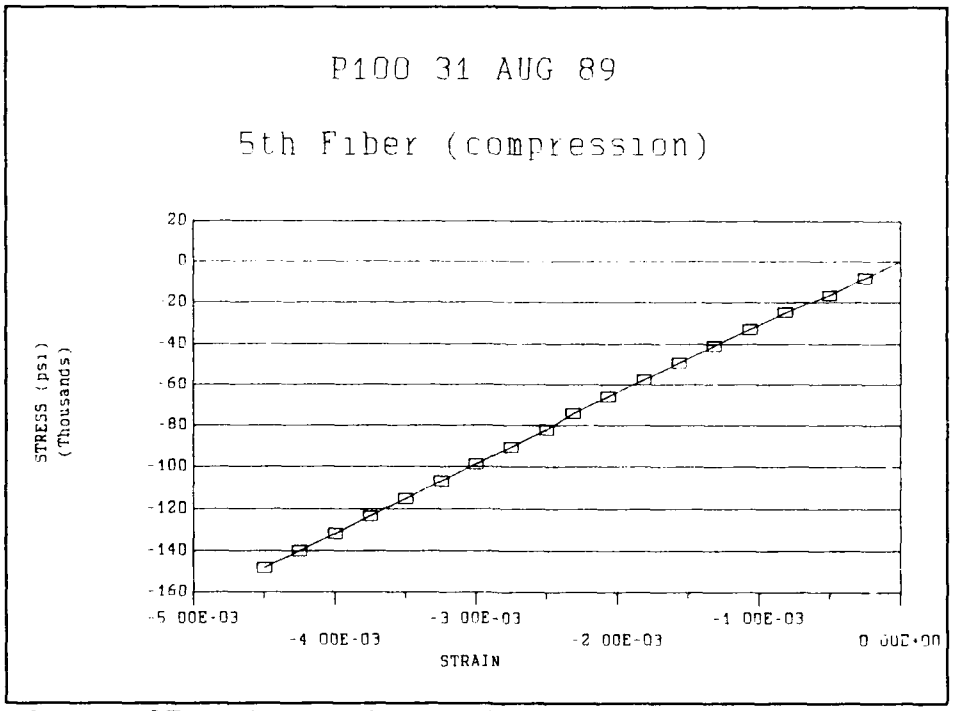

Figure 97 Thirty-fifth Fiber Tested In Compression

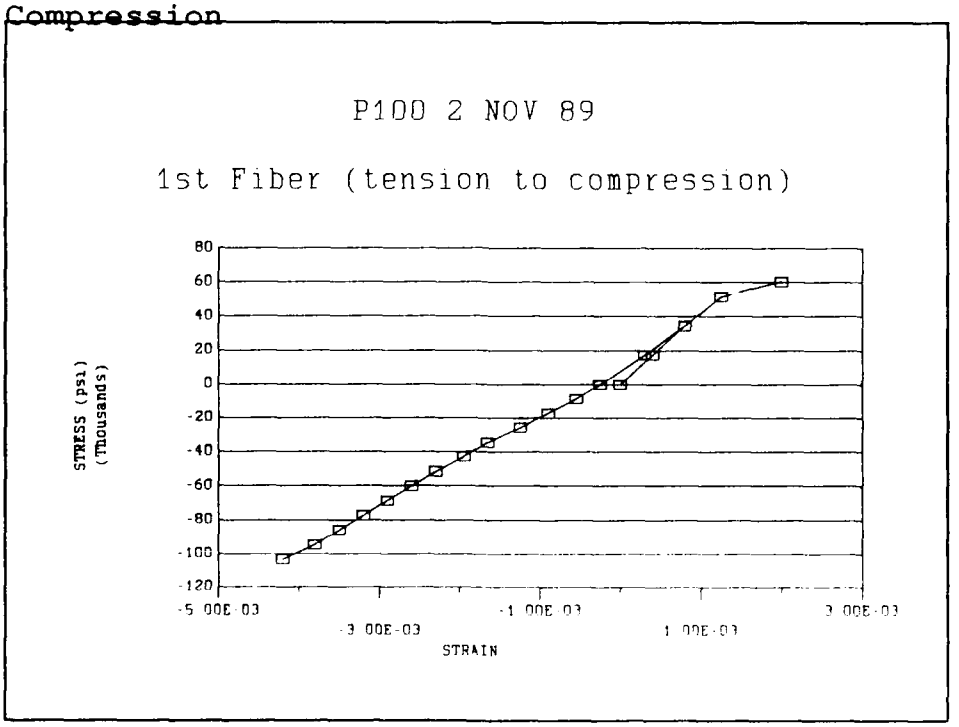

Figure 98 Thirty-sixth Fiber Tested In Compression

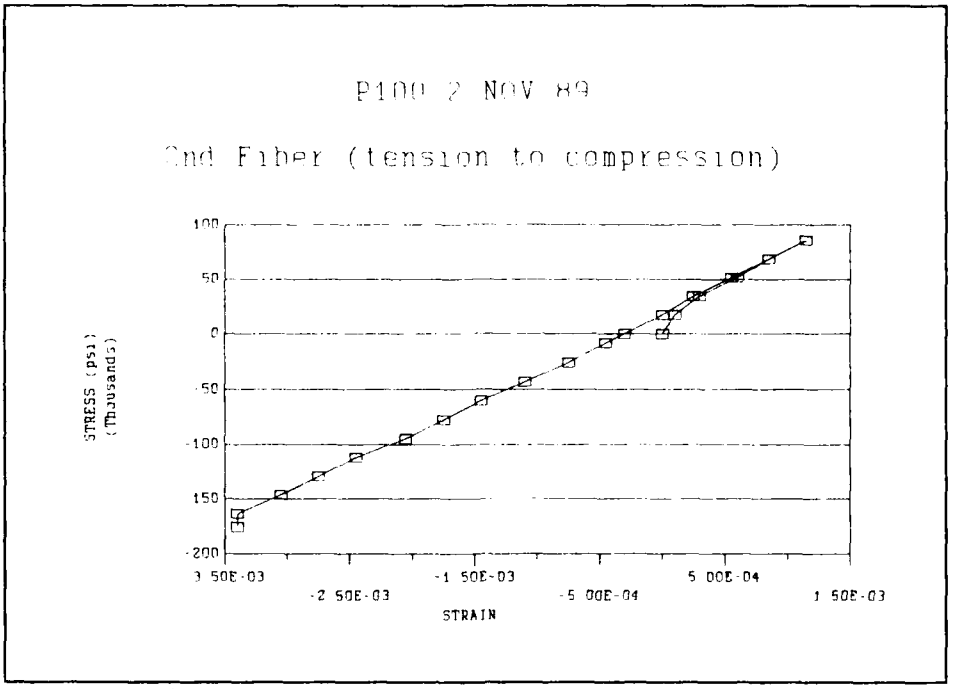

Figure 99 Thirty-seventh Fiber Tested In Compression

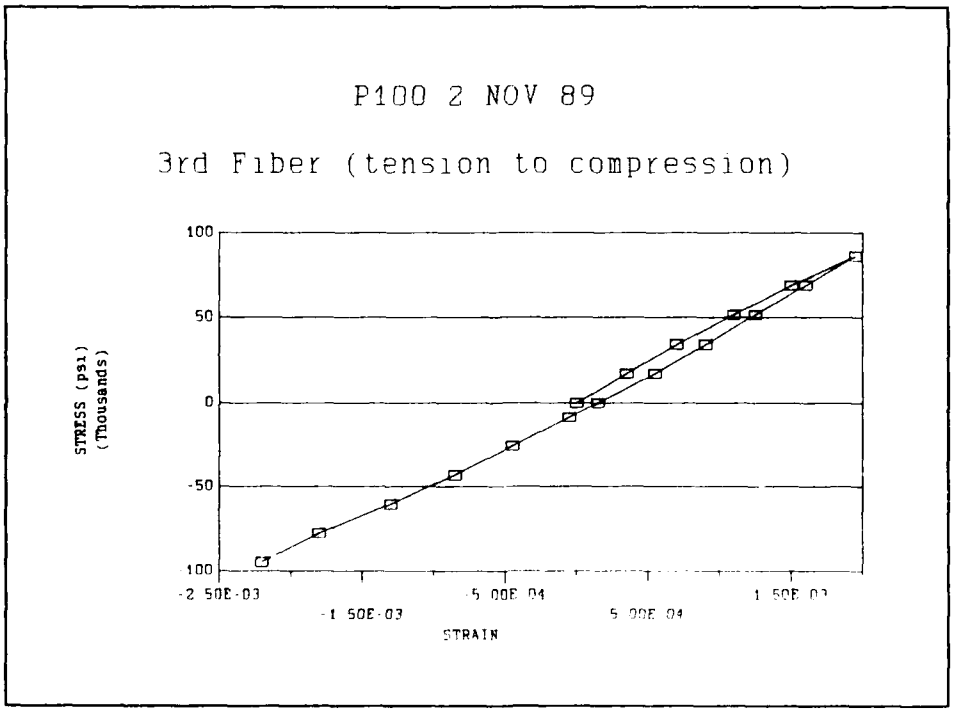

Figure 100 Thirty-eighth Fiber Tested In Compression

Table XXI P100 Fiber Data

#	DIAM μm	L_f mm	σ MPa	σ ksi	E. Mpsi	E. Mpsi
1	9.44	0.14	771.6	111.90	24.670	*
2	11.67	0.155	310.3	45.000	17.160	16.900
3	11.67	0.11	427.1	61.950	15.070	16.070
4	12.20	0.18	426.5	61.850	16.200	*
5	11.11	0.16	814.1	118.08	28.440	*
6	11.11	0.16	472.2	68.480	26.950	*
7	10.55	0.13	474.3	68.790	16.420	*
8	10.55	0.20	777.0	112.68	26.260	*
9	10.55	0.22	380.1	55.130	36.550	*
10	11.11	0.24	416.3	60.370	23.315	*
11	11.66	0.14	717.8	104.10	19.960	*
12	11.11	0.12	558.1	80.937	13.580	*
13	11.11	0.20	662.0	96.017	25.540	*
14	11.11	0.17	728.5	105.65	27.660	*
15	11.11	0.12	771.3	111.87	16.904	*
16	11.11	0.27	713.5	103.47	27.930	*
17	8.89	0.15	568.8	82.500	25.780	*
18	11.11	0.20	497.1	72.090	23.730	*
19	11.11	0.15	899.8	130.50	20.150	*
20	10.55	0.22	665.3	96.490	27.430	*
21	9.44	0.14	1053	152.79	31.560	*
22	11.11	0.195	385.7	55.932	25.750	*
23	9.63	0.20	912.0	132.26	34.970	*
24	9.44	0.21	1091	158.30	31.130	*
25	9.44	0.23	922.6	133.80	40.880	*
26	9.72	0.25	831.1	120.53	40.090	*
27	9.44	0.25	771.6	111.90	45.600	50.600
28	10.83	0.20	541.1	78.480	20.360	*
29	9.44	0.20	979.1	142.00	34.080	*
30	9.44	0.16	688.5	99.850	34.570	*
31	10.28	0.19	750.7	108.88	35.250	*
32	9.66	0.16	565.4	82.000	25.100	*
33	9.17	0.16	945.6	137.14	32.180	*
34	9.72	0.16	1276	185.00	28.610	*
35	9.66	0.16	1020	147.96	32.710	*

Appendix F: P55 Data

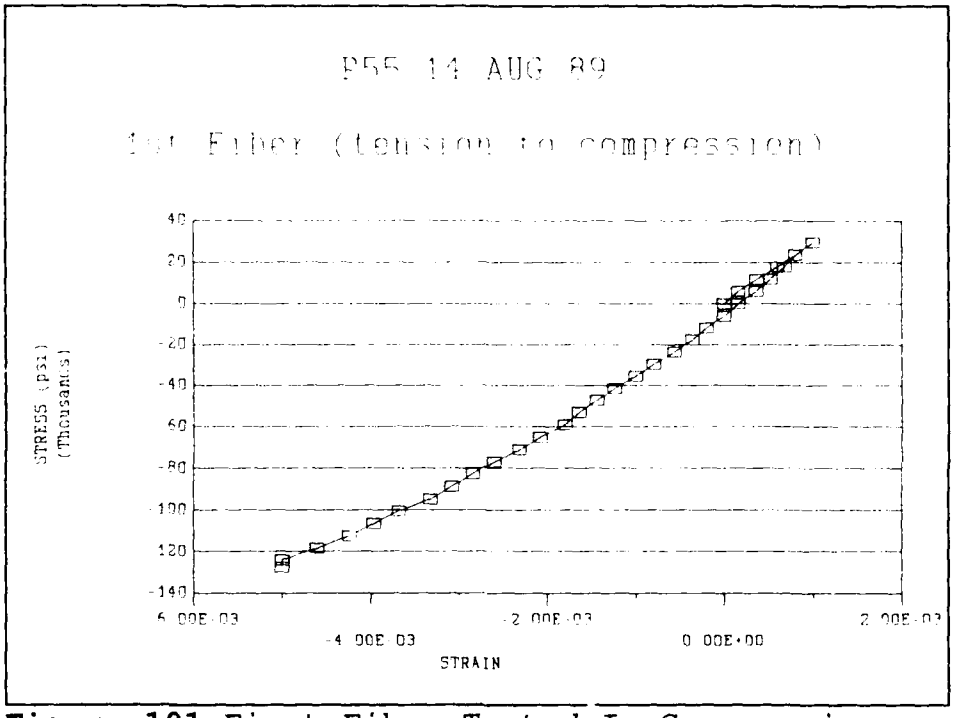

Figure 101 First Fiber Tested In Compression

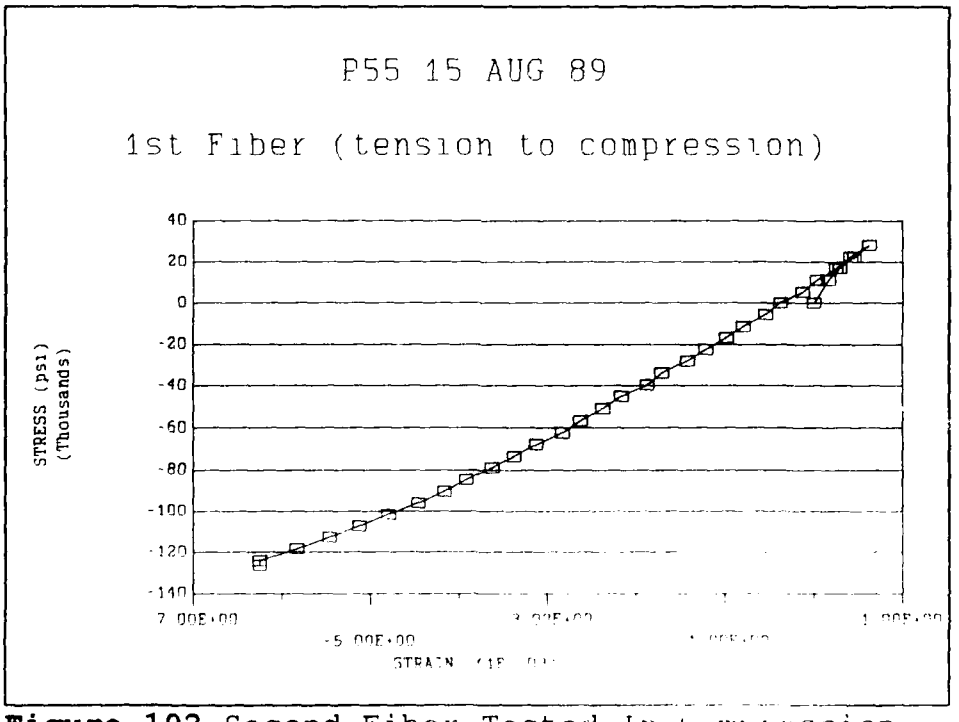

Figure 102 Second Fiber Tested In Compression

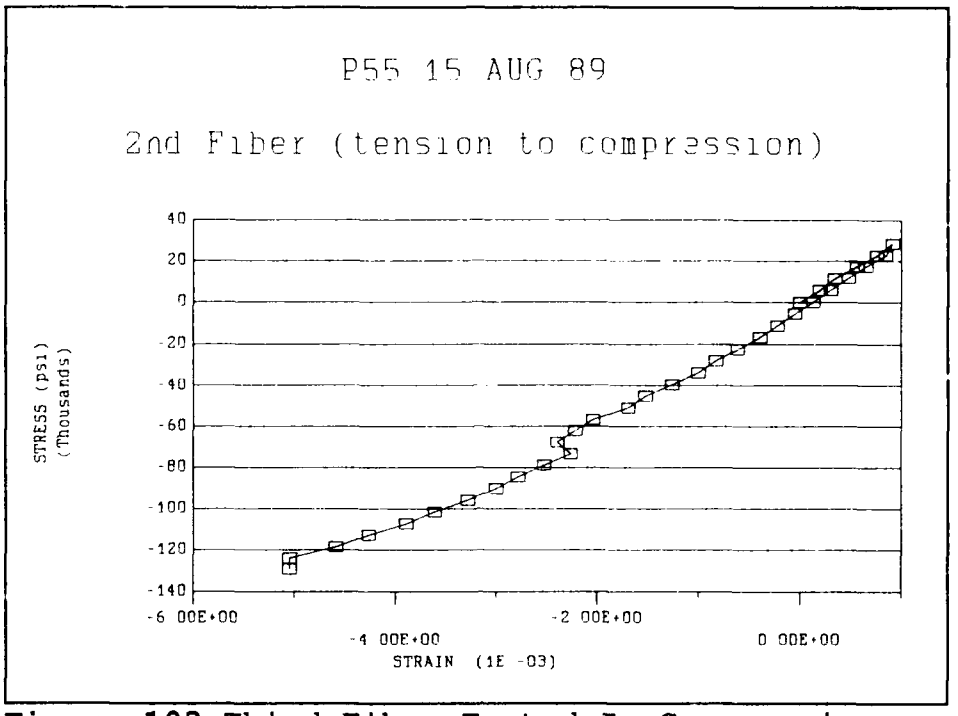

Figure 103 Third Fiber Tested In Compression

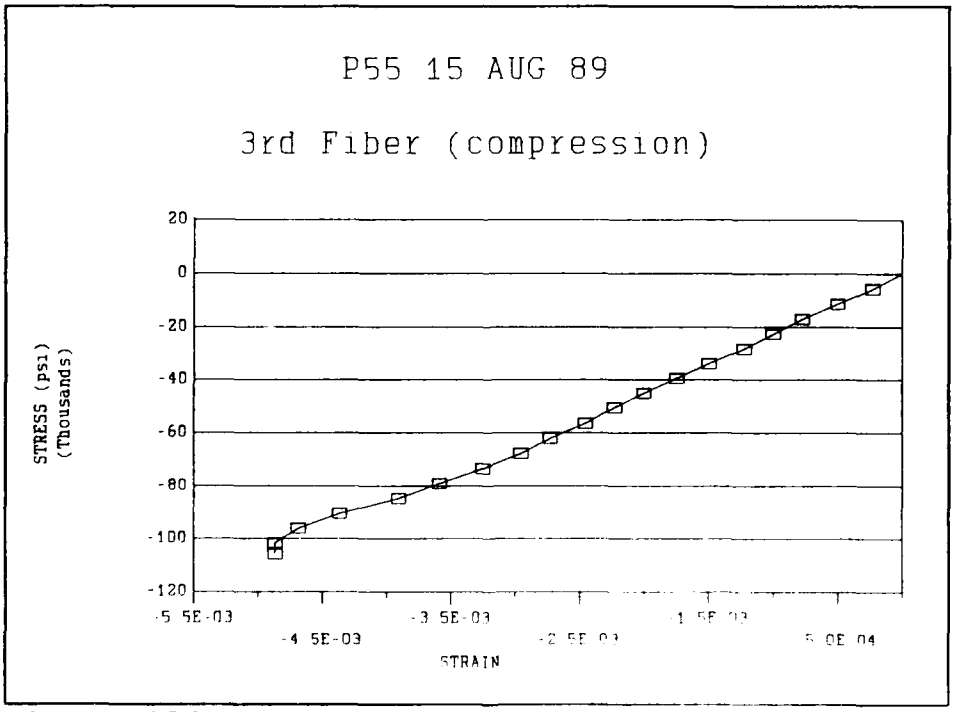

Figure 104 Fourth Fiber Tested In Compression

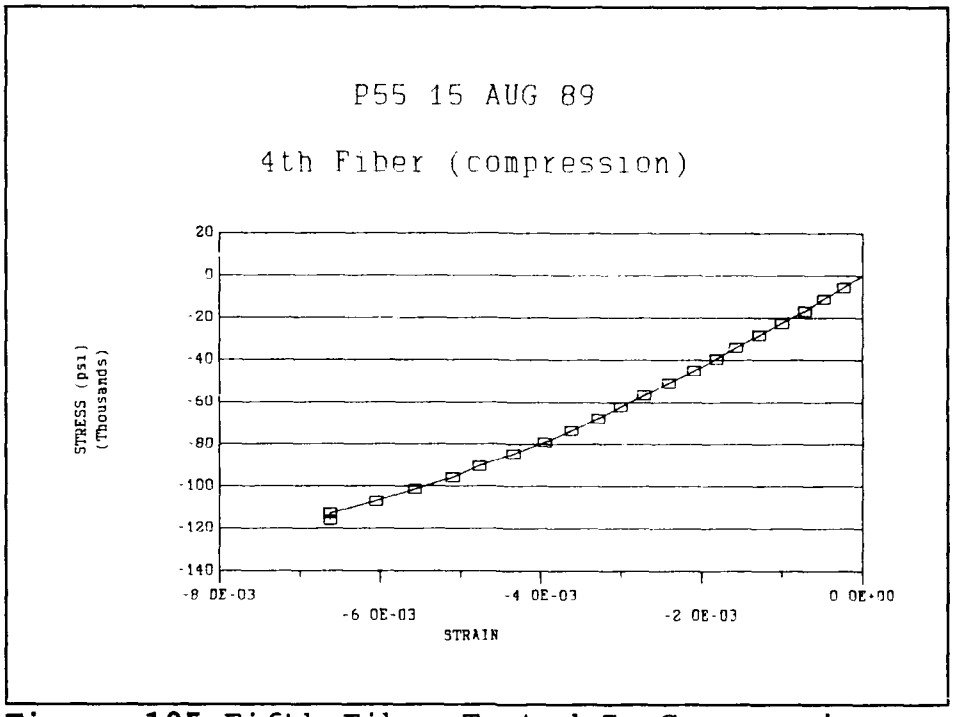

Figure 105 Fifth Fiber Tested In Compression

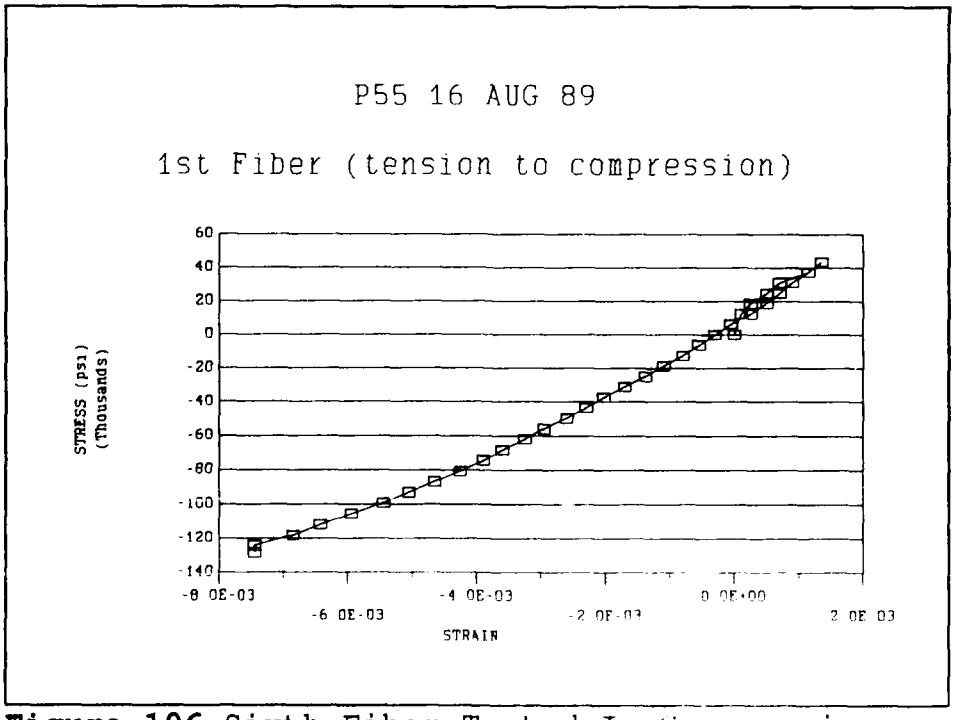

Figure 106 Sixth Fiber Tested In Compression

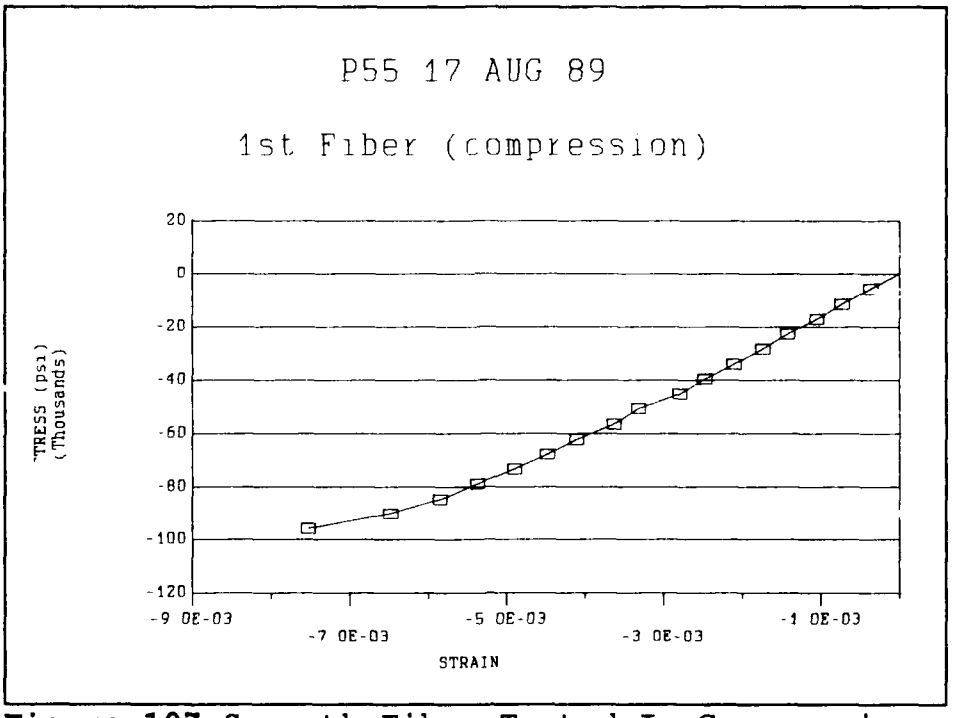

Figure 107 Seventh Fiber Tested In Compression

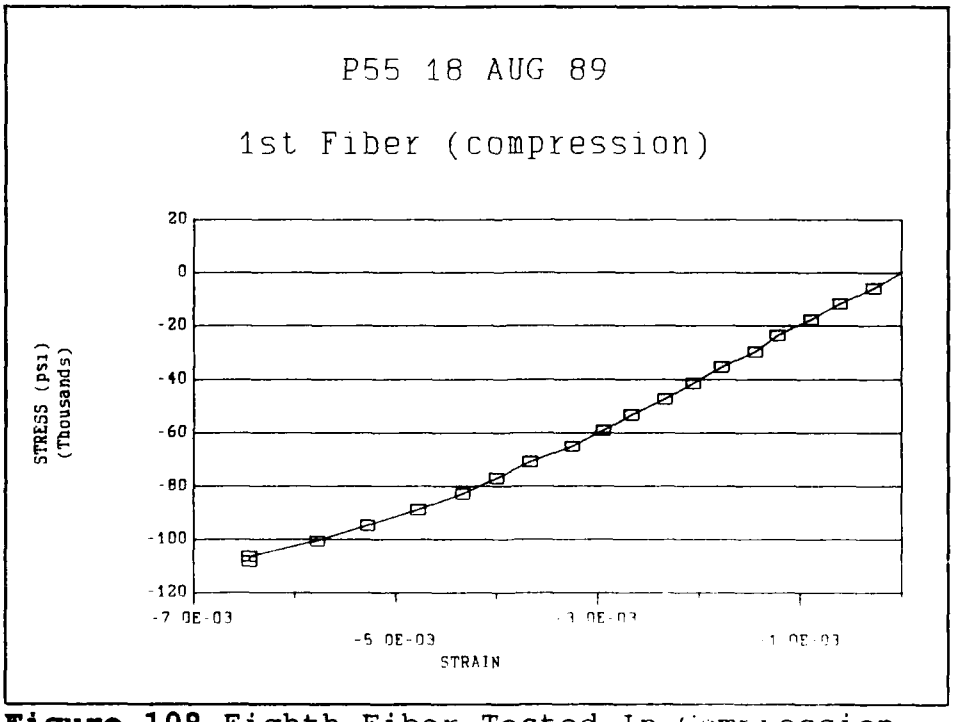

Figure 108 Eighth Fiber Tested In Compression

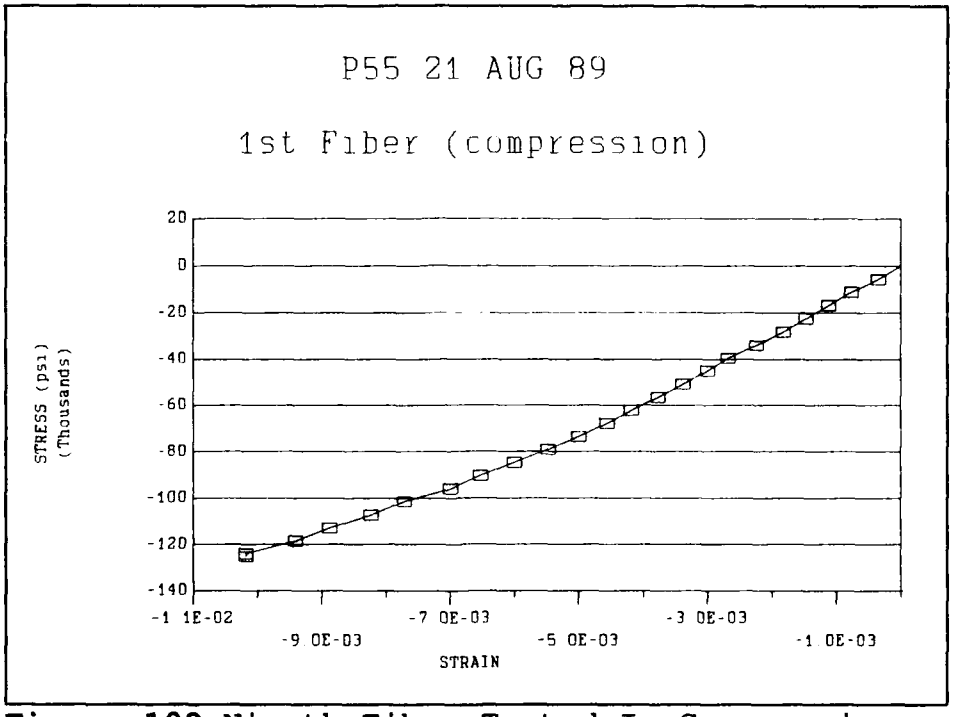

Figure 109 Nineth Fiber Tested In Compression

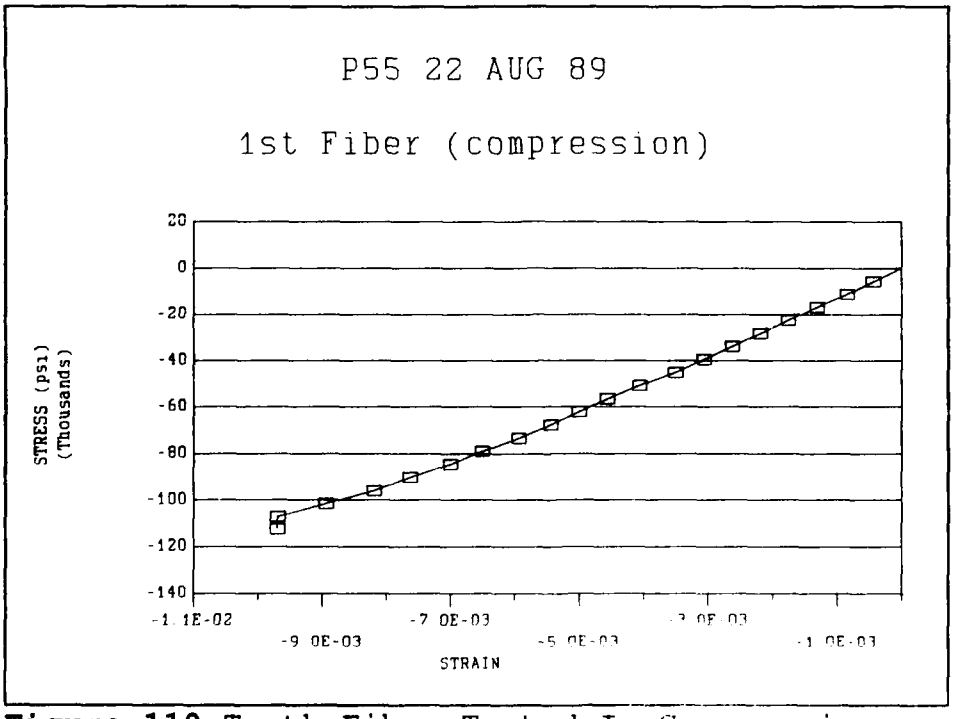

Figure 110 Tenth Fiber Tested In Compression

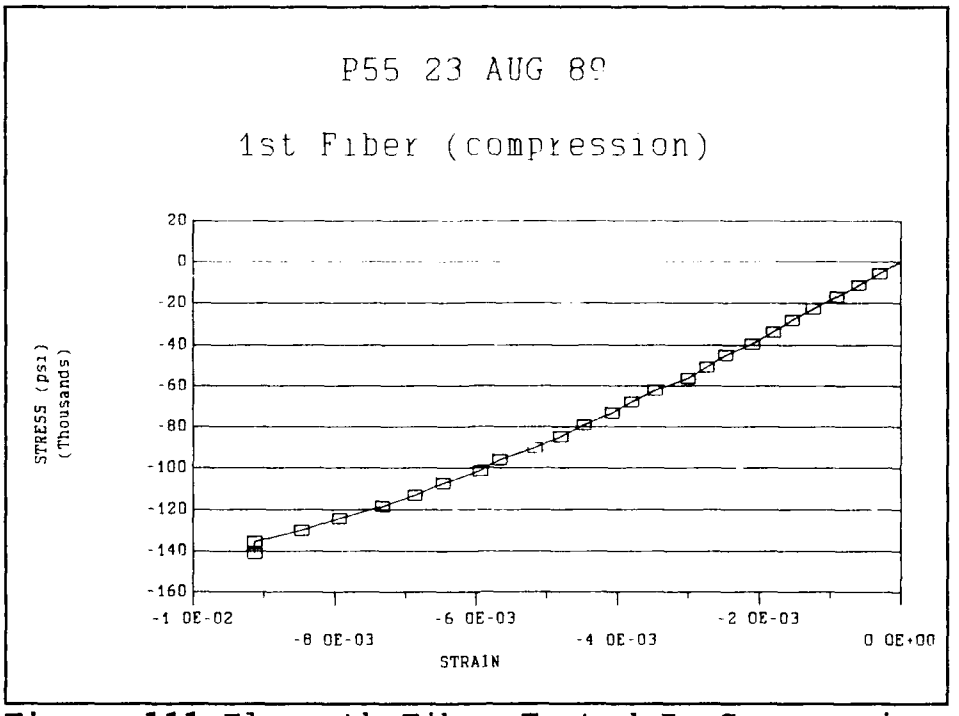

Figure 111 Eleventh Fiber Tested In Compression

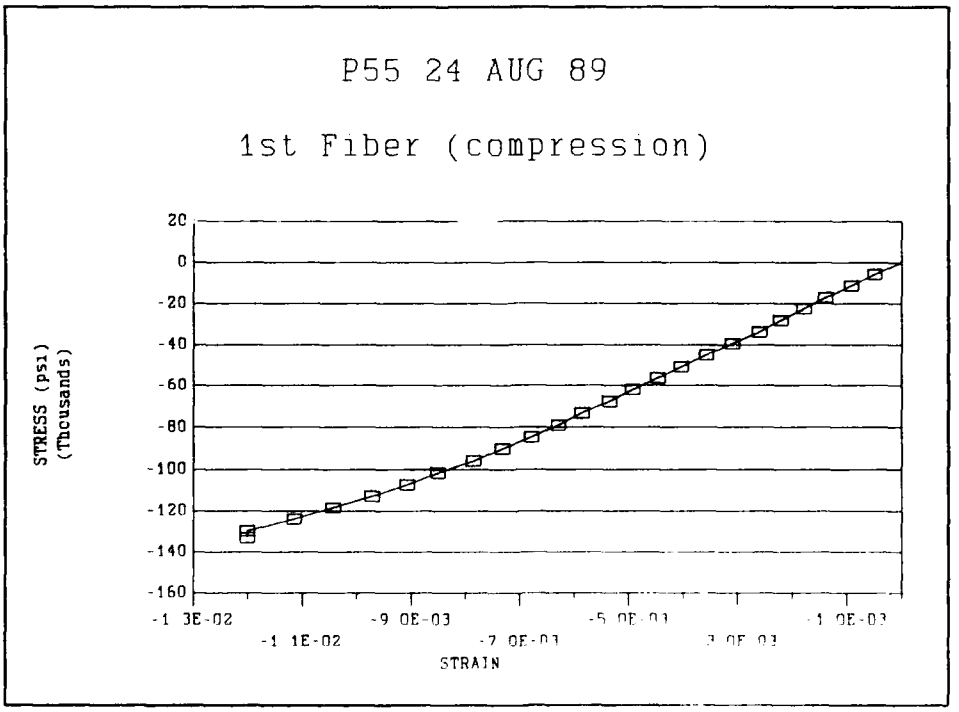

Figure 112 Twelfth Fiber Tested In Compression

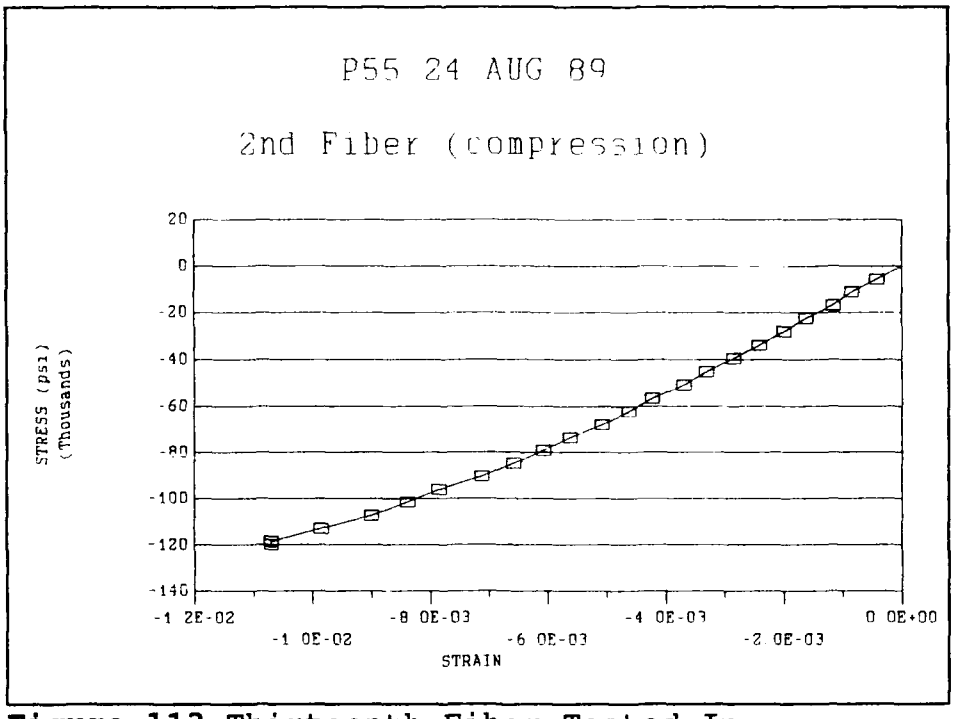

Figure 113 Thirteenth Fiber Tested In Compression

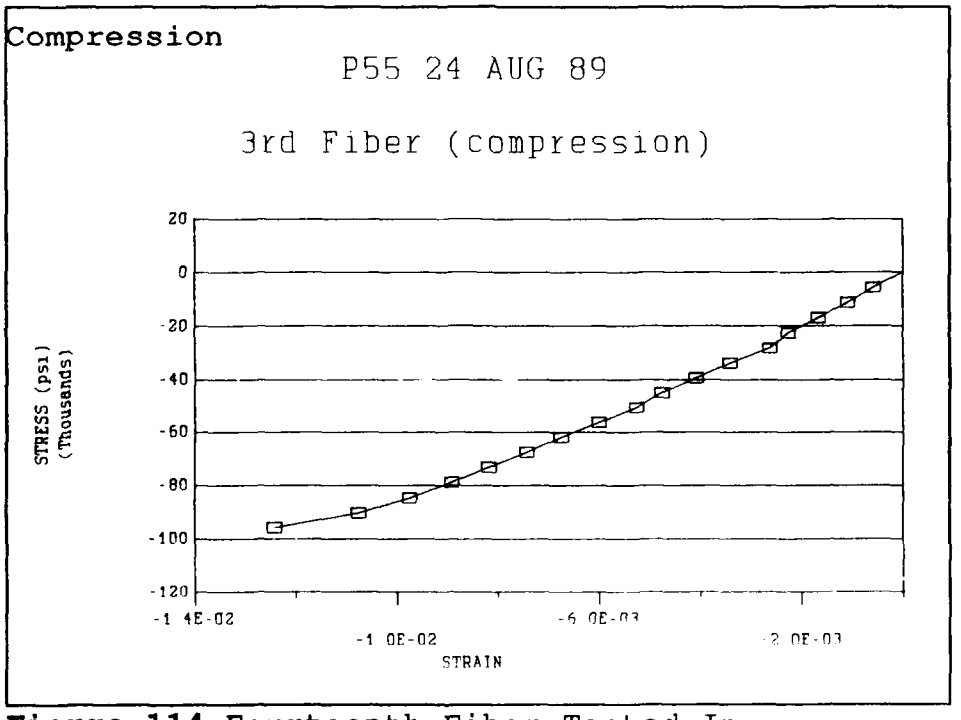

Figure 114 Fourteenth Fiber Tested In Compression

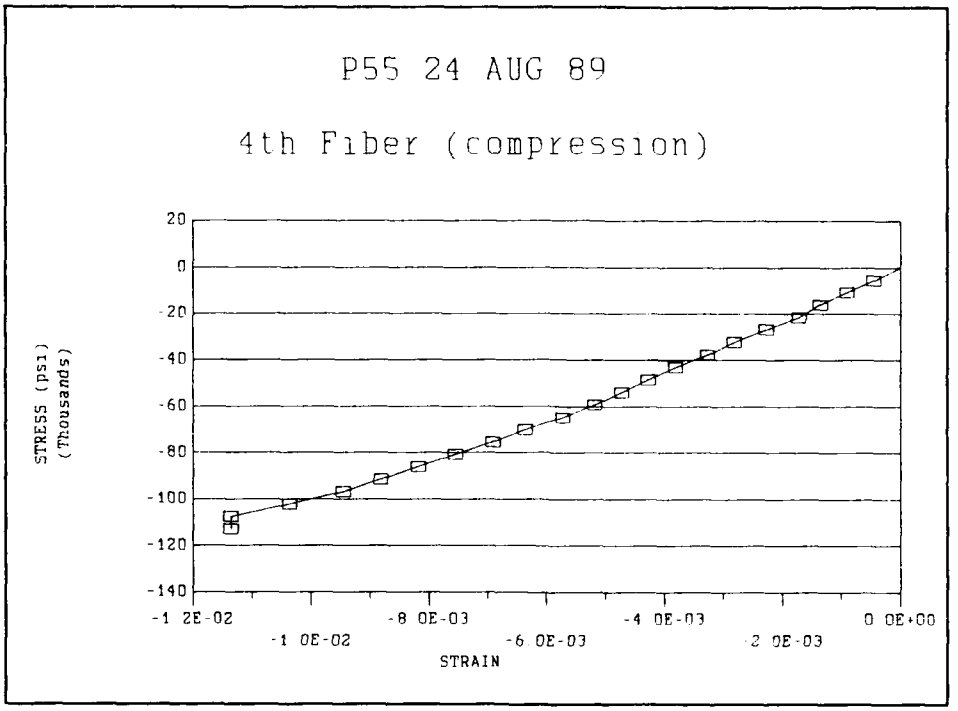

Figure 115 Fifteenth Fiber Tested In Compression

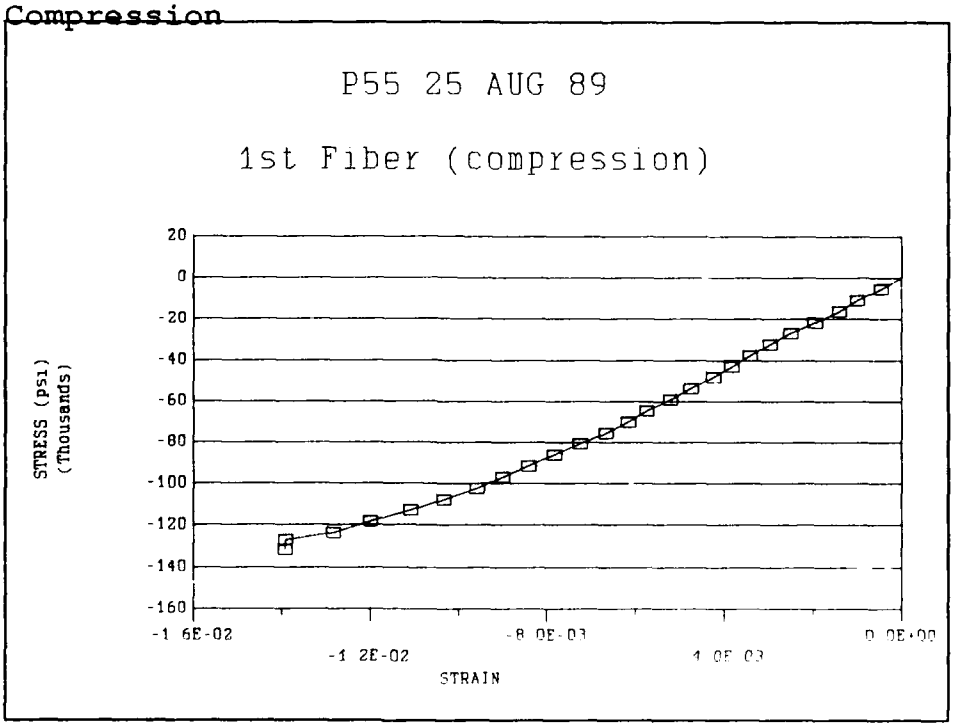

Figure 116 Sixteenth Fiber Tested In Compression

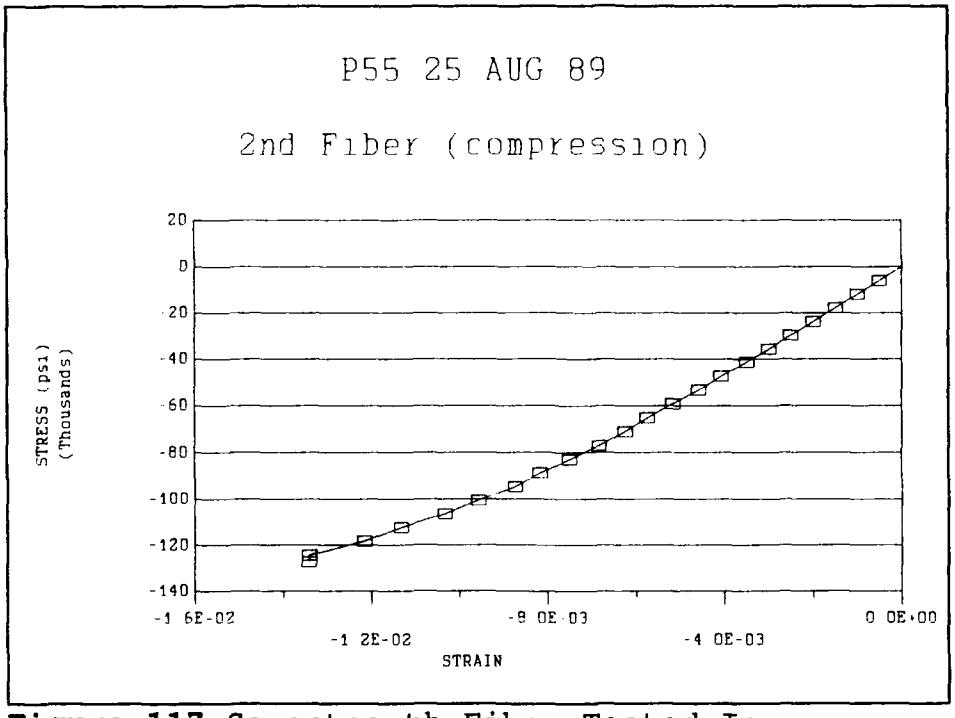

Figure 117 Seventeenth Fiber Tested In Compression

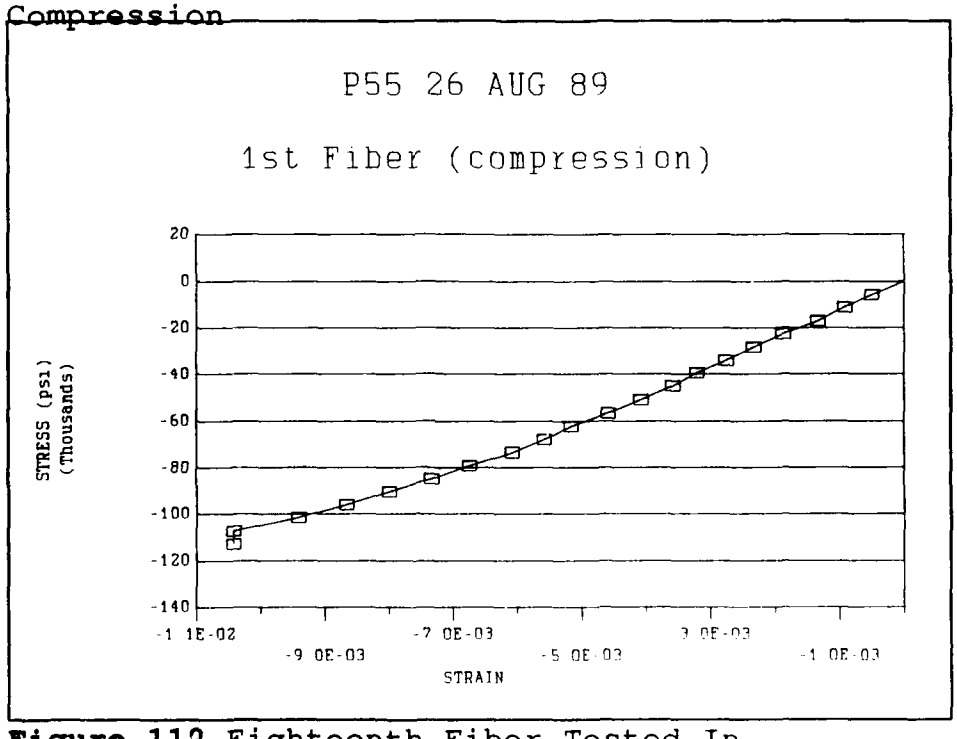

Figure 118 Eighteenth Fiber Tested In Compression

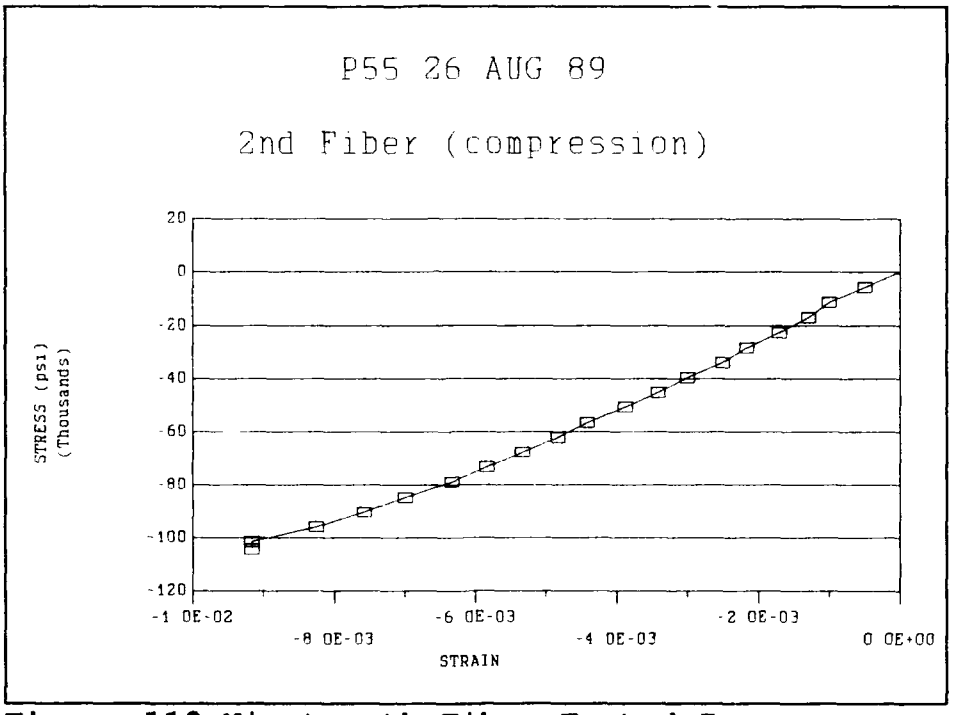

Figure 119 Nineteenth Fiber Tested In Compression

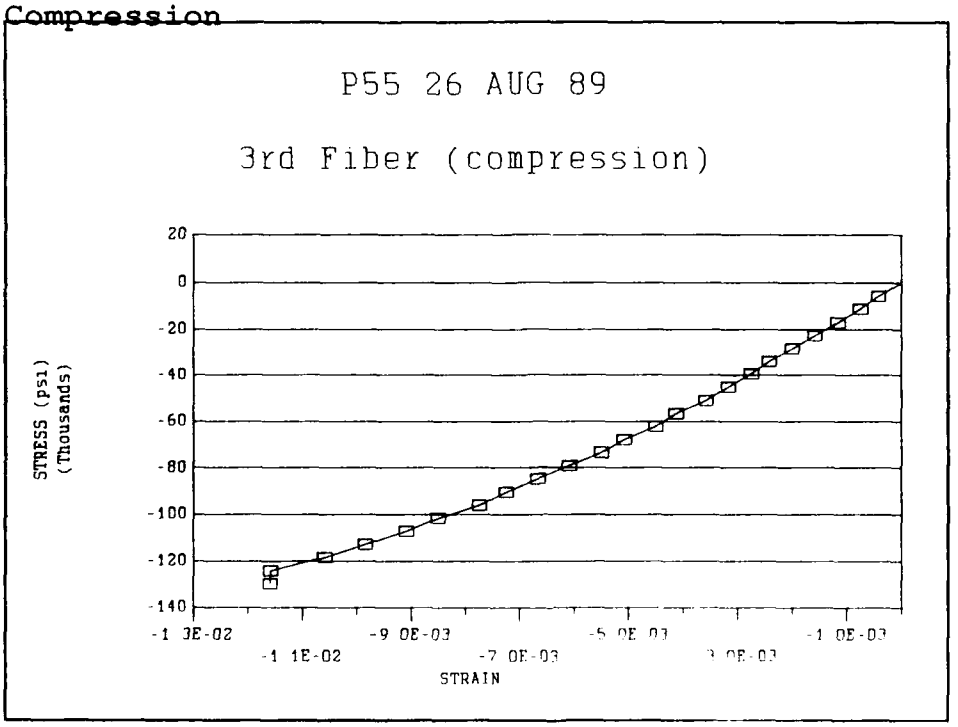

Figure 120 Twentieth Fiber Tested In Compression

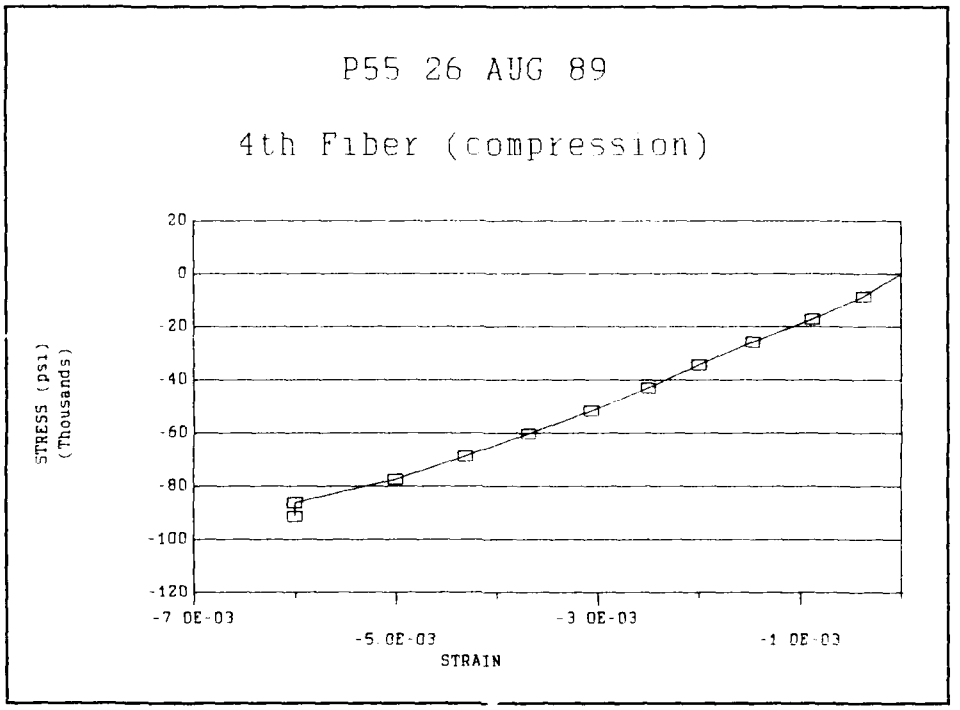

Figure 121 Twenty-first Fiber Tested In Compression

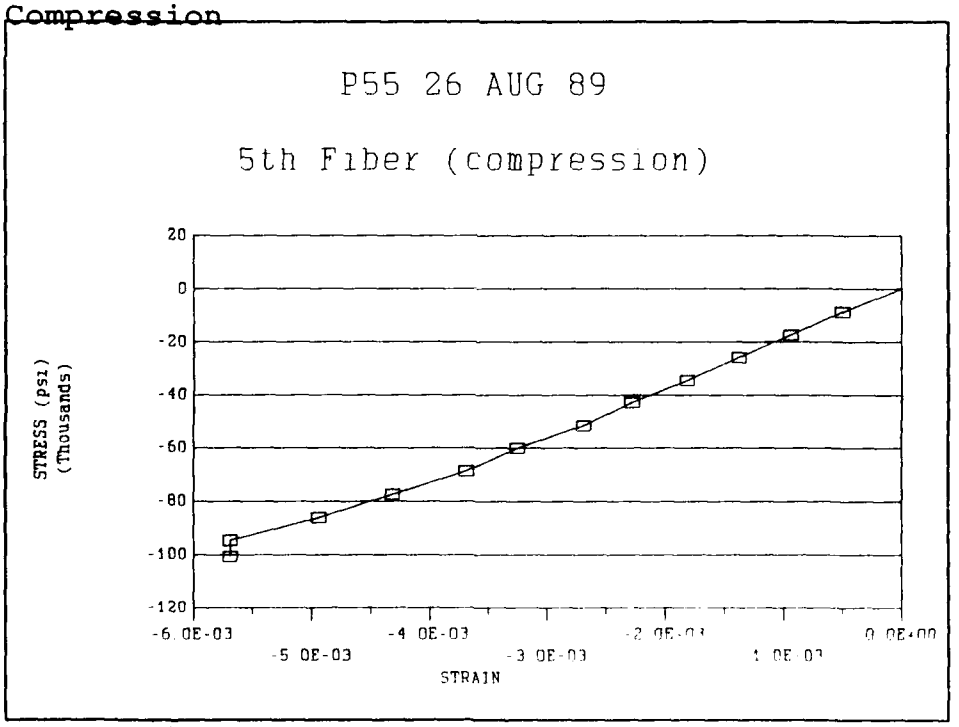

Figure 122 Twenty-second Fiber Tested In Compression

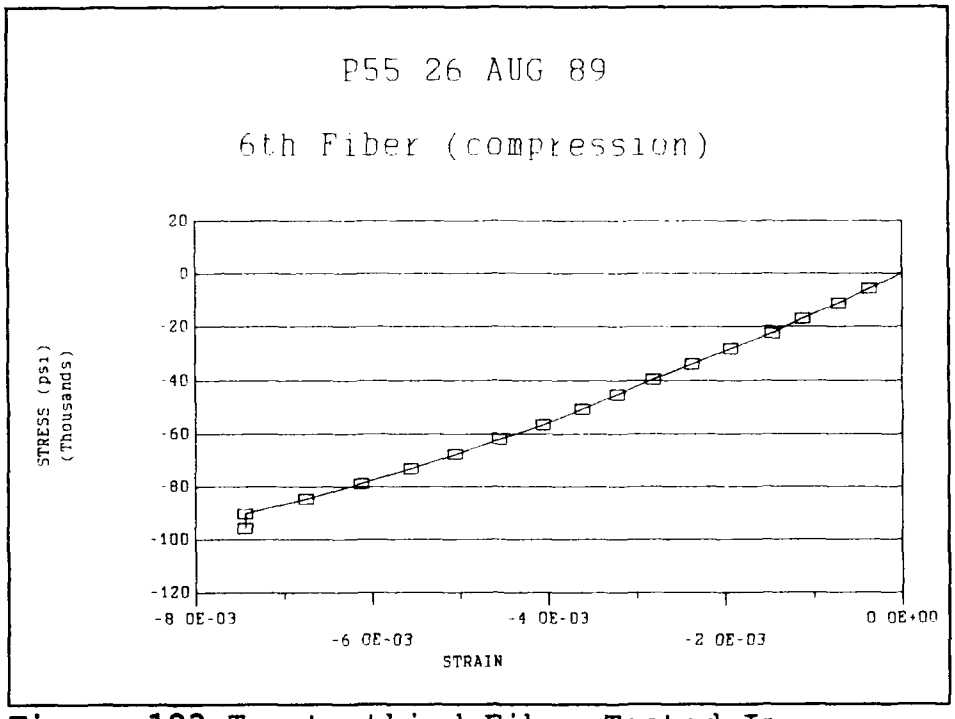

Figure 123 Twenty-third Fiber Tested In Compression

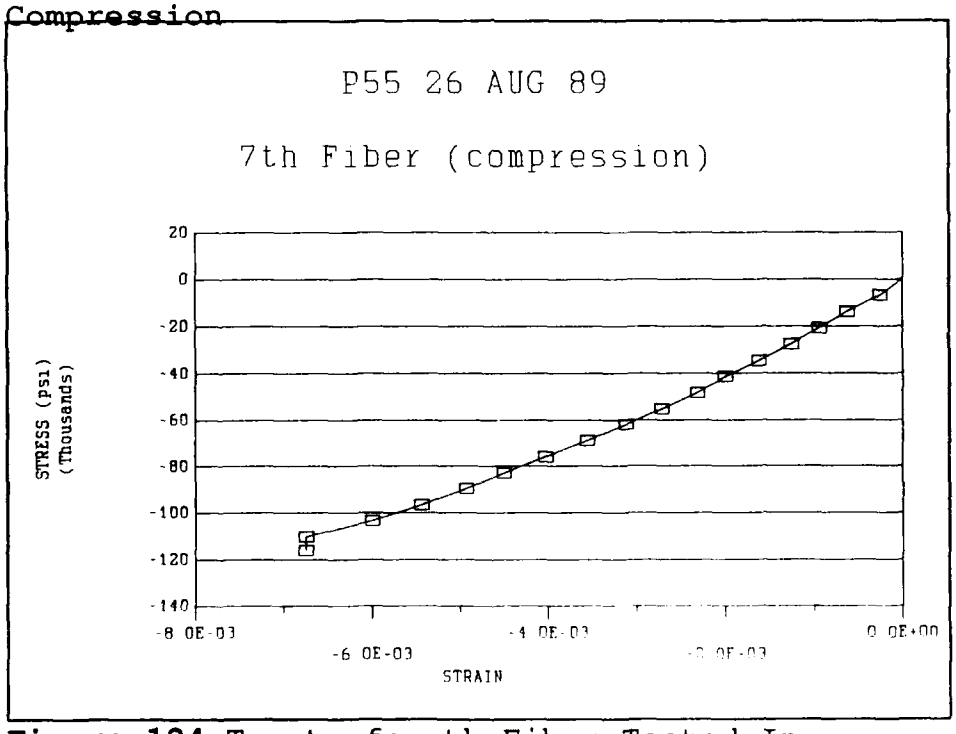

Figure 124 Twenty-fourth Fiber Tested In Compression

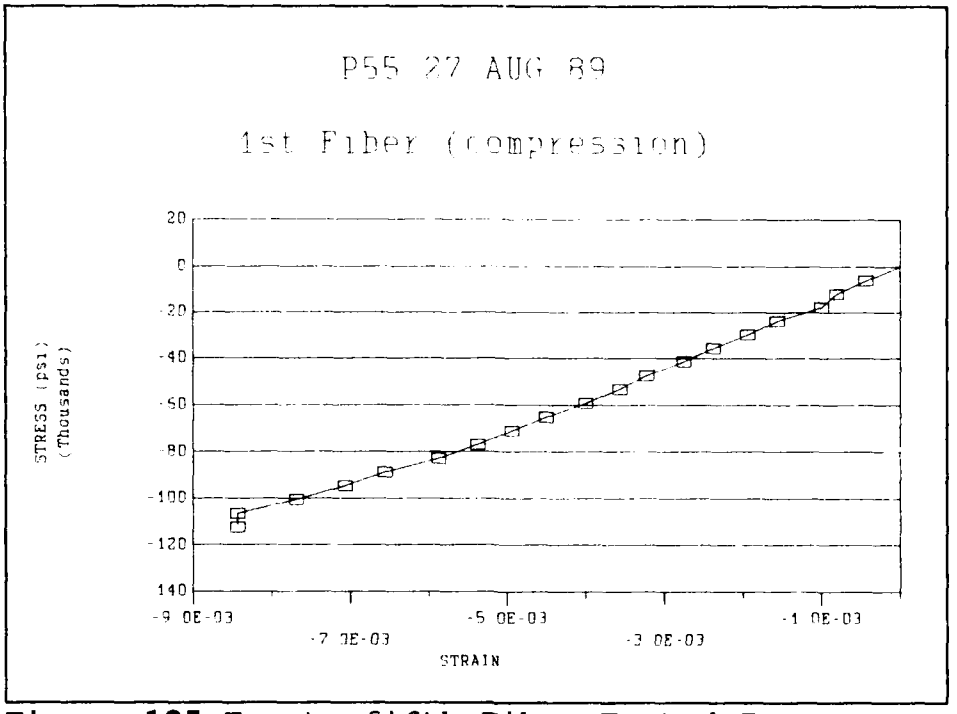

Figure 125 Twenty-fifth Fiber Tested In Compression

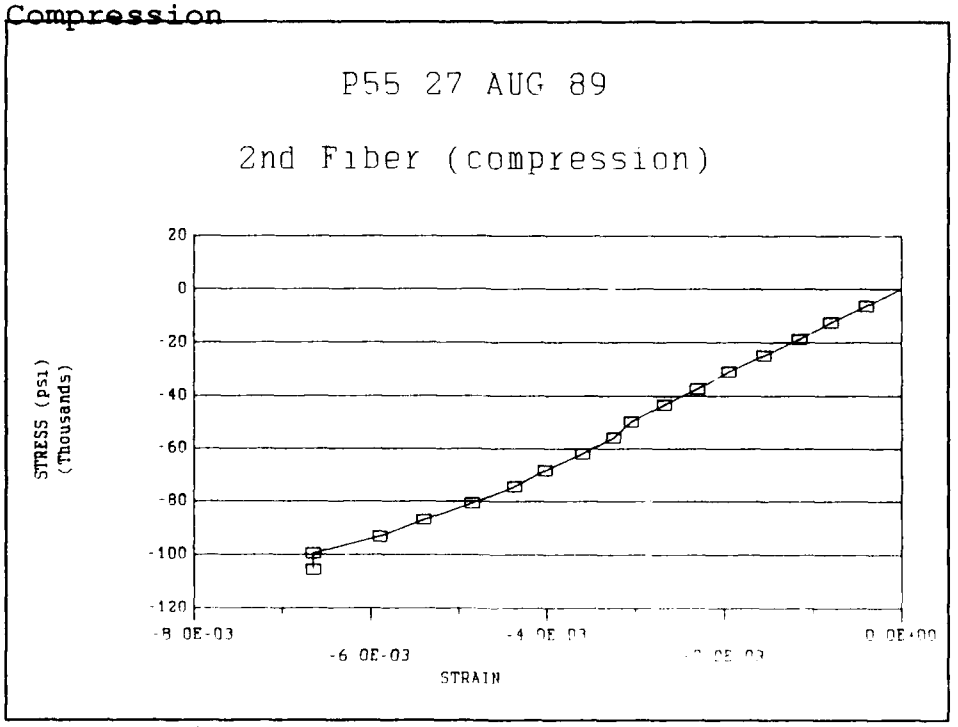

Figure 126 Twenty-sixth Fiber Tested In Compression

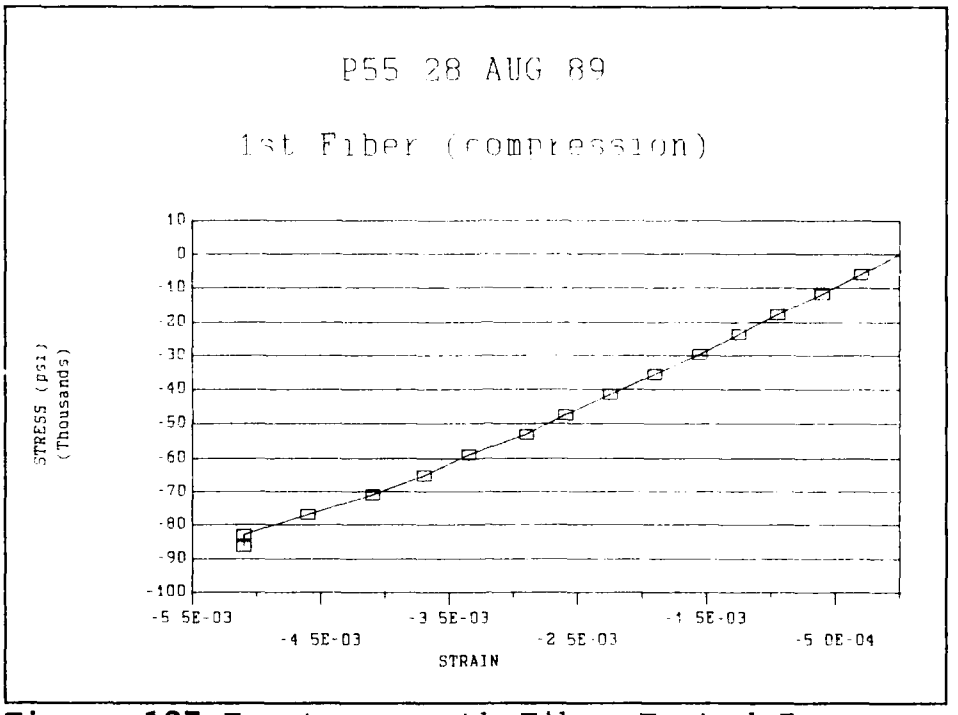

Figure 127 Twenty-seventh Fiber Tested In Compression

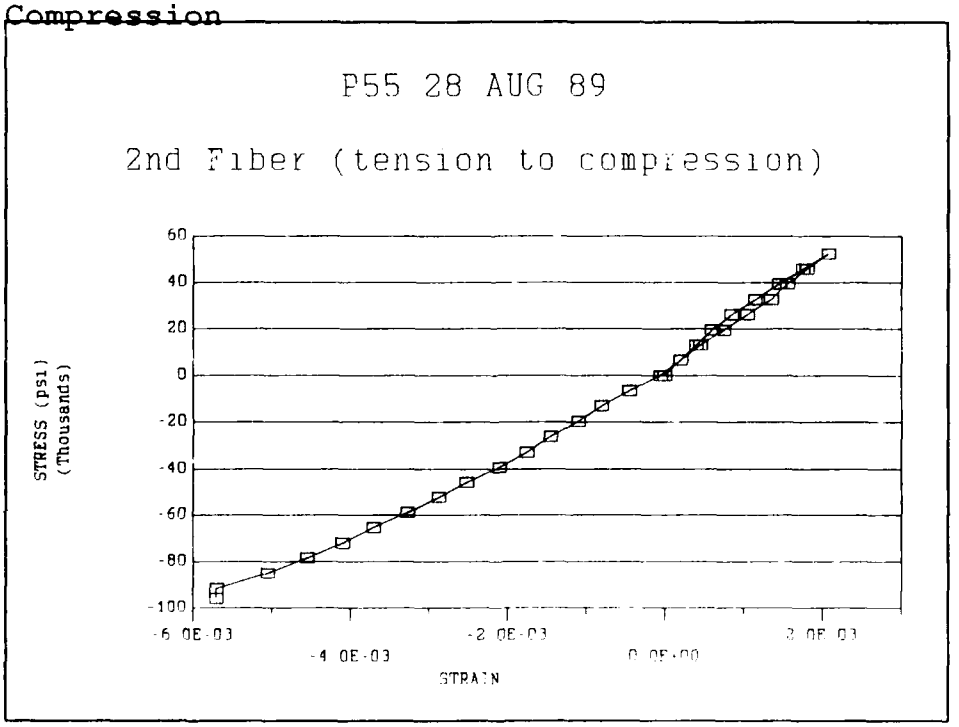

Figure 128 Twenty-eighth Fiber Tested In Compression

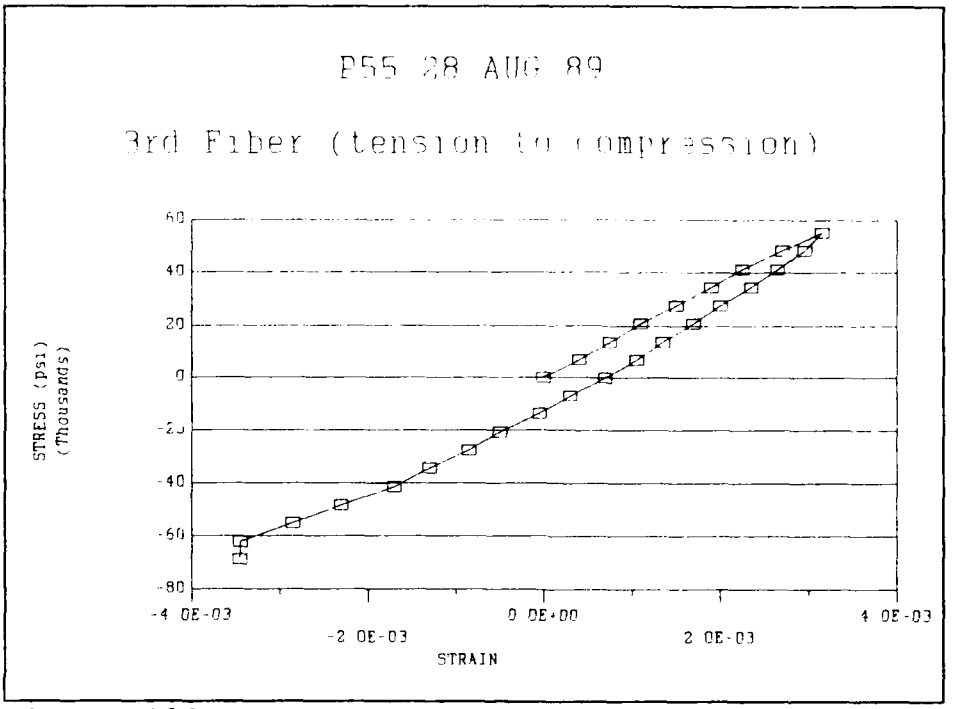

Figure 129 Twenty-ninth Fiber Tested In Compression

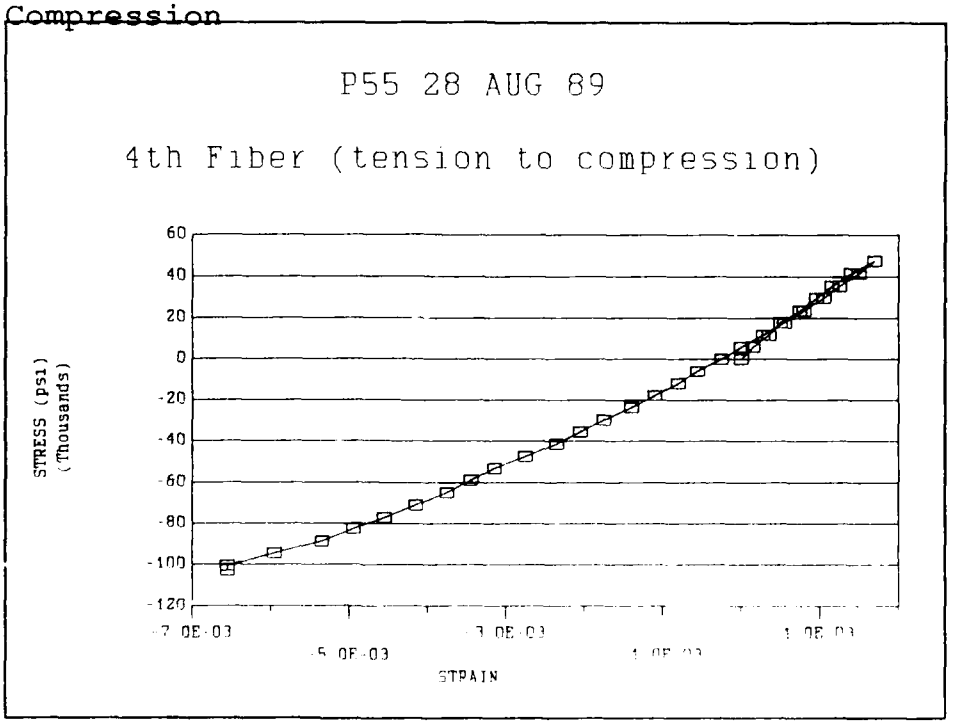

Figure 130 Thirtieth Fiber Tested In Compression

Table XXII P55 Fiber Data

#	DIAM μm	L_f mm	σ MPa	σ ksi	$E_{..}$ Mpsi	$E_{.}$ Mpsi
1	11.39	0.25	880.6	127.72	27.60	29.85
2	11.66	0.24	871.4	126.38	27.57	33.85
3	11.66	0.23	890.9	129.21	29.09	30.42
4	11.66	0.22	729.3	105.79	22.40	27.51
5	11.66	0.21	801.4	116.23	20.47	*
6	11.11	0.20	884.8	128.33	18.86	*
7	11.66	0.19	661.4	95.918	15.20	*
8	11.39	0.18	746.0	108.20	19.61	*
9	11.66	0.17	863.7	125.26	14.80	*
10	11.66	0.16	776.1	112.56	12.45	*
11	11.66	0.15	972.5	141.05	18.13	*
12	11.66	0.14	918.1	133.16	12.60	*
13	11.86	0.13	826.7	119.90	13.36	*
14	11.66	0.12	661.4	95.918	9.244	*
15	11.94	0.11	779.1	113.00	11.23	*
16	11.94	0.12	907.0	131.55	11.26	*
17	11.39	0.12	876.5	127.13	11.45	*
18	11.66	0.12	778.1	112.84	12.24	*
19	11.66	0.12	719.7	104.38	12.77	*
20	11.66	0.12	894.8	129.77	13.57	*
21	11.11	0.16	629.2	91.250	16.20	*
22	9.44	0.16	694.4	100.71	18.50	*
23	11.66	0.16	661.3	95.910	13.70	*
24	10.55	0.16	800.7	116.13	19.83	*
25	11.39	0.16	774.6	112.34	14.62	*
26	11.11	0.20	702.7	101.92	16.79	*
27	11.39	0.20	595.2	86.328	18.48	*
28	10.83	0.20	660.6	95.814	18.75	20.76
29	10.55	0.20	570.2	82.704	18.97	18.33
30	11.39	0.20	709.4	102.88	21.97	26.32

APPENDIX H: Recommended Experimental Design

The MTM-8 has demonstrated its ability to directly test fibers in compression. This testing can easily be incorporated into a larger research effort directed towards understanding the compressive behavior of composites. Response Surface Methodology (RSM) conveniently provides a means of describing an empirical relationship between fiber and matrix properties and the properties of a composite.

RSM is simply the application of statistical estimation procedures to relate variables (x_1, x_2, x_3,...,x_i) to a response Y over a specific region of interest. RSM can also be used to:

1) determine which x values will yield a product satsfying the constraints for different responses

2) explore the space of the x_i's to determine the maximum response and the nature of that response (3:iv)

RSM will be applied to the problem of relating the variables of fiber and matrix compressive properties to the response of composite compressive behavior. The proposed experimental design will be a 3 factor first order (linear) response surface design.

The object of RSM is to form a model in which the response is given as a function of controllable variables and associated variable parameters. This model may be represented as follows:

$$Y = F(E,\Theta) + \varepsilon$$

Y = response - composite strength
F = first order function
E = controllable variables - fiber and matrix
Θ = variable parameters - compressive strength, modulus
ε = experimental error (2:3-1)

The method by which the values for Θ are considered optimal for the function F will be the least squares regression.

The model building process by which the experimental design is formulated is called factorial design. The factorial design offers the ability to make multiple comparisons and provides a simple design structure (2:4-1). The proposed experimental set-up uses three variables (factors): fiber type, matrix type and volume fraction of the fiber in the composite. These factors will be set at two different levels. Thus the initial design is known as a 2^3 factorial design. Table XXIII lists the factors and their levels. The values listed

are hypothetical values and will be used to illustrate RSM techniques. The values are from an example listed in Empirical Model-Building and Response Surfaces by Box and Draper (3:107).

Table XXIII Factors of the 2^3 Design

FACTORS	VARIABLES (E_i)	LEVELS	
FIBER TYPE	STRENGTH (ksi)	250	350
MATRIX TYPE	STRENGTH (ksi)	8	10
VOLUME FRACTION	PERCENT	40	50

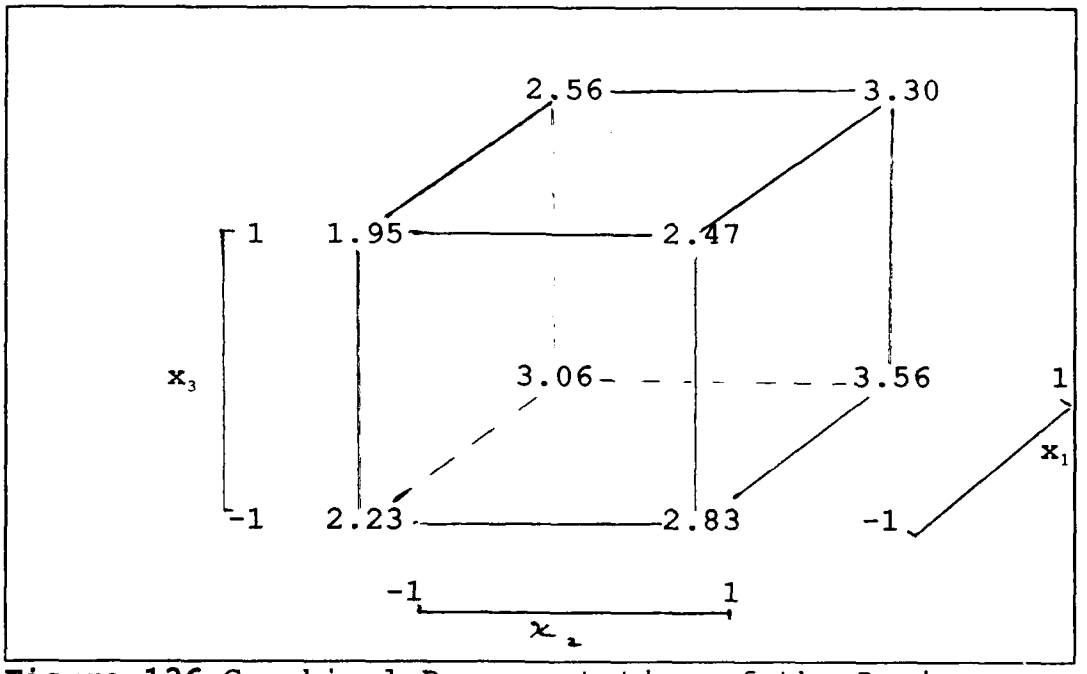

Figure 136 Graphical Representation of the Design

Graphically, the 2^3 design is represented in

Figure 1. The E_i's are coded so that the two levels of each variable equal -1 and +1, respectively. The coded variables (x_i's) are calculated in the following manner:

$$x_1 = (E_1-300)/25 \qquad x_2 = (E_2-9)/1 \qquad x_3 = (E_3-45)/5$$

Table XXIV lists the full 2^3 design, including the coded and uncoded variables.

Table XXIV Full 2^3 Design

UNCODED			CODED			
E_1	E_2	E_3	x_1	x_2	x_3	Y
250	8	40	-1	-1	-1	2.83
350	8	40	1	-1	-1	3.56
250	10	40	-1	1	-1	2.23
350	10	40	1	1	-1	3.06
250	8	50	-1	-1	1	2.47
350	8	50	1	-1	1	3.30
250	10	50	-1	1	1	1.95
350	10	50	1	1	1	2.56

Actual estimates for the E_1 values, the fibers' compressive properties, can be obtained from testing with the MTM-8. The E_2 estimates, the compressive properties of the matrix materials, can be found from testing with an Instron machine. Composite test specimens, fabricated with all the different fiber, matrix, and volume fraction combinations, can also be tested on an Instron machine in

order to estimate the E_3 values. After the data is collected, a multi-variate least squares analysis can be performed to determine the coefficient values for the following first order model:

$$Y = B_0+B_1x_1+B_2x_2+B_3x_3+B_4x_{12}+B_5x_{23}+B_6x_{13}$$

Replicate values at each design point are desirable because the replications will reduce the amount of pure deviation (2:3-35). Table XXV lists the first order regression results from the software package STATISTIX.

Table XXV First Order Regression Analysis

UNWEIGHTED LEAST SQUARES LINEAR REGRESSION OF Y

PREDICTOR VARIABLES	COEFFICIENT	STD ERROR	STUDENT'S T	P
CONSTANT	2.7545	1.8873E-02	145.95	0.0000
X_1	3.7500E-01	2.2131E-02	16.94	0.0001
X_2	-2.9500E-01	2.2131E-02	-13.33	0.0002
X_3	-1.7500E-01	2.2131E-02	-7.91	0.0014
X_{12}	-1.5000E-02	2.2131E-0	-0.68	0.5351
X_{23}	-2.0000E-02	2.2131E-02	-0.90	0.4173
X_{13}	-1.5000E-02	2.2131E-02	-0.68	0.5351

CASES INCLUDED	11	MISSING CASES	0
DEGREES OF FREEDOM	4		
OVERALL F	88.18	P VALUE	0.0003
ADJUSTED R SQUARED	0.9812		
R SQUARED	0.9925		
RESID. MEAN SQUARE	3.918E-03		

This analysis indicates the 1st order model that best fits the data is as follows:

$$Y = 2.745 + .375x_1 - .295x_2 - .035x_3$$

This initial design, while suitable for first order modeling, does not allow for any analysis to determine how well a second order model might fit the data. One additional composite specimen will allow for a fitness test of the following second order model:

$$Y = B_0+B_1x_1+B_2x_2+B_3x_3+B_4x_{12}+B_5x_{23}+B_6x_{13}+B_7x_{11}+B_8x_{22}+B_9x_{33}$$

The new composite specimen must be fabricated from a third fiber type, a third matrix material and a third fiber volume fraction. The new level of each variable should be at the mid point between the current levels (2:7-3). The coded values would then be equal to zero. Graphically, the new composite specimen represents the center of the cube depicted in Figure 1. The 2^3 design with the additional center point is listed in Table XXVI. The center point is replicated three times so that the

STATISIX software will perform the regression analysis.

Table XXVI Full Design with Center point

UNCODED			CODED			
E_1	E_2	E_3	x_1	x_2	x_3	Y
250	8	40	-1	-1	-1	2.83
350	8	40	1	-1	-1	3.56
250	10	40	-1	1	-1	2.23
350	10	40	1	1	-1	3.06
250	8	50	-1	-1	1	2.47
350	8	50	1	-1	1	3.30
250	10	50	-1	1	1	1.95
350	10	50	1	1	1	2.56
300	9	45	0	0	0	2.79
300	9	45	0	0	0	2.79
300	9	45	0	0	0	2.79

The results of the second order regression analysis for the augmented 2^3 design are listed in Table XXVII. The regression analysis (ANOVA lack of fit tests) shows clearly that the first order model gives the most adequate fit of the data.

Once the experiment is completed and the data is collected, a multi-variate least squares regression can be performed, assuming all of the appropriate assumptions for least squares regressions are found to be reasonable. If the statistical analysis shows that the response

Table XXVII 2nd Order Regression Analysis

UNWEIGHTED LEAST SQUARES LINEAR REGRESSION OF Y

NOTE: X22 AND X33 WERE DROPPED FROM THE MODEL BECAUSE OF HIGH CORRELATIONS WITH OTHER PREDICTOR VARIABLE(S).

PREDICTOR VARIABLES	COEFFICIENT	STD ERROR	STUDENT'S T	P
CONSTANT	2.7800	3.8006E-02	73.15	0.0000
X1	3.7500E-01	2.3274E-02	16.11	0.0005
X2	-2.9500E-01	2.3274E-02	-12.68	0.0011
X3	-1.7500E-01	2.3274E-02	-7.52	0.0049
X12	-1.5000E-02	2.3274E-02	-0.64	0.5651
X23	-2.0000E-02	2.3274E-02	-0.86	0.4533
X13	-1.5000E-02	2.3274E-02	-0.64	0.5651
X11	-3.5000E-02	4.4566E-02	0.79	0.4896

CASES INCLUDED	11	MISSING CASES	0
DEGREES OF FREEDOM	3		
OVERALL F	68.43	P VALUE	0.0026
ADJUSTED R SQUARED	0.9793		
R SQUARED	0.9938		
RESID. MEAN SQUARE	4.333E-03		

STEPWISE ANALYSIS OF VARIANCE OF Y

SOURCE	INDIVIDUAL SS	CUM DF	CUMULATIVE SS	CUMULATIVE MS	ADJUSTED R-SQUARED
CONSTANT	83.463				
X1	1.125	1	1.125	1.125	0.4874
X2	6.96E-01	2	1.821	9.11E-01	0.8399
X3	2.45E-01	3	2.066	6.89E-01	0.9846
X12	1.80E-03	4	2.068	5.17E-01	0.9835
X23	3.20E-03	5	2.071	4.14E-01	0.9833
X13	1.80E-03	6	2.073	3.45E-01	0.9812
X11	2.67E-03	7	2.076	2.96E-01	0.9793
RESIDUAL	1.30E-02	10	2.089	2.09E-01	

CASES INCLUDED	11	MISSING CASES	0
DEGREES OF FREEDOM	3		

surface can be approximated with a second order function, other test designs based on RSM concepts, such as those suggested by Box and Behnken, can be used to find second order or higher relationships.

As previously mentioned, actual data points can be collected with the MTM-8 and the Instron Testing machines. One of the key assumptions used in this RSM analysis is that the levels of each variable are continuous, not discrete, data points. This assumption impacts the choice of fibers and matrix materials that can be used. Choosing fibers that are made from different starting materials, such as carbon or polymers, probably would invalidate this assumption of continuity. An example of an appropriate choice of fibers would be P25, P55 and P100 fibers. These fibers are all made from carbon pitch, but have different mechanical properties. The matrix materials should be chosen in an analogous fashion.

RSM is a powerful experimental design tool that can be applied to the study of composite material compressive properties. The design presented is only a suggestion and is meant to be a starting point. Additional

variables can be added without altering the underlying RSM concepts. The assumptions made during the analysis must not be ignored. If the assumptions are for some reason invalidated, then any inferences drawn from the resulting model will be suspect.

Bibliography

1. Allen, Steven R. Mechanical and Morphological Correlations in Poly(p-phenylenebenzobisthiazole) Fibers, July 1983. Contract AFWAL-TR-83-4045. Amherst MA: University of Massachuettes, July 1983.

2. Bauer, Kenneth, W. Class handout distributed in OPER 699, Response Surface Methodology. Air Force Institute of Technology (AU), Wright-Patterson AFB OH, July 1989.

3. Box, George P. and Norman R. Draper. Empirical Model Building and Response Surfaces. New York: John Wiley and Sons Inc., 1987.

4. Brush, D. O. and Bo O. Almroth. Buckling of Bars, Plates, and Shells. New York: McGraw-Hill Book Company, 1975.

5. Devore, Jay L. Probability and Statistics For Engineering and the Sciences (Second Edition). Monterey, California: Brooks/Cole Publishing Company, 1987.

6. Deteresa, S. J. The Axial Compressive Strengths of High Performance Polymer Fibers: Interim Report, 1 September 1982 - 1 April 1983. Contract AFWAL-TR-85-4013. Amherst MA: University of Massachuettes, March 1985 (AD-A165 065).

7. Dobbs, M.G. and others. "Compressional Behaviour of Kevlar Fibers", Polymer,22: 960-965 July 1981.

8. Fawaz, 2Lt Scott A. Compressive Properties of High Performance Polymeric Fibers. Ms Thesis, AFIT/GAE/AA/88D-13. School of Engineering, Air Force Institute of Technology (AU), Wright-Patterson AFB OH, December 1988.

9. Hawthorne H.M. and E. Teghtsoonian. "Axial Compression Fracture in Carbon Fibres", Journal of Material Science, 10: 40-47 1975.

10. Jones, Robert M. Mechanics of Composite Materials. Washington, D.C.: McGraw-Hill Book Company, 1975.

11. Keller, Capt Russel L. Examination of High Performance Polymer Fibers Under Compressive Deformation. Ms Thesis, AFIT/GAE/AA/86D-5. School of Engineering, Air Force Institute of Technology (AU), Wright-Patterson AFB OH, December 1986.

12. Kumar, Satish and T. E. Helminiak. "Compressive Strength of High Performance Fibers", Proceedings of the Materials Research Society Symposium, Volume 134. Pittsburgh, Penna.: 1989.

13. Kumar, Satish and others. "Uniaxial Compressive Strength of High Modulus Fibers for Composites", Journal of Reinforced Plastics and Composites, 7: 108-119 (March 1988).

14. Neter, John and others. Applied Linear Statistical Models (Second Edition). Homewood, Illinois: Irwin Inc., 1985.

15. NH Analytic Software. STATISTIX - An Interactive Statistical Analysis Program for Microcomputers. Software User's Manual. NH Analytic Software, Roseville MN, 1987.

16. Palazotto, A. M., Professor, School of Engineering, Air Force Institute of Technology, Personal Interview, Air Force Institute of Technology (AU), Wright-Patterson AFB OH, [illegible] February through 1 November 1989.

17. Riggs, Dennis M. and others. "Graphite Fibers and Composites," Handbook of Composites. edited by George Lubin. New York: Van Nostrand Reinnold Company, 1982.

18. Schenck, Hilbert. Theories of Engineering Experimentation, (Third Edition). New York: McGraw-Hill Book Company, 1979.

19. Tecam Micro-Tensile Testing Machin[illegible] Instruction Book. Techne Inc., Princeton NJ, January 1968.

20. Wang, C. S., Research Chemist, Universiy of Dayton Research Institute, Personal Interview, Air Force Materials Laboratory, *Polymer Branch*, Wright-Patterson AFB OH, 9 February through 25 October 1989.

21. Wang, C. S. and others. "Axial Compressive Strengths of High-Performance Fibers By Tensile Recoil Technique", Proceedings from American Chemical Society Meeting. Miami Beach: September 1989.

Vita

Thomas A. Doyne [redacted] He graduated from Radnor Senior High School in Radnor PA in 1980. He attended the United States Air Force Academy, where he graduated in the Class of 1984 with a Bachelor of Science in Engineering Mechanics. As a lieutenant, he was stationed at Peterson AFB, CO and was part of the initial cadre who activated the First Satellite Control Squadron (1SCS), Second Space Wing. As a member of the 1SCS, Lt. Doyne served as lead ground systems control officer on a satellite operations crew. In May 1988, he started his graduate study for a Master of Science in Space Operations at the Air Force Institute of Technology.

[redacted]